Spring 2015

Design and synthesis of fluoroquinolones to overcome resistance in bacteria

Benjamin Howard Williamson
University of Iowa

DESIGN AND SYNTHESIS OF FLUOROQUINOLONES TO OVERCOME RESISTANCE IN BACTERIA

by

Benjamin Howard Williamson

A thesis submitted in partial fulfillment
of the requirements for the Doctor of
Philosophy degree in Pharmacy
in the Graduate College of
The University of Iowa

May 2015

Thesis Supervisor: Professor Robert J. Kerns

Graduate College
The University of Iowa
Iowa City, Iowa

CERTIFICATE OF APPROVAL

_____

PH.D. THESIS

_____

This is to certify that the Ph.D. thesis of

Benjamin Howard Williamson

has been approved by the Examining Committee
for the thesis requirement for the Doctor of Philosophy
degree in at the graduation.

Thesis Committee: _____
Robert J. Kerns, Thesis Supervisor

_____
Jonathan A. Doorn

_____
Zhendong Jin

_____
Horacio Olivo

_____
F. Christopher Pigge

ACKNOWLEDGMENTS

I wish first to thank my graduate advisor Robert Kerns, who accepted me into his lab and his fluoroquinolone project. His continued guidance, support, encouragement, and patience made me into the scientist I am today. I also wish to thank the members of my thesis committee Jonathan Doorn, Horacio Olivo, Zhendong Jin, and Christopher Pigge for their time and support. I also must thank the many professors under which I have studied during my graduate education. Their extensive training will serve as the foundation of my career. This work would have been impossible without the dedicated administration of Patricia Sadowski, Lois Baker, Kelly Walsh, and Kellie Northup.

I owe a great debt to Lei Chen and Luis Hernandez, who taught (and retaught) me a variety of laboratory techniques (both traditional and not-so traditional) in organic synthesis and research. In particular Heidi Schwanz was very important for my training in fluoroquinolone research, and the research described herein would not have been possible without her. I would be remiss if I did not thank all members of the Kerns lab, past and present, for their advice and encouragement. I must thank my undergraduate professors Melvin Hall and Hank Parker, mentors who began my studies in organic chemistry and encouraged my career in academic science.

I have enjoyed the companionship of many wonderful people over the past six years. I came to Iowa knowing absolutely no one, and in a few short years you all have become the finest group of friends that anyone could ever ask for. For that, you each have my sincerest gratitude. I wish had space to list you all here by name, but you know who you are. Finally, I would like to thank my wonderful parents, John and Susan Williamson. They have been ever-present sources of love, encouragement, advice, and support my entire life, and without them I never would have succeeded in these endeavors. All that I have done has been made possible by God above. He is my rock, my salvation, and the source of all good things.

ABSTRACT

Fluoroquinolones, a class of type-II topoisomerase inhibitors, have successfully been used as antibiotics for the last several decades, beginning with the use of nalidixic acid in urinary tract infections. This led to the broad-spectrum activity of ciprofloxacin in the 1980s. Unfortunately, use of fluoroquinolones has led to the emergence of resistant bacteria. Recently, this has generated new bacteria such as multidrug-resistant and extensive-drug-resistant strains of *M. tuberculosis* that are also fluoroquinolone-resistant. Infections caused by these bacterial strains are widespread, with high mortality rate in immune-compromised populations such as the elderly, infants, and in AIDS or HIV-positive patients.

Fluoroquinolone resistance is acquired through amino acid substitutions of key fluoroquinolone-binding residues of the type-II bacterial topoisomerases DNA Gyrase and Topoisomerase IV, the enzyme targets of fluoroquinolones. Amino acid substitutions that result in fluoroquinolone resistance are located on Helix-4 of these enzymes, which is the site of a magnesium (Mg)-water bridge that is a crucial binding interaction for fluoroquinolones. When certain substitutions to Helix-4 occur, the Mg-water bridge is compromised and no longer available to anchor fluoroquinolones into a ternary complex composed of topoisomerase, fluoroquinolone, and DNA. This results in drug resistance. Herein are described attempts to generate fluoroquinolones that are capable of overcoming this mechanism of resistance.

In the first study, attempts were made to generate a series of novel tricyclic fluoroquinolones and diones designed to exploit intercalative or pi-stacking binding interactions with the bacterial DNA in the ternary complex in order to lessen the importance of the Mg-water bridge interaction. Despite numerous attempts, no complete synthetic pathway to these core structures was ever discovered.

The second study investigated the utility of a C7-aminomethylpyrrolidine group on the fluoroquinolone structure. This was done in order to explore the mechanistic reasons why previously generated fluoroquinolones possessing this C7-aminomethylpyrrolidine group maintained activity against common Helix-4 mutants. A panel of fluoroquinolones with C7-aminomethylpyrrolidine groups and diverse core structures was synthesized and docking studies with the original C7-aminomethylpyrrolidine fluoroquinolone and other fluoroquinolones were performed. Target compounds were synthesized and evaluated for inhibition/poisoning purified enzyme and for the ability to inhibit growth with wild-type and fluoroquinolone-resistant cells. In a third study, fluoroquinolones possessing structural variations of the C7-aminomethylpyrrolidine were designed and synthesized to explore structural requirements of the aminomethylpyrrolidine group binding and overcoming fluoroquinolone-resistance caused by alterations of Helix-4. This led to further exploration of the binding space around the C7-position of the fluoroquinolones. In both the second and third studies, the new fluoroquinolones were evaluated for the ability to specifically target bacterial topoisomerases over human topoisomerase. The results of these studies have contributed new knowledge to the binding requirements of fluoroquinolones that maintain potency against fluoroquinolone-resistant type-II topoisomerases, and represent a step towards methodology to overcome bacteria resistant to fluoroquinolones.

PUBLIC ABSTRACT

Fluoroquinolones are highly successful antibiotics that, through widespread use, suffer diminishing clinical utility due to emerging antibiotic resistance. The emergence of fluoroquinolone-resistant bacteria is believed to be caused by evolution-driven changes in the targets of fluoroquinolone action, namely the type-II bacterial topoisomerases DNA Gyrase and Topoisomerase IV. The function of type-II topoisomerases is the untangling of knots in bacterial DNA and the separation of newly replicated bacterial DNA. Type-II topoisomerases are crucial to the replication of bacterial DNA, and ultimately cellular reproduction in bacteria. Fluoroquinolones are able to bind into a structure composed of bacterial DNA bound into topoisomerase. This entire structure, which is composed of fluoroquinolone, DNA, and topoisomerase, is called the ternary complex. The binding of the fluoroquinolone into the ternary complex stops the process of DNA untangling by topoisomerase, which in turn halts cellular growth and leads to cell death. Fluoroquinolones that are able to stabilize the ternary complex are referred to as topoisomerase poisons.

The goal of the research described herein is the development of new fluoroquinolones that are able to poison both wild-type bacteria and fluoroquinolone-resistant bacteria. This was accomplished by the generation of fluoroquinolones that possess side chain structures that bind to places in the ternary complex that are separate from the resistance-causing alterations within topoisomerase. The ability of these new fluoroquinolones to 1) poison bacterial topoisomerases and 2) not poison human topoisomerase was tested in purified bacterial and human topoisomerase enzymes. The ability of these new fluoroquinolones to inhibit bacteria cell growth was tested in wild-type and fluoroquinolone-resistant cell cultures.

TABLE OF CONTENTS

LIST OF TABLES ix

LIST OF FIGURES xi

LIST OF SCHEMES xvi

LIST OF COLLABORATING INVESTIGATORS xvii

LIST OF ABBREVIATIONS xviii

CHAPTER

I. INTRODUCTION 1

1.1: A Brief History of Fluoroquinolones 1
1.2: SAR of the Quinolone Scaffold 3
1.3: Structure and Function of Type-II Bacterial Topoisomerases 8
1.4: Mechanism of Flouroquinolone Activity 10
1.5: Mechanisms of Fluoroquinolone Resistance 12
1.6: Targeting Human Topoisomerase as a Result of Overcoming Fluoroquinolone Resistance 15

II. STATEMENT OF PURPOSE 18

III. ATTEMPTS TO GENERATE INTERCALATIVE TRICYCLIC FLUOROQUINOLONE AND DIONE CORES 22

3.1: Introductuion 22
3.2: Goals of the Study 24
3.3: Docking Studies with Topoisomerase IV and Tricyclic Fluoroquinolones and Diones 25
3.4: Attempts to Synthesize 5, 6-phenyl Napthyridone, 4, 5-Pyrimidine Fluoroquinolone, and 5, 6-phenyl Dione Cores 27
3.5: Conclusions and Future Directions 35

IV. EFFECT OF C-7 AMINOMETHYLPYRROLIDINE SIDE CHAIN ON FLUOROQUINOLONE ACTIVITY 37

4.1: Introduction 37
4.2: Goals of the Study 40
4.3: Synthesis of Core-Diverse C7-Aminomethylpyrrolidine Fluoroquinolone Series 41
4.4: Docking Studies with Core-Diverse C7-Aminomethylpyrrolidine Fluoroquinolones 43
4.5: Enzyme Inhibition Activity by C7-Aminomethylpyrrolidine Fluoroquinolones 44
4.6: Growth Inhibition Activity by Core-Diverse C7-Aminomethylpyrrolidine Fluoroquinolones 50
4.7: Antimutant Activity Profiles of Core-Diverse C7-Aminomethylpyrrolidine Fluoroquinolones 53

V. THE EFFECT OF MODIFICATIONS TO THE C7-AMINOMETHYLPYRROLIDINE SIDE CHAIN 67

5.1: Introduction 67
5.2: Goals of the Study 69
5.3: Synthesis of C7-variant Fluoroquinolones 70
5.4: Docking Studies with C7-Variant Fluoroquinolones 71
5.5: Enzyme Inhibition by C7-Variant Fluoroquinolones 73
5.6: Growth Inhibition Activity by C7-Variant Fluoroquinolones 78
5.7: Antimutant Activity of C7-Variant Fluoroquinolones 81

VI. EXPERIMENTAL SECTION 91

6.1: General Methods 91
6.2: Synthesis of Intermediates to Obtain 5, 6-phenyl Fluoroquinolone and Dione Cores (Chapter 3) 92
6.2.1: Preparation of Isoquinolone-1, 3 (2H, 4H)-dione (**6**) (**UIBW01-236**) 92
6.2.2: Preparation of 1, 3-dichloroisoquinolone (**7**) (**UIBW01-239**) 93
6.2.3: Preparation of 1,3-dichloroisoquinoline-4-carboxylic acid (**8**) (**UIBW02-121**) 93
6.2.4: Preparation of 1,3-dichloroisoquinoline-4-carboxamide (**9**) (**UIBW02-297**) 95
6.2.5: Preparation of ethyl 3-(1,3-dichloroisoquinoline-4-yl)-3-oxopropanoate (**10**) (**UIBW02-299**) 96
6.3: Synthesis of Intermediates to Obtain 4, 5-pyrimidine Fluoroquinolone Core (Chapter 3) 97
6.3.1: Preparation of 1-cyclopropyl-6,7-difluoro-8-methoxy-5-nitro-4-oxo-1,4-dihydroquinoline-3-carboxylic acid (**21**) (**UIBW02-067**) 97
6.3.2: Preparation of methyl 1-cyclopropyl-6,7-difluoro-8-methoxy-5-nitro-4-oxo-1,4-dihydroquinoline-3-carboxylate (**22**) (**UIBW02-068**) 98
6.3.3: Preparation of methyl 5-amino-1-cyclopropyl-6,7-difluoro-8-methoxy-4-oxo-1,4-dihydroquinoline-3-carboxylate (**23**) (**UIBW02-196**) 98
6.3.4: Preparation of methyl 6-cyclopropyl-8,9-difluoro-7-methoxy-6H-pyrido[4,3,2-de]quinazoline-4-carboxylate (**24**) (**UIBW02-157**) 99
6.4: Synthesis of Core-Diverse 7-Aminomethylpyrrolidine Fluoroquinolones (Chapter 4) 100
6.4.1: Preparation of (S)-7-(3-(aminomethyl)pyrrolidin-1-yl)-1-cyclopropyl-6-fluoro-8-methoxy-4-oxo-1,4 dihydroquinoline-3-carboxylic acid (**UING05-249/ UIHS02a-077**) 100
6.4.2: Preparation of (S)-7-(3-(aminomethyl)pyrrolidin-1-yl)-1-cyclopropyl-6-fluoro-8-methoxy-5-methyl-4-oxo-1,4-dihydroquinoline-3-carboxylic acid (**UIHS02a-215**) 101
6.4.3: Preparation of (S)-7-(3-(aminomethyl)pyrrolidin-1-yl)-6-fluoro-8-methoxy-4-oxo-1-(prop-1-en-2-yl)-1,4-dihydroquinoline-3-carboxylic acid (**UITT03-245**) 101
6.4.4: Preparation of (S)-5-amino-7-(3-(aminomethyl)pyrrolidin-1-yl)-1-cyclopropyl-6-fluoro-8-methoxy-4-oxo-1,4-dihydroquinoline-3-carboxylic acid (**UIBW04-123B**) 102

6.4.5: Preparation of (S)-7-(3-(aminomethyl)pyrrolidin-1-yl)-1-cyclopropyl-6-fluoro-4-oxo-1,4-dihydro-1,8-naphthyridine-3-carboxylic acid (**UIBW04-234**) 103
6.4.6: Preparation of (S)-10-((S)-3-(aminomethyl)pyrrolidin-1-yl)-9-fluoro-3-methyl-7-oxo-3,7-dihydro-2H-[1,4]oxazino[2,3,4-ij]quinoline-6-carboxylic acid (**UIBW04-235**) 104
6.4.7: Preparation of (S)-6-((S)-3-(aminomethyl)pyrrolidin-1-yl)-5-fluoro-8-oxo-3H,8H-4-Oxa-1-thia-9b-azacyclopenta[cd]phenalene-9-carboxylic acid (**UIBW04-236**) 105
6.4.8: Preparation of (S)-7-(3-(aminomethyl)pyrrolidin-1-yl)-1-ethyl-6-fluoro-4-oxo-1,4-dihydroquinoline-3-carboxylic acid (**UIBW04-237**) 106
6.4.9: Preparation of 7-((S)-3-(aminomethyl)pyrrolidin-1-yl)-6,8-difluoro-1-(2-fluorocyclopropyl)-4-oxo-1,4-dihydroquinoline-3-carboxylic acid (**UIBW04-238**) 106
6.4.10: Preparation of (S)-7-(3-(aminomethyl)pyrrolidin-1-yl)-1-(2,4-difluorophenyl)-6-fluoro-4-oxo-1,4-dihydro-1,8-naphthyridine-3-carboxylic acid (**UIBW04-255**) 107
6.5: Synthesis of C7-Diverse Fluoroquinolones (Chapter 5) 108
6.5.1: Preparation of (R)-7-(3-carbamoylpyrrolidin-1-yl)-1-cyclopropyl-6-fluoro-8-methoxy-4-oxo-1,4-dihydroquinoline-3-carboxylic acid (**UIBW04-259**) 108
6.5.2: Preparation of (R)-7-(3-aminopyrrolidin-1-yl)-1-cyclopropyl-6-fluoro-8-methoxy-4-oxo-1,4-dihydroquinoline-3-carboxylic acid (**UIBW04-261**) 109
6.5.3: Preparation of (R)-1-cyclopropyl-6-fluoro-7-(3-(hydroxymethyl)pyrrolidin-1-yl)-8-methoxy-4-oxo-1,4-dihydroquinoline-3-carboxylic acid (**UIB04-263**) 110
6.5.4: Preparation of (S)-1-cyclopropyl-6-fluoro-8-methoxy-7-(3-((methylamino)methyl)pyrrolidin-1-yl)-4-oxo-1,4-dihydroquinoline-3-carboxylic acid (**UIBW04-267**) 110
6.6: *In-silico* Docking Studies with SYBYL Software 111
6.7: Analysis of Compound Activity 112

VII. CONCLUSIONS AND FUTURE DIRECTIONS 115

7.1: Brief Restatement of Theory 115
7.2: Studies with Tricyclic Fluoroquinolones 116
7.3: Studies with Core-Diverse C7-Aminomethylpyrrolidine Fluoroquinolones 116
7.4: Studies with C7-Variant Fluoroquinolones 121
7.5: Future Directions 126

APPENDIX A: CHAPTER 3 SELECTED NMR SPECTRA 127

APPENDIX B: CHAPTER 4 AND 5 SELECTED NMR SPECTRA AND HPLC CHROMATOGRAMS 132

REFERENCES 146

LIST OF TABLES

1. Table 4.1: Supercoiling inhibition with wild-type E. coli DNA gyrase by core-diverse, C7- aminomethylpyrrolidine fluoroquinolones. The fold-difference between IC50 of each compound and the IC50 of a previously studied C7-aminomethylpyrrolidine compound, UING-05-249 is listed in the right column.. 45

2. Table 4.2: Cleaved complex formation and poisoning activity measured by formation of linear DNA complexes as a result of incubation with core-diverse series of fluoroquinolones. Poisoning activity is listed at supercoiling IC_{50}. CC_3 is the concentration of fluoroquinolone required to triple the amount of released cleaved complexes. 48

3. Table 4.3: Supercoiling inhibition activity by core-diverse, C7-aminomethylpyrrolidine fluoroquinolones with human topoisomerase IIα. Poisoning fold-stimulation is measured at supercoiling IC_{50}.. 50

4. Table 4.4: Minimum inhibitory concentrations of core-diverse, C7-aminomethylpyrrolidine fluoroquinolones with *tolC* KO *E. coli* cells. The fold-difference between MIC's of each compound are compared to the MIC of UING-05-249.....51

5. Table 4.5: Bacteriostatic activities of C7-variant fluoroquinolones in wild-type *M. smegmatis* cells. The fold-difference between compound MIC and the MIC of UING-05-249 is listed to in the center-right column. The fold-difference between compound MIC in wild-type *M. smegmatis* cells ($MIC_{M. smeg}$) and MIC in *tolC* KO *E. coli* cells is listed in the far right column 52

6. Table 4.6: Average MIC values, standard deviations, and antimutant activities of core-diverse C7-aminomethylpyrrolidine fluoroquinolones *E. coli* strains containing serine 83 mutations.....57

7. Table 4.7: Average MIC values, standard deviations, and antimutant activities of core-diverse C7-aminomethylpyrrolidine fluoroquinolones *E. coli* strains containing aspartic acid 87 mutations 58

8. Table 4.8: Average MIC values, standard deviations, and antimutant activities of core-diverse C7-aminomethylpyrrolidine fluoroquinolones *E. coli* strains containing glycine 81 and aspartic acid 82 mutations.....60

9. Table 4.9: Average MIC values, standard deviations, and antimutant activities of core-diverse C7-aminomethylpyrrolidine fluoroquinolones *E. coli* strains containing adenine 84 mutations.....61

10. Table 4.10: Average MIC values, standard deviations, and antimutant activities of core-diverse C7-aminomethylpyrrolidine fluoroquinolones *E. coli* strains containing GyrB/ParE-region mutations D426N and K447E 62

11. Table 5.1: Inhibition of supercoiling activity of purified wild-type *E. coli* DNA gyrase by C7-variant fluoroquinolones. In the right column is a comparison between the activity of each C7-variant fluoroquinolone and the

parent C7-aminomethylpyrrolidine fluoroquinolone, UING-05-249, listed as a ratio of their respective IC_{50} values.....74

12. Table 5.2: Poisoning activity measured by formation of cleaved (linear) complexes of DNA as a result of ternary complex formation with C7-variant fluoroquinolones. Poisoning activity was determined as the supercoiling inhibition IC_{50} of each compound, which are listed in Table 5.1.....76

13. Table 5.3: Decatenation inhibition and poisoning fold-stimulation activity of C7-variant fluoroquinolones with human topoisomerase IIα. Poisoning fold-stimulation by was determined at decatenation inhibition IC_{50}. 78

14. Table 5.4: Bacteriostatic activities of C7-variant fluoroquinolones in *tolC* KO *E. coli* cells. The MIC value for Moxifloxacin in *tolC* KO *E. coli* cells was obtained from a separate study 79

15. Table 5.5: Bacteriostatic activities of C7-variant fluoroquinolones in wild-type *M. smegmatis* cells. The fold-difference between compound MIC and the MIC of UING-05-249 is listed to in the center-right column. The fold-difference between compound MIC in wild-type *M. smegmatis* cells ($MIC_{M. smeg}$) and MIC in *tolC* KO *E. coli* cells ($MIC_{E.coli}$) is listed in the far right column.....80

16. Table 5.6: Average MIC values and standard deviations of C7-variant fluoroquinolones with *E. coli* mutant strains containing serine 83 mutations. The calculated antimutant activity of each compound in the serine 83 mutant strain is listed in the far-right column as "mut/wt."....83

17. Table 5.7: Average MIC values and standard deviations of C7-variant fluoroquinolones with *E. coli* mutant strains containing aspartic acid 87 mutations. The calculated antimutant activity of each compound in the aspartic acid 87 mutant strain is listed in the far-right column as "mut/wt."....84

18. Table 5.8: Average MIC values and standard deviations of C7-variant fluoroquinolones with *E. coli* mutant strains containing Helix-4 mutations separate from residues that coordinate the Mg-water bridge. The calculated antimutant activity of each compound in the listed mutant strain in each subsection of the table is listed in the far-right column as "mut/wt."....85

19. Table 5.9 Average MIC values and standard deviations of C7-variant fluoroquinolones with *E. coli* mutant strains containing GyrB-region mutations. The calculated antimutant activity of each compound with the given mutant strain of each subsection of the table is listed in the far-right column as "mut/wt" 86

Table 6.1: The cell cultures used in bacteriostatic activity (MIC) assays, later used to determine antimutant activity profiles for the compounds. 114

LIST OF FIGURES

1. Figure 1.1: Evolution of initially discovered quinolone structures to modern fluoroquinolones 2

2. Figure 1.2: Left: Diagram of established SAR for fluoroquinolone scaffold Right: Schematic of the Mg-water bridge.....4

3. Figure 1.3: Diversification of the C7- and C8-positions of the fluoroquinolone scaffold.....6

4. Figure 1.4: Examples of N1-C8 linked fluoroquinolones.....7

5. Figure 1.5: **Left**-The regulation of superhelical topology by DNA Gyrase and topoisomerase IV (adapted from Redgrave et. al. [2]). **Right**- ParC of *A. baumannii* topoisomerase IV (Adapted from PDB: 2XKK structure).....8

6. Figure 1.6: ATP-driven mechanism of type-II topoisomerases. DNA binds GyrA/ParC and a pair of single-stranded nicks on each strand of DNA are introduced, creating a transient DNA gate through which a second strand can pass. Superhelical density is regulated and unknotting/untangling of bacterial DNA is performed with DNA Gyrase and daughter chromatids are segregated with Topoisomerase IV. (Adapted from DNA topoisomerase II and its growing repertoire of biological functions. *Nature Reviews Cancer*).....9

7. Figure 1.7: Moxifloxacin bound within ternary complex in *A. baumannii* topoisomerase IV via the Mg-water bridge (adapted from 2XKK, Wohlkonig et. al). Other interactions are believed to exist through DNA nucleoside bases and riboses, via interactions through the C7 side chain. 12

8. Figure 1.8: The binding site of fluoroquinolones. Point mutations to the Helix-4 region of GyrA/ParC subunits of type-II bacterial topoisomerases represent the greatest threat to the clinical utility of fluoroquinolones. There is evidence of resistance-causing mutations in GyrB/ParE subunits, however as yet these appear to be less prevalent and less able to cause high-level fluoroquinolone resistance. 14

9. Figure 1.9: Comparison of *A. baumannii* topoisomerase IV (adapted from 2XKK) and human topoisomerase IIα (adapted from 4FM9)[102] both bound to DNA. The central structure Helix-4 is highlighted in gold. Topoisomerase IV is bound to moxifloxacin through the Mg-water bridge. The coordinating acidic residues of the Mg-water bridge in Topoisomerase IV are in bold and numbered, as are the corresponding methionine residues in human topoisomerase IIα. Similarities in sequence are also highlighted in red… 16

10. Figure 1.10: General fluoroquinolone and quinazolinedione (“dione”) scaffolds (C2-position highlighted in red) 17

11. Figure 3.1 Initial *in silico* modeling of 5,6-phenyl quinolone (black-ball and stick) forming a pi-stacking interaction with bound DNA (nucleoside residues highlighted in green-stick) within drug-enzyme-DNA ternary complex. Docking study performed with Wohlkonig et. al. [1] 2XKK *A. baumannii* structure.. 23

12. Figure 3.2: Proposed modifications to the fluoroquinolone and dione scaffolds to extend aromatic character of compound and increase compound ability to form pi-stacking binding contacts. 24

13. Figure 3.3: Docking scores of hypothetical fluoroquinolone and dione skeletons with aryl extensions of their core structure in order to form intercalative/ π-stacking interactions with nucleoside bases, along with known fluoroquinolone and dione structures as controls. Each compound was docked into the 2XKK crystal structure. The "Score" is a composite CScore generated by SYBYL.. 26

14. Figure 3.4: Proposed modifications to fluoroquinolone and dione drug skeletons. Once core structures had been made it was believed that side chains would be facile to attach and thus the compounds could be diversified as required. 27

15. Figure 4.1: DNA cleavage activity with *B. anthracis* TopoIV as a result of the binding of fluoroquinolones containing a C7 piperazine, diazabicyclononane, or aminomethylpyrrolidine group. The wild-type activities (black lines) observed with the C7 piperazine and diazabicyclononane fluoroquinolones are lost when serine 81 is substituted with phenylalanine (blue lines) or tyrosine (red lines). In *B. anthracis* serine 81 is a key residue that coordinates the Mg-water bridge to Helix-4. The C7-aminomethylpyrrolidine fluoroquinolones are able to either maintain or have improved activity with these substitutions. Adapted from previous work by Schwanz and colleagues. 38

16. Figure 4.2: Docking studies with UING-05-249 in *A. baumannii* topoisomerase IV structure (2XKK). The highest scoring pose is depicted and consists of a bridging interaction of the primary amine of the C7-aminomethylpyrrolidine between the Glu437 side chain of ParE and a backbone carbonyl of R418 (orange circle). In other docking poses it is also possible for the C7-aminomethylpyrrolidine chain to twist around and interact with the ribose oxygen of DA-20 (blue circle), mimicking the binding of the moxifloxacin diazabicyclononane C7-side chain or the C7-piperazine of ciprofloxacin.. 39

17. Figure 4.3: The panel of core-diverse C7-aminomethylpyrrolidine fluoroquinolones. 42

18. Figure 4.4: C7-aminomethylpyrrolidine fluoroquinolones with the control compounds ciprofloxacin, moxifloxacin, and UING-05-249. Beneath each compound is its SYBYL-generated docking score for docking into a crystal structure of a ternary complex of *A. baumannii* topoisomerase IV (PDB:2XKK). Higher scores represent increased binding affinity. All compounds dock with comparable affinity into the fluoroquinolone binding-pocket with the Mg-water bridge as the main binding contact 43

19. Figure 4.5: Simplified depiction of *in silico* docking of the core-diverse C7-aminomethylpyrrolidine fluoroquinolones and moxifloxacin in *A. baumannii* topoisomerase IV crystal structure 2XKK. The binding orientation is conserved across all compounds. 44

20. Figure 4.6: *In silico* depiction of Helix-4 residues (*E. coli* numbering) of Topoisomerase IV. Moxifloxacin (black stick) is bound to Helix-4 through the Mg-water bridge (green and red spheres) and is oriented into the DNA (gold stick) nicked site. The serine and aspartate residues that coordinate the Mg-water bridge are highlighted in green. Other Helix-4 residues of note are G81, D82 and A84. D426 and K447 (not shown) are GyrB/ParE residues that may interact with the C7-aminomethylpyrrolidine. 55

21. Figure 4.7: Bar-graph representation of antimutant activities of core-diverse C7-aminomethylpyrrolidine fluoroquinolone series *E. coli* strains possessing mutations of the S83L(blue), S83W (dark blue), D87N (purple), and D87Y (light purple). The residues S83 and D87 coordinate the Mg-water bridge and mutations to these residues are highly correlative to fluoroquinolone resistance. Lower antimutant activity represents greater retention of compound activity. 59

22. Figure 4.8: Antimutant activities of core-diverse C7-aminomethylpyrrolidine fluoroquinolones with *E. coli* strains containing the Helix-4 mutations G81C (olive), D82A (brown), and A84P (green) as well as strains with the GyrB mutations D426N (orange) and K447E (yellow). 63

23. Figure 4.9: Bar graph of antimutant activities of C7-aminomethylpyrrolidine-containing fluoroquinolones with data for current fluoroquinolones PD160788 (left structure) and moxifloxacin (right structure). Antimutant profiles against S83/D87 substitutions are shown in the left graph and other Helix-4 and GyrB/ParE substitutions are shown in the right graph. The antimutant activities for PD160788 and moxifloxacin were adapted from previous studies. 66

24. Figure 5.1: Panel A- Binding pose of UING-05-249 with the C7-aminomethylpyrrolidine primary amine forming a divalent binding pose between E437 and the backbone carbonyl of R418 in the 2XKK crystal structure. Panel B- Overlay of moxifloxacin and UING-05-249 binding poses in the 2XKK DNA nicked site. The DA-20 ribose oxygen binding contact of the moxifloxacin C7-group 2^{o}-amine is shared by a binding pose of the C7-aminomethylpyrrolidine group of UING-05-249 (not shown). 68

25. Figure 5.2: The C7-variant fluoroquinolone series, structurally based on the original C7-aminomethylpyrrolidine fluoroquinolone UING-05-249. 69

26. Figure 5.3: The C7-variant fluoroquinolones with SYBYL-generated docking scores as a composite measurement of binding affinity. All C7-variant fluoroquinolones, UING-05-249 and moxifloxacin are able to dock with comparable affinity to each other. All compounds dock into the fluoroquinolone binding-pocket with the Mg-water bridge as the main binding contact. 72

27. Figure 5.4: Simplified picture of C7-variant fluoroquinolones and UING-05-249 binding into *A. baumannii* crystal structure 2XKK. The highest

scoring binding pose of each of the C7-variant fluoroquinolones uses the Mg-water bridge as the major binding contact in wild-type topoisomerase IV.. 72

28. Figure 5.5: Antimutant activities (y-axis) for each of the C7-variant fluoroquinolones (x-axis) with *E. coli* Helix-4 mutants (G81C- dark green, D82A- brown, S83L-blue, S83W- dark purple, A84P-light green, D87N- purple, D87Y- gray) and *E. coli* GyrB mutants (D426N- orange, K447E- yellow). The antimutant activities shown for moxifloxacin were adapted from a previous study.....87

29. Figure 5.6: Summary of global observations from antimutant activities determined for C7-variant fluoroquinolones, comparing their overall abilities to maintain activity with fluoroquinolone-resistant *E. coli* mutant strains. 90

30. Figure 7.1: Structural diversification of fluoroquinolone cores studied with C7-aminomethylpyrrolidine (AMP) group in Chapter 4. 117

31. Figure 7.2: The C7-variant fluoroquinolones (C7-groups highlighted in red) with parent compound UING-05-249 and brief descriptions of structural diversification. 122

32. Figure 7.3: Proposed binding for fluoroquinolone with bis-substituted C7-pyrrolidine group.. 126

33. Figure A1. ^{1}H-NMR (300 MHz, $CHCl_3$) of **6** (**UIBW01-236**).....127

34. Figure A2. ^{1}H-NMR (300 MHz, DMSO-d_6) of **7** (**UIBW01-239**) 127

35. Figure A3. ^{1}H-NMR (300 MHz, $CHCl_3$) of **8** (**UIBW02-121**).....128

36. Figure A4. ^{1}H-NMR (300 MHz, $CHCl_3$) of **10 (UIBW02-299)**.....128

37. Figure A5. ^{1}H-NMR (300 MHz, $CHCl_3$) of **9** (**UIBW02-297**).....129

38. Figure A6. ^{1}H-NMR (300 MHz, DMSO-d_6) of **21** (**UIBW02-067**) 129

39. Figure A7. ^{1}H-NMR (300 MHz, $CHCl_3$) of **22** (**UIBW02-068**).....130

40. Figure A8. ^{1}H-NMR (300 MHz, $CHCl_3$) of **23** (**UIBW02-196**).....130

41. Figure A9. ^{1}H-NMR (300 MHz, $CHCl_3$) of **24** (**UIBW02-157**).....131

42. Figure B1. ^{1}H-NMR (300 MHz, DMSO-d_6) of (**UIBW-04-123B**).....132

43. Figure B2. HPLC chromatogram of (**UIBW-04-123B**) 132

44. Figure B3. ^{1}H-NMR (300 MHz, DMSO-d_6) of (**UIBW-04-234**) 133

45. Figure B4. HPLC chromatogram of (**UIBW-04-234**) 133

46. Figure B5. ^{1}H-NMR (300 MHz, DMSO-d_6) of (**UIBW-04-235**) 134

47. Figure B6. HPLC chromatogram of (**UIBW-04-235**) 134

48. Figure B7. ^{1}H-NMR (300 MHz, DMSO-d_6) of (**UIBW-04-236**) 135

49. Figure B8. HPLC chromatogram of (**UIBW-04-236**) 135

50. Figure B9. ^{1}H-NMR (300 MHz, DMSO-d_6) of (**UIBW-04-237**) 136

51. Figure B10. HPLC chromatogram of (**UIBW-04-237**) 136

52. Figure B11. ^{1}H-NMR (300 MHz, DMSO-d_6) of (**UIBW-04-238**) 137

53. Figure B12. HPLC chromatogram of (**UIBW-04-238**) 137

54. Figure B13. ^{1}H-NMR (300 MHz, DMSO-d_6) of (**UIBW-04-255**) 138

55. Figure B14. HPLC chromatogram of (**UIBW-04-255**) 138

56. Figure B15. ^{1}H-NMR (300 MHz, DMSO-d_6) of (**UIHS-IIa-77 / UING-05-249**) 139

57. Figure B16. HPLC chromatogram of (**UIHS-IIa-77 / UING-05-249**) 139

58. Figure B17. ^{1}H-NMR (300 MHz, DMSO-d_6) of (**UIHS-IIa-215**) 140

59. Figure B18. HPLC chromatogram of (**UIHS-IIa-215**) 140

60. Figure B19. ^{1}H-NMR (300 MHz, DMSO-d_6) of (**UITT-03-245**).....141

61. Figure B20. HPLC chromatogram of (**UITT-03-245**) 141

62. Figure B21. ^{1}H-NMR (300 MHz, DMSO-d_6) of (**UIBW-04-259**) 142

63. Figure B22. HPLC chromatogram of (**UIBW-04-259**) 142

64. Figure B23. ^{1}H-NMR (300 MHz, DMSO-d_6) of (**UIBW-04-261**) 143

65. Figure B24. HPLC chromatogram of (**UIBW-04-261**) 143

66. Figure B25. ^{1}H-NMR (300 MHz, DMSO-d_6) of (**UIBW-04-263**) 144

67. Figure B26. HPLC chromatogram of (**UIBW-04-263**) 144

68. Figure B27. ^{1}H-NMR (300 MHz, DMSO-d_6) of (**UIBW-04-267**) 145

69. Figure B28. HPLC chromatogram of (**UIBW-04-267**) 145

LIST OF SCHEMES

1. Scheme 3.1: Typical synthesis of basic fluoroquinolone core structure prior to side chain addition.[6] 28

2. Scheme 3.2: Synthesis of 5,6-phenyl napthyridone and dione precursors. 29

3. Scheme 3.3: Proposed synthesis of 5,6-phenyl napthyridone derivatives, following established methodology for creating many fluoroquinolone cores. 30

4. Scheme 3.4: Attempts to progress in the synthesis of the 5, 6-phenyl napthyridone core from the C4 β-ketoester dichloroisoquinolone. 31

5. Scheme 3.5: Synthesis of the 4,5-pyrimidine fluoroquinolone core.....33

6. Scheme 3.6: Proposed synthesis of the 5,6-phenyl dione cores and the C4-nitrile product resulting from the unfavorable rearrangement of the carbonyl isocyanate.....34

7. Scheme 4.1: General methodology used to perform nucleophilic aromatic substitution of the C7-position on a variety of structurally diverse fluoroquinolone cores possessing either a C7-chlorine or fluorine. 42

8. Scheme 5.1: Synthesis of C7-variant fluoroquinolones. Nucleophilic aromatic substitution is used to add the four C7-side chains to an N1-cylcopropyl, C8-methoxy fluoroquinolone core.....71

LIST OF COLLABORATING INVESTIGATORS

Rutgers University

Karl Drlica
Arkada Mustaev
Muhammed Malik

University of Minnesota

Hiroshi Hiasa

LIST OF ABBREVIATIONS

ABC: ATP-binding cassette

AMP: aminomethylpyrrolidine

ATP: adenosine triphosphate

DA: DNA attribute

d-DMSO: deuterated dimethylsulfoxide

DIPEA: diisopropylethylamine

DMF: dimethylformamide

DMSO: dimethylsulfoxide

DNA: deoxyribonucleic acid

EDTA: Ethylenediaminetetraacetic acid

ESI-MS: electrospray ionization mass spectrometry

ESKAPE: *Enterococcus faecium, Staphylococcus aureus, Klebsiella pneumoniae, Acinetobacter baumannii, Pseudomonas aeruginosa, Enterobacter* species

Glu: glutamine

HPLC: high-pressure liquid chromatography

IC_{50}: inhibitory concentration of 50% enzyme activity

LDA: lithium diisopropylamide

LHMDS: lithium bis(trimethylsilyl)amide

LRMS: low-resolution mass spectrometry

MDR: multidrug resistant

MFS: major facilitator superfamily

Mg: magnesium

MIC: minimum inhibitory concentration

MPC: mutant prevention concentration

MSW: mutant selection window

Mut/wt: MIC_{mutant}/ $MIC_{wild\text{-}type}$

NMR: nuclear magnetic resonance

Pd/C: palladium on activated carbon

PFP: pentafluorophenyl

QRDR: quinolone-resistance determining region

SAR: structure-activity relationship

S.C. IC_{50}: supercoiling inhibitory concentration

Ser: serine

SMR: small multidrug resistance

TEA: triethylamine

TFA: trifluoroacetic acid

THF: tetrahyrdofuran

tRNA: transfer ribonucleic acid

XDR: extensively drug resistant

CHAPTER I: INTRODUCTION

1.1: A Brief History of Fluoroquinolones

The history of quinolones begins with the discovery of 3-carboxy substituted quinolones by Price *et. al*. in 1949.[1] Between 1957-1960 the synthesis and antibacterial characterization of similar quinolones by Imperial Chemical Industries was disclosed in a patent which included the 1,8-napthyridone substructure (Figure 1.1).[1] This would later lead to the discovery and characterization of the nalidixic acid 1,8-napthyridone structure (Figure 1.1) by Lesher et. al. at Sterling in 1962.[1 2] The 3-carboxy substituted quinolone substructure would later lead to the synthesis of norfloxacin, the first fluoroquinolone.[1 3] Nalidixic acid proved to be a useful way of treating uncomplicated infections of the urinary tract caused by Gram-negative bacteria, but lacked activity against Gram-positive bacteria and had numerous negative side effects. [4 5 6] Norfloxacin was the first quinolone-based agent to contain a 6-fluorine moiety and was the beginning of the fluoroquinolone scaffold. [7] This modification broadened activity of quinolones against additional Gram-negative bacteria such as *P. aeruginosa.* [7] Unfortunately, the low bioavailability of norfloxacin continued to limit the use of this quinolone and other fluoroquinolone-type agents to treating urinary tract infections. [6] The introduction of a N1-cyclopropyl substitution led to one of the most successful fluoroquinolones to date: ciprofloxacin. [8] Ciprofloxacin possessed enhanced Gram-positive activity and could achieve adequate serum concentration to treat infections outside of the urinary tract. [8] However, ciprofloxacin had limited use in respiratory infections as it possessed relatively low activity against *S. pneumonia*. [9 10] Despite these limitations, since its discovery in the 1980's ciprofloxacin has been one of the most widely used clinical fluoroquinolones. [11]

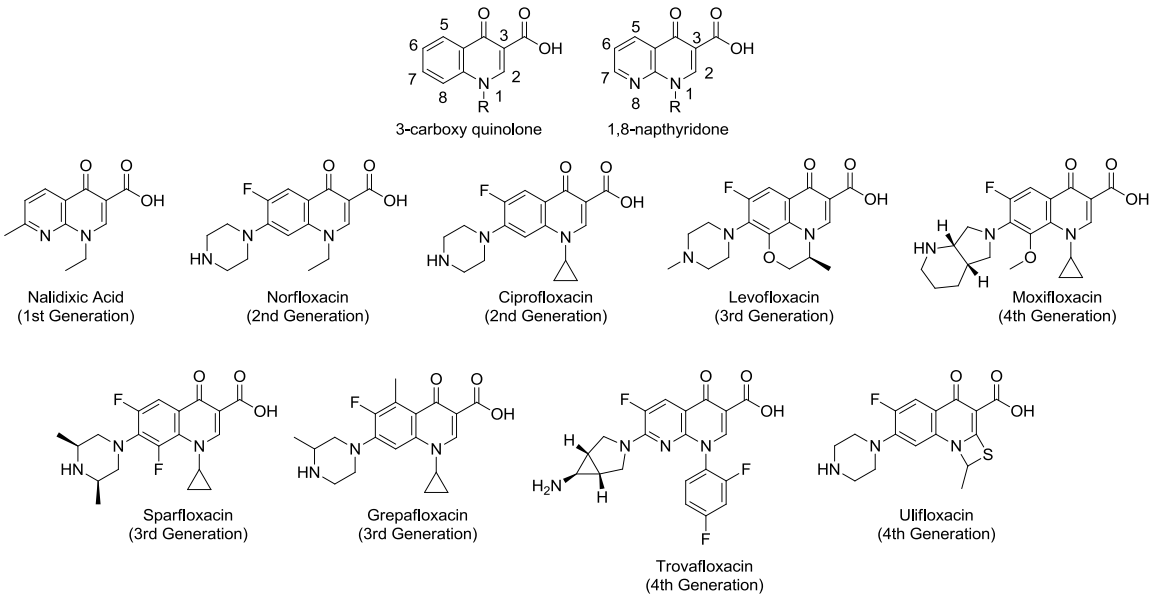

Figure 1.1: Evolution of initially discovered quinolone structures to modern fluoroquinolones

Several modifications were made to ciprofloxacin in order to identify better derivatives to combat respiratory infections; in particular many attempts were made to expand activity of fluoroquinolones against Gram-positive cocci and to decrease the selection for resistant strains. [12 13 14] These modifications resulted in the development of the compounds levofloxacin, moxifloxacin, sparfloxacin, grepafloxacin, and trovafloxacin, (Figure 1.1) among several others. [11 15] In particular, levofloxacin (Figure 1.1) is a 3rd-generation fluoroquinolone and the active (*S*)-isomer of ofloxacin, a racemic 2nd-generation fluoroquinolone. Levofloxacin is today widely used and has good activity against respiratory infections such as *S. pnuemoniae.* [11] Levofloxacin also maintains activity against additional Gram-positive and Gram-negative bacteria, and possesses a favorable pharmacokinetic profile that permits once-a-day dosing. [16]

Sparfloxacin (Figure 1.1) has performed well in extensive studies of its utility in treating respiratory infections, in particular chronic obstructive pulmonary disease and chronic bronchitis. [15] [17] [17b] [18] Unfortunately, sparfloxacin has demonstrated severe side effects such as prolongation of the QT-interval and severe phototoxicity. [19] [20] Trovafloxacin, grepafloxacin, and moxifloxacin (Figure 1.1) represent a more recent generation of fluoroquinolones that possess enhanced activity against Gram-positive bacteria and retain activity against a broad spectrum of Gram-negative pathogens. [21] [22] [23]. Specifically, these compounds have good activity against penicillin-resistant *S. pnuemoniae, H. influenza, K. pneumoniae,* and other respiratory pathogens, fulfilling the goal of discovering fluoroquinolone agents that have utility against respiratory infections. [21] Recent efforts have been largely devoted to adapting fluoroquinolones to combat drug-resistant infections, such as vancomycin-resistant enterococci and methicillin-resistant *S. aureus*, as well as the newly developing problem of fluoroquinolone-resistant strains of *E. coli* and *N. gonorrhoeae*. [10, 24] Moxifloxacin has proven useful against some infections resistant to earlier-generation fluoroquinolones like ciprofloxacin, however more agents are needed.

1.2: SAR of the Quinolone Scaffold

Since the discovery of norfloxacin several modifications to the fluoroquinolone scaffold have been made and some general trends in structure-activity-relationship (SAR) have been elucidated, as shown in Figure 1.2 There are three principle necessities of the fluoroquinolone structure: a 3,4 β-ketoacid, a C6-fluorine and a cyclic N1-amine. [25] Together these features form the skeleton of the fluoroquinolone drug scaffold.

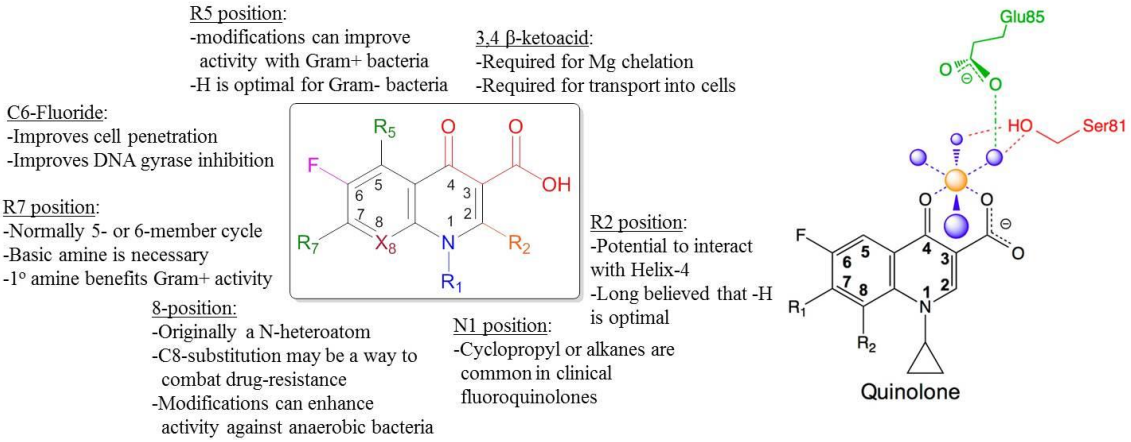

Figure 1.2: Left: Diagram of established SAR for fluoroquinolone scaffold [11] [15] Right: Schematic of the Mg-water bridge.[26]

The 3,4 β-ketoacid serves as the chelation site of a divalent magnesium^{+2} ion (Mg), and is necessary for cell penetration and is a major factor in drug binding. [13] [27] [28] [29] The recent crystal structure published by Wohlkonig et. al demonstrated that the ability of the drug skeleton to chelate divalent magnesium is necessary to anchor the fluoroquinolone into a drug-bacterial DNA-topoisomerase ternary complex via a water-magnesium bridge (Figure 1.2).[26] [30] The Mg-water bridge will be discussed in more detail in later sections. The proximity of the C2 position to the crucial C3-carboxylate has resulted in the prevailing theory that a C2-hydrogen is optimal, to prevent steric impedance between the fluoroquinolone and the binding site in the DNA/topoisomerase interface region. [13] [25] [31] However, the invention of ulifloxacin (Figure 1.1) as its dioxolan-2-one-modified prodrug, prulifloxacin, has demonstrated that the C2 position

can tolerate a sulphur atom within a cyclic thioether. [32] This concept will be explored further in Chapter 4 of this dissertation.

The addition of the 6-fluorine moiety in norfloxacin was revolutionary as it increased Gram-positive activity and allowed for greater cell penetration and enhanced pharmacodynamics. [33] Because all clinical quinolone agents developed during and after the second generation of quinolone antibiotics contain this C6-fluorine, the drug class is referred to as fluoroquinolones. However, some studies suggest that non-fluorinated quinolones may be useful in combating fluoroquinolone-resistant bacteria strains. [34 35]

A great deal of effort has gone into the exploration of binding space around the N1-position of the fluoroquinolone scaffold. The original quinolones nalidixic acid and norfloxacin possessed an N1 ethyl group (Figure 1.1). Later modifications demonstrated that steric bulk and spatial effects of the N1 position affect the overall potency of fluoroquinolones. [5] In particular, a cyclopropyl ring is considered optimal and is featured in many clinical fluoroquinolones (Figure 1.1). [5 33 36] Levofloxacin is unique in this manner due the presence of a 1,8-(2-methyl)-morpholone ring system (Figure 1.1), which improved activity against *P. aeruginosa* and proved to be a useful modification to treat ocular and respiratory infections. [5 16] Trovafloxacin possess a 2,4-difluorophenyl group at N1 (Figure 1.1), which enhances potency compared to norfloxacin, however not to the same extent as the cyclopropyl group. [13] More hydrophobic groups have also been studied, such as an N1-*tert*-butyl group from studies at Bristol-Myers showed promising Gram-positive activity. [37]

Perhaps the most diversified position of the fluoroquinolone scaffold is the C7 position, which often features a nitrogen heterocycle. A general trend is that a 5-

membered aliphatic heterocycle containing a peripheral amine increases potency against Gram-positive bacteria, while a piperazinyl side chain increases potency against Gram-negative bacteria. [25] It has been demonstrated in compounds such as sparfloxacin and grepafloxacin (Figure 1.3) that small alkyl substituents on piperazine or pyrrolidine side chains grant pharmacokinetic advantages, such as increased solubility, longer half-life, and enhanced Gram-positive activity. [13] Similarly, azabicyclic structures such as those featured on moxifloxacin and trovafloxacin (Figure 1.3) have demonstrated enhanced Gram-positive activity. [38]

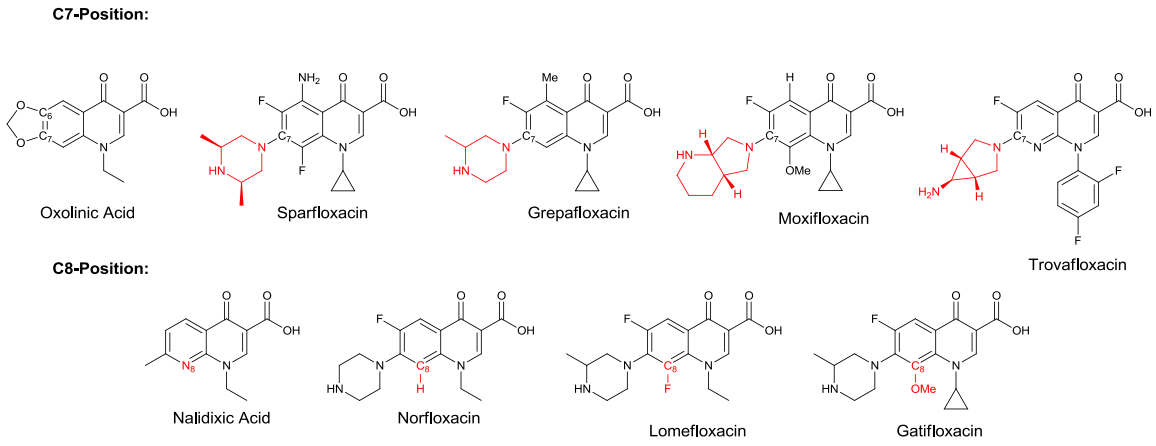

Figure 1.3: Diversification of the C7- and C8-positions of the fluoroquinolone scaffold.

Substitution of groups on the C8-position of the fluoroquinolone scaffold has been extensively explored. One of the original modifications to the 1,8-napthyridone nalidixic acid (Figure 1.3) was the removal of the 8-heteroatom along with modifications to C6 and C7, resulting in oxolinic acid (Figure 1.3) which possessed better inhibitory activity against *E. coli*. [39] This modification was also present in the first fluoroquinolone norfloxacin. Substitution of halogens onto the C8-position, such as the 8-fluorine in

lomefloxacin (Figure 1.3), have been shown to expand fluoroquinolone activity in anaerobic bacteria, but unfortunately are often found to result in increased instances of phototoxicity. [13] An 8-methoxy group also improves activity against anaerobes and has a lower propensity to aggravate phototoxicity than 8-halogen groups. [13] Many clinically used recent fluoroquinolones such as moxifloxacin and gatifloxacin feature an 8-methoxy group (Figure 1.3). It has also been shown that the structure at the 8-position can increase interactions with other drugs, such as theophylline in the case of the 8-nitrogen heteroatom featured in trovafloxacin (Figure 1.3). [27]

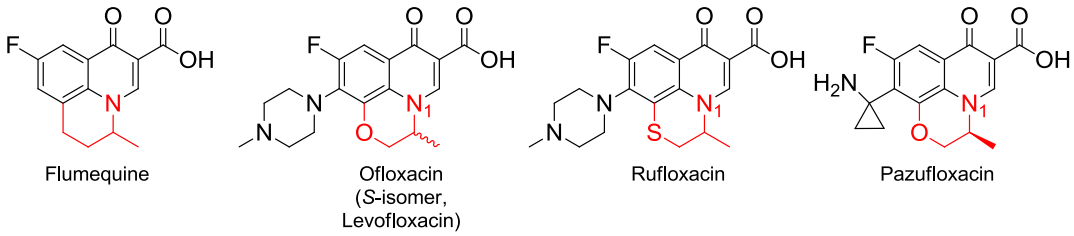

Figure 1.4: Examples of N1-C8 linked fluoroquinolones

Studies in linking the N1-C8 position of the fluoroquinolone scaffold began with 1st-generation quinolone flumequine (Figure 1.4), which had activity in murine models of urinary tract infections and *P. mirabilis*-induced prostatitis. [40] Ofloxacin has a racemic 1, 8-methylmorpholine system (Figure 1.4), and was shown to possess potent activity against several *Pseudomonas* pathogens as well as promising Gram-positive activity and was employed against ocular infections. [41] However, it was later discovered that the (*S*)-isomer of ofloxacin, levofloxacin, was the active component and able to target *E. coli* cells. [42] Other N1-C8-linked fluoroquinolones include rufloxacin, and pazufloxacin

(Figure 1.4), which exhibit less potent activity against *E. coli* bacteria in the absence of protein synthesis. [43] The C5-position has been shown to affect Gram-positive activity, likely through steric interactions. [25] Small groups are tolerated in this position, such as methyl (grepafloxacin) and amine (sparfloxacin) groups, but for the majority of clinical fluoroquinolones a C5-hydrogen is retained in order to maintain Gram-negative activity.[13]

1.3: Structure and Function of Type-II Bacterial Topoisomerases

The enzyme targets of fluoroquinolones are type-II bacterial topoisomerases, DNA gyrase and topoisomerase IV. [44] [45] The majority of bacteria possess both enzymes, and each performs essential roles in regulating the superhelical density and separation of chromosome strands during bacterial DNA replication, which is depicted in Figure 1.5 (left). [46] [47] [48]

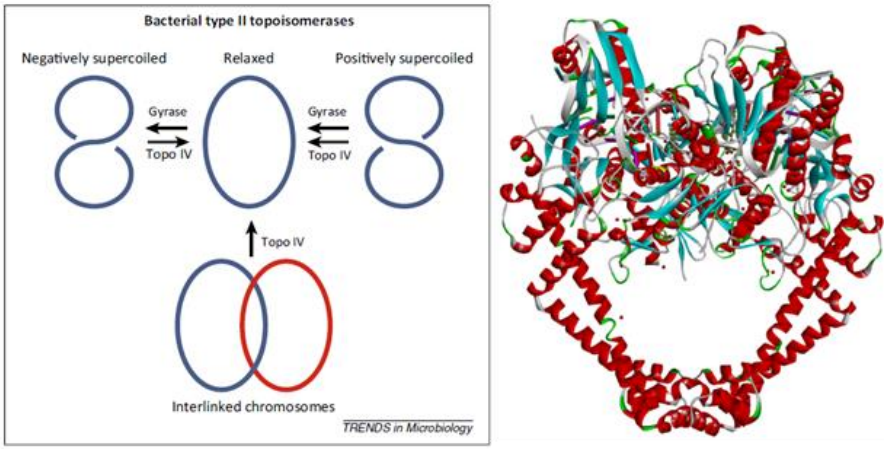

Figure 1.5: **Left**-The regulation of superhelical topology by DNA Gyrase and topoisomerase IV (adapted from Redgrave et. al. [49]). **Right**- ParC of *A. baumannii* topoisomerase IV (adapted from PDB: 2XKK structure) [30]

DNA gyrase and topoisomerase IV are A_2B_2 heterotetramer structures, each composed of two dimeric subunits. GyrA in DNA Gyrase and ParC in Topoisomerase IV (Figure 1.5; right) are the sites of DNA nicking and religation, and GyrB in DNA Gyrase and ParE in topoisomerase IV are the sites of ATP binding and hydrolysis which drives the action of the enzyme. [50] The GyrA/ParC subunits of gyrase and topoisomerase IV contain a tyrosine residue at the catalytic site of DNA cleavage and religation. [45]

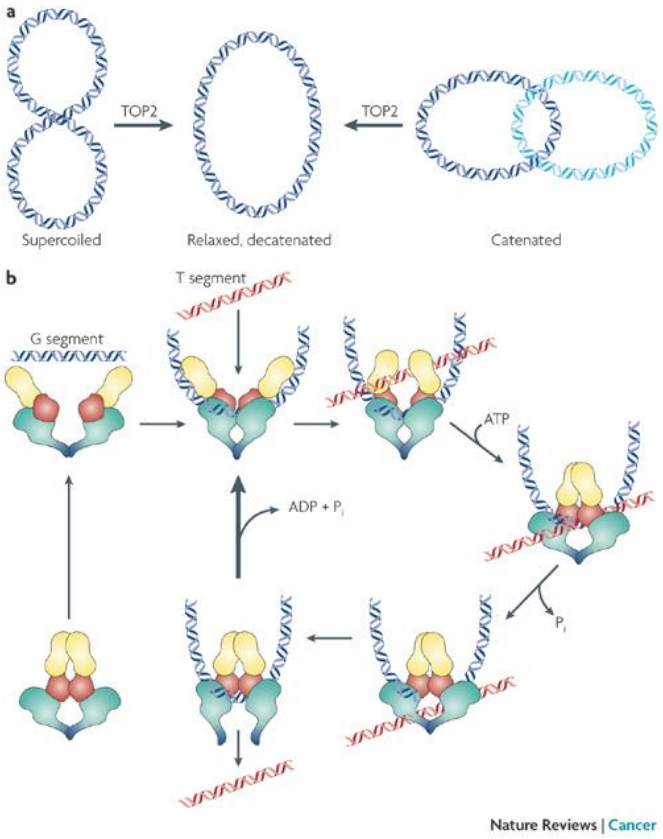

Figure 1.6: ATP-driven mechanism of type-II topoisomerases. DNA binds GyrA/ParC and a pair of single-stranded nicks on each strand of DNA are introduced, creating a transient DNA gate through which a second strand can pass. Superhelical density is regulated and unknotting/untangling of bacterial DNA is performed with DNA Gyrase and daughter chromatids are segregated with Topoisomerase IV. (Adapted from DNA topoisomerase II and its growing repertoire of biological functions. *Nature Reviews Cancer*) [51]

The function of DNA gyrase is the introduction of negative supercoils into positively coiled bacterial DNA to relieve superhelical tension generated during replication (Figure 1.6). [52] DNA gyrase also relieves torsional stress that is accumulated in front of replication forks. [47] [48] [50] Topoisomerase IV, however, is mainly responsible for removing knots and tangles in DNA and is necessary for the separation of daughter chromosomes. [53] In both enzymes a pair of single-stranded nicks on each strand of DNA which are four nucleotide-base pairs apart are generated and covalently bound to catalytic tyrosine residues within the A subunit of each enzyme using a two-metal ion mechanism. [46] [47] [48] [50] [54] This process creates a transient DNA gate through which another chromosome strand is able to pass. Because these enzymes generate two single-stranded nicks they are classified as "type II" topoisomerases. [45]

1.4: Mechanism of Fluoroquinolone Activity

Fluoroquinolones bind and stabilize a ternary complex composed of the bacterial DNA, the topoisomerase, and the fluoroquinolone. In this way, fluoroquinolones act as topoisomerase poison by preventing religation of the DNA nicks caused by topoisomerase IV and DNA gyrase, causing bacteriostasis. [52] This process halts cell growth and replication, and it is reversible upon removal of the fluoroquinolone. It has been found that the binding of some fluoroquinolones to type-II bacterial topoisomerases lead to increases in fragmented DNA in cells, which ultimately leads to rapid cell death. [55] [56] The mechanism of rapid lethality by fluoroquinolones is as yet poorly understood.

The site of fluoroquinolone binding is on the interface region of the ternary complex between the bacterial DNA and Helix-4 of GyrA/ ParC, near the catalytic tyrosine residue. Specifically, previous studies have shown that a primary binding contact

for fluoroquinolones is a Mg-water bridge that anchors the 3,4 β-ketoacid of the fluoroquinolone skeleton onto Helix-4 through coordination with conserved serine and acidic residues (Ser84 and Glu87 in *A. baumannii* topoisomerase IV, for example),[57] as shown in Figure 1.7. [26 58 57b] This binding interaction is complementary to the long-standing observation that the fluoroquinolone β-ketoacid is crucial to drug activity. It must be considered, however that this static image of fluoroquinolone binding is an incomplete representation of the fluoroquinolone binding site. For one consideration, topoisomerases are dynamic proteins and the binding pocket may undergo drastic conformational changes. Additionally, many differences in activity have been observed through modifications of the C7 position of the fluoroquinolone scaffold. It is believed that in some fluoroquinolones the C7-group often binds through the bound DNA of the ternary complex. For example, the secondary amine of the C7-diazabicyclononane of moxifloxacin has been shown to bind through a ribose oxygen (Figure 1.7). Conversely, docking studies have shown that current fluoroquinolones, such as ciprofloxacin and moxifloxacin (Figure 1.7), do not make binding contacts with the ParE region. The work here seeks to characterize and explain some of the reasons for structure-activity relationships of the C7-position. Future chapters will discuss theories of binding between novel fluoroquinolone C7-substituents and the GyrB/ParE region of the ternary complex, in particular a conserved acidic residue (Glu437 in Figure 1.7).

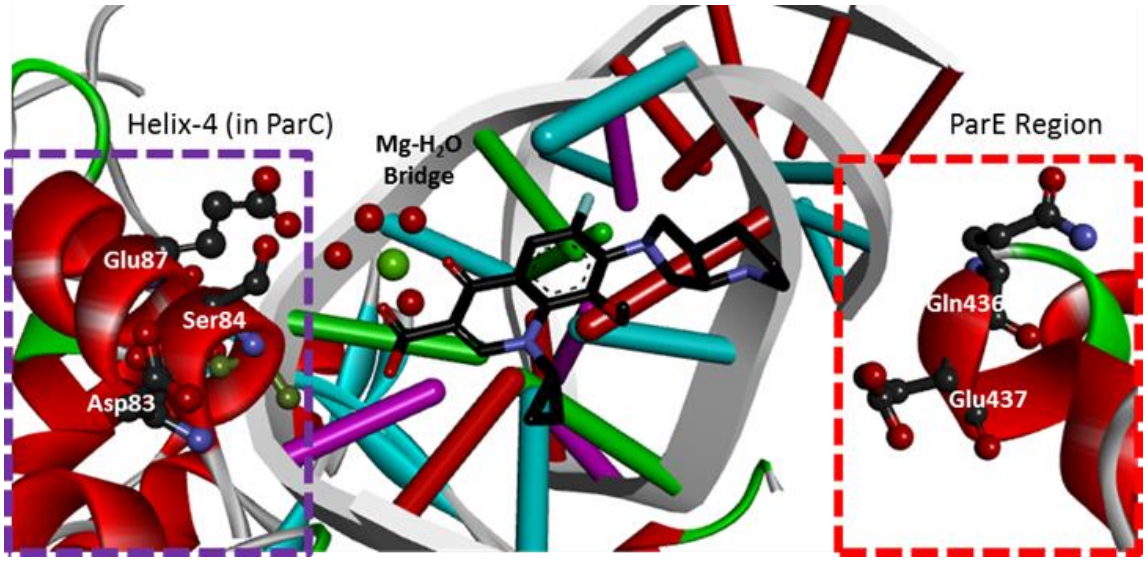

Figure 1.7: Moxifloxacin bound within ternary complex in *A. baumannii* topoisomerase IV via the Mg-water bridge (adapted from 2XKK, Wohlkonig et. al). Other interactions are believed to exist through DNA nucleoside bases and riboses, via interactions through the C7 side chain.

1.5: Mechanisms of Fluoroquinolone Resistance

Resistance ultimately arises in every instance of treatment with antimicrobial agents. The prevalence of antibiotics has resulted in a number of drug-resistant bacteria, including multidrug-resistant (MDR) and extensively-drug resistant (XDR) strains of tuberculosis. As recently as 2012, an estimated 8.6 million new cases of tuberculosis were discovered with a death toll of 1.3 million. [59] Of those cases, 450,000 were MDR infections, which accounted for 13% of the tuberculosis deaths worldwide. [59] The clinical utility of fluoroquinolones has greatly expanded since the 1980's advent of norfloxacin and ciprofloxacin. [60] [61] The increasing clinical use, and possibly overuse, of fluoroquinolones has led to the rising occurrence of fluoroquinolone-resistance in nearly every bacterial species that have been treated. [62] [63] [64] Gram-positive species of note that exhibit high levels of fluoroquinolone resistance are *S. aureus*, a common human skin colonizer [65] and *S. pnuemoniae*, which is common in respiratory infections. [66] [67] The Gram-negative

species *P. aeruginosa* also exhibits high levels of fluoroquinolone-resistance. [10, 68] The known mechanisms of resistance in bacteria can be collected into three categories: target-mediated, plasmid-mediated, and chromosomal-mediated resistance. [69]

Target-mediated resistance (Figure 1.8) arises from point mutations of DNA gyrase and topoisomerase IV. In many cases mutation of either enzyme confers 10-fold resistance to fluoroquinolone agents; however isolates that contain mutations of both DNA gyrase and topoisomerase IV may possess 10 to100-fold resistance to fluoroquinolones. [63 70 46, 71 72 73] As previously mentioned, a key binding interaction between fluoroquinolone agents and type-II topoisomerases is believed to be a Mg-water bridge located on Helix-4 within the A subunit of the enzymes. Concurrent with this theory, mutations to the conserved serine and acidic residues on Helix-4 that bind the Mg-water bridge are found in 90% of clinical isolates of fluoroquinolone-resistant infections.[74 75] The genes that encode for such mutations in GyrA of Gram-negative bacteria group together into a specific region of the genome that is referred to as the quinolone-resistance determining region (QRDR). [76 77] For such mutants, in most cases cellular poisoning by fluoroquinolones via stabilization of the ternary complex is impeded. [78 79 80 81 82 83 84] It has been observed that mutations to the conserved serine residue that helps anchor the Mg-water bridge does not impede the function of the enzyme, however less common mutations to the acidic residue reduces turnover of the enzyme 5 to 10-fold. [78 79 80 85 86] This dissertation will explore methods of overcoming fluoroquinolone-resistance caused by point mutations in the Helix-4 region of GyrA/ParC of topoisomerases. As stated before, such mutations have been linked to the majority of clinically observed fluoroquinolone-resistance, and as of now represent the greatest threat to the clinical use of fluoroquinolones.

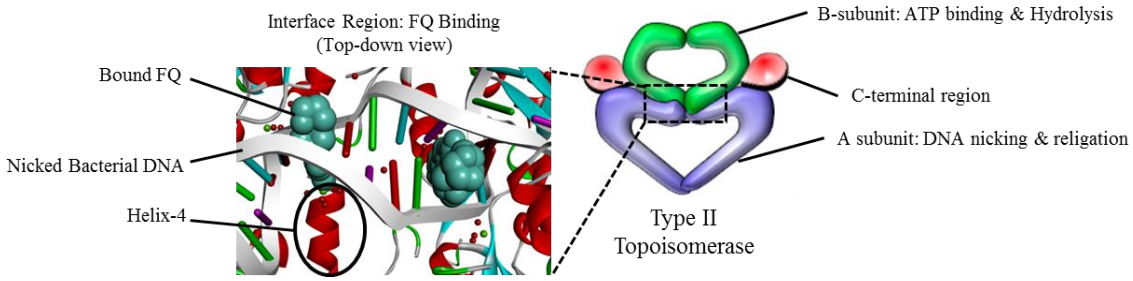

Figure 1.8: The binding site of fluoroquinolones. Point mutations to the Helix-4 region of GyrA/ParC subunits of type-II bacterial topoisomerases represent the greatest threat to the clinical utility of fluoroquinolones. There is evidence of resistance-causing mutations in GyrB/ParE subunits, however as yet these appear to be less prevalent and less able to cause high-level fluoroquinolone resistance. [69]

Plasmid-mediated resistance is a unique challenge because it can be transmuted both generation-to-generation and through bacterial conjugation. The Qnr family of genes has been shown to cause fluoroquinolone resistance by two mechanisms: the reduction of DNA binding to topoisomerases and preventing fluoroquinolones from entering the DNA-enzyme complex. [87] [88] [89] [90] In this way, the downstream products of these genes are able to reduce the number of available intercellular targets of fluoroquinolones and are able to block binding outright. A more targeted mechanism against fluoroquinolones is the ability of certain proteins to modify fluoroquinolones inside the cell. Specifically, an aac(6′)-Ib-cr-variant aminoglycoside acetyltransferase with point mutations that allow it to acylate the basic secondary amine of the norfloxacin or ciprofloxacin piperazine side chain, thus lowering its ability to bind topoisomerase. [91] [92] Finally, the QepA1, and QepA2 are gene families that encode for efflux pumps that remove intracellular fluoroquinolones. [88] [93] [94] Curiously enough, these seem to only be present in human infections.

Mechanistically similar to some forms of plasmid-mediated resistance, chromosomal-mediated resistance influences the penetration of fluoroquinolones into the cell and efflux of drug out of the cell. In Gram-positive species, fluoroquinolones are able to diffuse through the cell wall; this action is opposed by chromosomal-upregulation of MFS-superfamily, ABC and SMR-families of drug efflux pumps. [95] [96] In Gram-negative bacteria cell penetration requires the action of porin transport channels, which can be chromosomally down-regulated, thus decreasing intercellular fluoroquinolone concentration. This form of resistance, however, is less common than plasmid or target-mediated fluoroquinolone resistance. [88] [97] [98] Chromosomal-mediated disruption of fluoroquinolone transport into cells is not a major threat to clinical fluoroquinolone use by itself, yet this mechanism deserves attention because it promotes the development other resistance mechanisms. [99] [100] [101]

1.6: Targeting Human Topoisomerase as a Result of Overcoming Fluoroquinolone Resistance

For many years, bacterial type-II topoisomerases have proven to be valuable targets for antibiotics, in part because the sequences of bacterial type-II topoisomerases are not conserved in mammalian type-II topoisomerases. Specifically, human type-II topoisomerases do not possess serine and acidic residues on Helix-4 with similar positioning to bacterial type-II topoisomerases. Instead, for example, human topoisomerase IIα possesses methionine residues in these positions. A result of this structural difference is that human topoisomerase is unable to coordinate waters within the Mg-water bridge on Helix-4 in the same way that bacterial topoisomerases do. Therefore, human type-II topoisomerases do not form the Mg-water bridge with fluoroquinolones. Previous studies have shown that the structural difference between

type-II bacterial and human topoisomerase is likely the source of specificity for fluoroquinolone action on bacteria.[26] Human type-II topoisomerases, aside from sequence differences, are otherwise macro-structurally similar to bacterial topoisomerases, as shown in Figure 1.9.

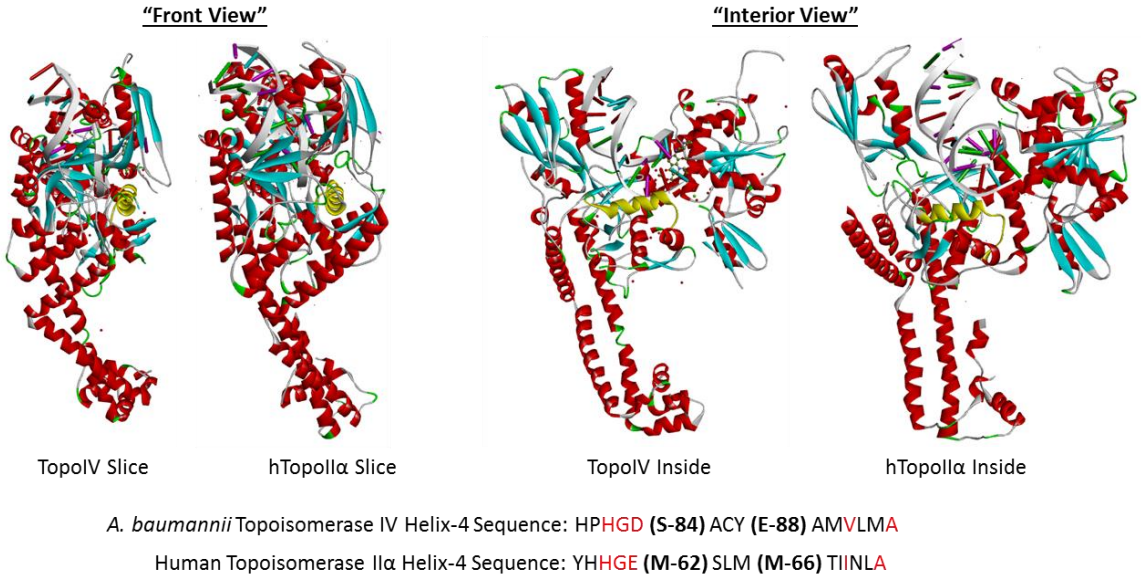

Figure 1.9: Comparison of *A. baumannii* topoisomerase IV (adapted from 2XKK) and human topoisomerase IIα (adapted from 4FM9)[102] both bound to DNA. The central structure Helix-4 is highlighted in gold. Topoisomerase IV is bound to moxifloxacin through the Mg-water bridge. The coordinating acidic residues of the Mg-water bridge in Topoisomerase IV are in bold and numbered, as are the corresponding methionine residues in human topoisomerase IIα. Similarities in sequence are also highlighted in red.

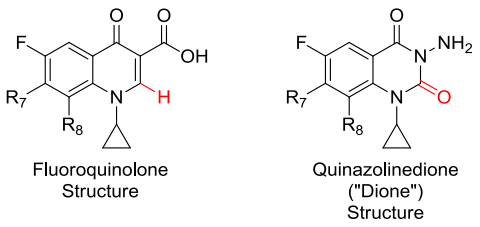

Figure 1.10: General fluoroquinolone and quinazolinediones ("dione") scaffolds (C2-position highlighted in red)

Quinazolinediones (diones) are bacterial type-II topoisomerase inhibitors that are structurally similar to fluoroquinolones, as shown in Figure 1.10. Diones are distinct from fluoroquinolones in that they are able to bind to Helix-4 within the ternary complex, however they do not require the Mg-water bridge to do so. Instead, it is hypothesized that the diones bind to Helix-4 via H-bond donating interaction through the C2-carbonyl (Figure 1.10, shown in red). It has been demonstrated in previous studies that some diones are able to cross over and inhibit human topoisomerase IIα as well as bacterial type-II topoisomerases. The binding interaction through the dione C2-carbonyl is possibly mimicked in Helix-4 of human topoisomerase IIα, thus explaining that ability of diones to cross over and inhibit human enzyme as well as bacterial enzyme. Similarly, it was found that some fluoroquinolones that possess a C7-aminomethylpyrrolidine side chain can also cross over to human topoisomerase IIα.[26] It is believed that crossover activity to human topoisomerase IIα by C7-aminomethylpyrrolidine fluoroquinolones is due to conserved acidic residues in the GyrB region of human topoisomerase IIα that interact with the basic primary nitrogen of the side chain. We therefore sought to mechanistically understand the binding of the fluoroquinolone core in conjunction with the C7-aminomethylpyrrolidine group. This understanding is crucial to creating fluoroquinolones that are capable of specifically targeting bacterial type-II topoisomerases over human type-II topoisomerases. This will be an important step to the C7-aminomethylpyrrolidine side chain achieving clinical utility.

CHAPTER II: STATEMENT OF PURPOSE

Drug-resistance is becoming more pervasive in bacterial infections. A particularly distressing trend is the rise of drug-resistance in several pathogens that are responsible for the majority of hospital infections, which have been dubbed the "ESKAPE" pathogens (*Enterococcus faecium, Staphylococcus aureus, Klebsiella pneumoniae, Acinetobacter baumannii, Pseudomonas aeruginosa,* and several *Enterobacter* species).[103] This fact represents a dire and immediate threat to many populations: the elderly, the very young, and individuals with compromised immune systems. More importantly, drug-resistant bacteria represent a critical world-wide threat due to the spread of MDR and XDR bacterial strains in developing countries. These "hotspots" of emerging drug-resistant bacteria are connected to all other countries through international travel. Therefore it is imperative that methods to halt and reverse the increasing emergence of drug-resistant bacteria be found.

When bacterial colonies are treated with antibiotics, genetic random chance and evolutionary forces facilitate the emergence of viable, drug-resistant bacteria. A factor that contributes heavily to this trend is the mutant selection window (MSW), which is a range of antibiotic agent dosing between the minimum inhibitory concentration (MIC) and mutant prevention concentration (MPC). Clinical practice commonly places antibiotic dosing regimens to within the MSW. [104] Antibiotic dosing above the MIC for wild-type cells is required to lower an infectious bacterial population and suppress and/or cure the infection. Unfortunately this level of dosing allows for the emergence of drug-resistant species variants. [105] Dosing at or above the MPC may prevent the emergence of such bacterial subpopulations but this is often within the range of human toxicity of the antibiotic agent. It is imperative that the prior research practice of searching for potent bactericidal drugs be redirected towards a focus on generating new antibiotics that when used in the clinic have been designed specifically for the simultaneous rapid killing of

wild-type and drug-resistant strains with limited selection for new resistant mutants. Rapid killing is likely to be necessary to best suppress the emergence of drug-resistance.

The investigations described herein where undertaken with the goal of overcoming the most common cause of fluoroquinolone-resistance in bacteria: target-mediated resistance in the form of substitutions to the fluoroquinolone-binding Helix-4 amino acids of DNA gyrase and Topoisomerase IV. Previous studies have demonstrated the importance of a magnesium-chelated water bridge that anchors fluoroquinolones into the ternary complex. [26] Substitutions to Helix-4 amino acids that disrupt the Mg-water bridge interaction have been found in the vast majority of fluoroquinolone-resistant bacterial subpopulations. [75] It is therefore hypothesized that a fluoroquinolone-type agent that is able to use the Mg-water bridge as a binding interaction and is able to form additional binding contacts independent of the Mg-water bridge would be able to simultaneously target both wild-type and common fluoroquinolone-resistant bacteria. To test this hypothesis, two major structural modifications to fluoroquinolones at positions separate from the Mg-water bridge connection for the fluoroquinolone scaffold (the 3,4 β-ketoacid structure) were planned: modifications to the 5,6-position and the 7-position of the fluoroquinolone.

In the first study, the attempt was made to generate fluoroquinolones and diones with a novel 5,6-conjugated phenyl system to promote π-stacking binding interactions with bacterial DNA as a way of increasing diminishing the importance of the Mg-water bridge for fluoroquinolone binding and increasing the overall binding affinity of the diones. In theory, the activity of fluoroquinolones and diones that are able to exploit binding contacts on bacterial DNA within the ternary complex would be less affected or unaffected at all by mutations that disrupt the Mg-water bridge. Such a concept was supported by *in silico* binding studies. As a continuation of this concept, a 4,5-pyrrimidine modification of the fluoroquinolone and dione scaffold was conceived. It was believed such a modification that overlapped with the 3,4 β-ketoacid part of the molecule

would still allow for anchoring through the Mg-water bridge while supporting a π-stacking interaction with bacterial DNA, and thus such compounds would be able to inhibit fluoroquinolone-resistant topoisomerases. Unfortunately, though a great deal of time and effort was absorbed by these endeavors and interesting synthetic methods were employed, no successful synthetic routes to the 5,6-phenyl fluoroquinolone core, the 5,6-phenyl dione core, or the 4,5-pyrrimidine core were discovered. However, the synthetic methodology that was employed over the course of these efforts will be described with the hope that such chemistry will be of use to future studies.

During the course of this study, fluoroquinolone derivatives with a C7-aminomethylpyrrolidine side chain were shown to be able to maintain activity against common fluoroquinolone-resistant bacterial type-II topoisomerase by overcoming Helix-4 amino acid substitutions that are disruptive to Mg-water bridge formation. It was observed that a fluoroquinolone with an 8-methoxy core and a C7-aminomethylpyrrolidine group maintained activity against wild-type enzyme and two common fluoroquinolone-resistant Helix-4 mutants of *B. anthracis* Topoisomerase IV. Then, in the second study, a panel of fluoroquinolone featuring a diversity of core structures and a C7- aminomethylpyrrolidine side chain were synthesized in order to explore the role of core structure for novel interactions through the C7 position. Initially, catalytic inhibition and poisoning activity of the fluoroquinolone derivatives was first measured in purified wild-type *E. coli* DNA gyrase with a supercoiling assay and DNA cleavage assay, respectively. Inhibition of *E. coli* topoisomerase IV was tested with a DNA decatenation assay. To test for crossover activity, the DNA decatenation and DNA cleavage assays were repeated with human topoisomerase IIα. Further studies were performed with *tolC* KO *E. coli* and wild-type *M. smegmatis* cells and several forms of *tolC* KO *E. coli* strains with fluoroquinolone-resistant mutations to Helix-4.

In the third study, structural derivatives of the C7-aminomethylpyrrolidine side chain were attached to the N1-cyclopropyl C8-methoxy fluoroquinolone core (this core is

present in the clinical fluoroquinolone moxifloxacin) in order to explore the structural requirements of the C7-aminomethylpyrrolidine group to impart activity against fluoroquinolone-resistant topoisomerases. These studies together constitute a significant contribution to the knowledge base of fluoroquinolone-topoisomerase interactions and will serve to direct future studies to overcome target-mediated fluoroquinolone-resistance in bacteria.

CHAPTER III: ATTEMPTS TO GENERATE INTERCALATIVE TRICYCLIC FLUOROQUINOLONE AND DIONE CORES

3.1: Introduction

The principle binding contact of fluoroquinolones in the topoisomerase interface region is a Mg-water bridge. This Mg-water bridge is composed of a divalent magnesium atom chelated to the 3,4 β-ketoacid of the fluoroquinolone skeleton. The magnesium is also bound to four water molecules, which themselves are bound to a conserved serine and either aspartate or glutamate residues on Helix-4 of type-II bacterial topoisomerases (Figure 3.1). As previously mentioned, there exist point mutations of the genes that code for bacterial type-II topoisomerase enzymes which cause amino acid substitution of the Helix-4 residues that participate in the formation of the Mg-water bridge. When these substitutions occur, the formation of the Mg-water bridge is compromised, resulting in fluoroquinolone resistance. Mutations that cause these substitutions are highly prevalent in fluoroquinolone-resistant bacteria. My general approach to overcoming this mechanism of fluoroquinolone resistance was to generate a modified fluoroquinolone scaffold capable of binding via the Mg-water bridge, yet also capable of exploiting novel binding interactions separate from the Mg-water bridge. It was hypothesized that such a compound would be able to bind within the ternary complex regardless of disruption to the Mg-water bridge binding contact. This line of reasoning led to the conceptualization of a tricyclic fluoroquinolone with a 5,6 conjugated phenyl system.

During the course of these studies a crystal structure of the clinical fluoroquinolone moxifloxacin bound to topoisomerase IV of *A. baumannii* was published by Wohlkonig et. al. This structure showed that the fluoroquinolone binding site, which is within a type-II topoisomerase-generated DNA dual-strand nicked site, contains a nucleoside base that is well oriented to form a π-stacking interaction with a theoretical 4,5- or 5,6-position aryl extension of the fluoroquinolone scaffold. This is shown in

Figure 3.1. With this concept in mind several iterations of 5,6-aryl motifs were generated for docking studies using SYBYL software.

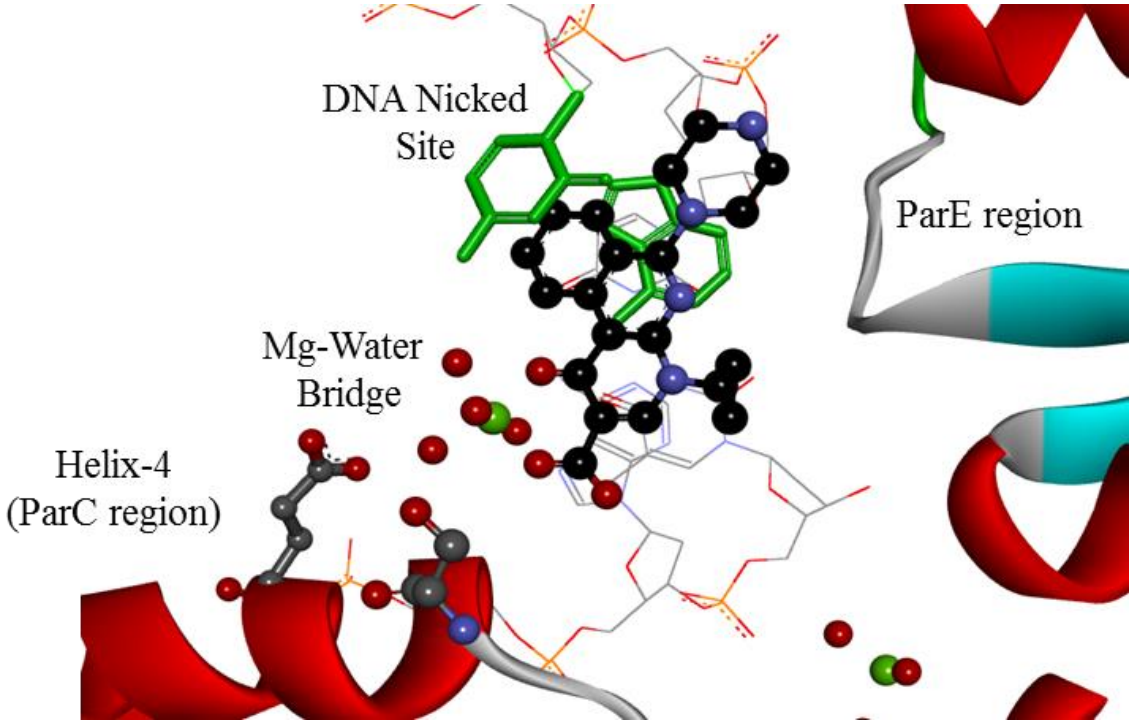

Figure 3.1: Initial *in silico* modeling of 5,6-phenyl quinolone (black-ball and stick) forming a pi-stacking interaction with bound DNA (nucleoside residues highlighted in green-stick) within drug-enzyme-DNA ternary complex. Docking study performed with Wohlkonig et. al. [30] 2XKK *A. baumannii* structure.

3.2: Goals of the Study

There were three goals in this first study: 1) to generate a series of 5,6-phenyl quinolones, 2) to generate a series of 4,5-pyrimidine fluoroquinolones, and 3) to generate a series of 5,6-phenyl diones. These concepts are depicted in Figure 3.2. The compounds from each of the three series would then be tested for ability to inhibit purified wild-type and fluoroquinolone-resistant bacterial topoisomerases and to test the bacteriostatic/ bactericidal activity of these compounds in whole-cell assays with wild-type and fluoroquinolone-resistant mutant bacteria.

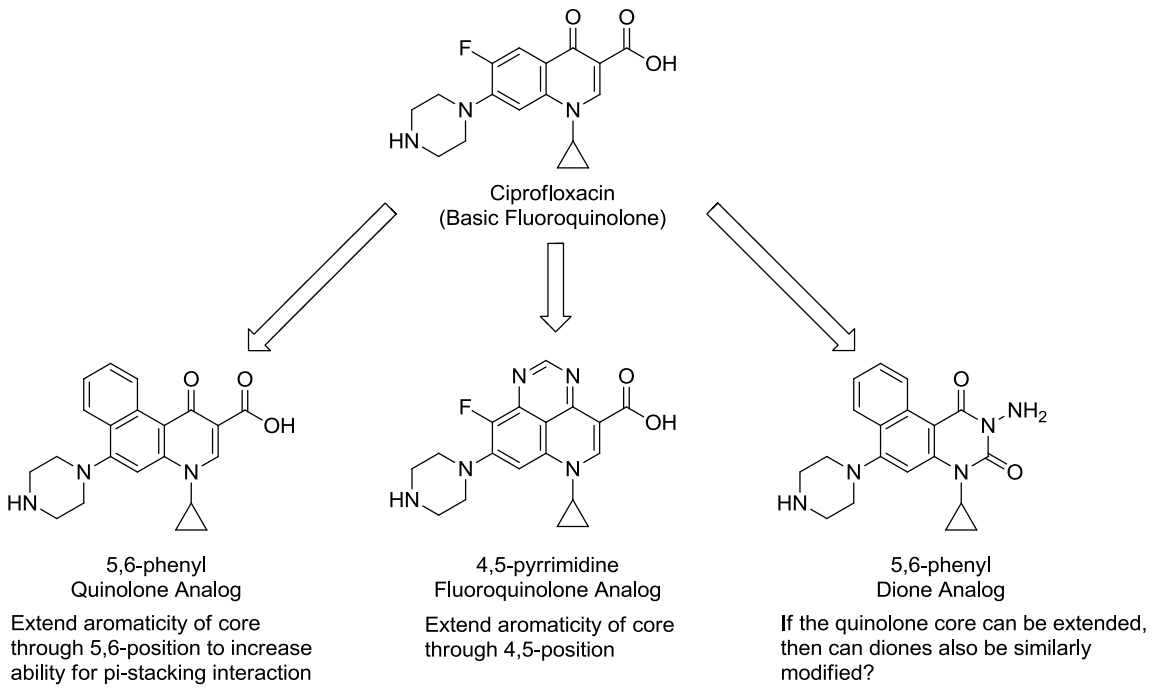

Figure 3.2: Proposed modifications to the fluoroquinolone and dione scaffolds to extend aromatic character of compound and increase compound ability to form pi-stacking binding contacts.

Attempts to overcome fluoroquinolone resistance via point mutations led the search for novel binding contacts independent from Helix-4. The recent Wohlkonig[30] and

Laponagov[106] crystal structures depicted the fluoroquinolone binding orientation to anchor to Helix-4 through the Mg-water bridge and the aromatic core structure partially intercalating into bound bacterial DNA. It was believed that aromatic extensions of the fluoroquinolone skeleton through the 4,5- and 5,6-position to exploit π-stacking interactions with nucleoside base rings. If this proved to be possible, it would be likely that the dione skeleton could be similarly augmented to increase binding potential, which was already believed to be independent of the Mg-water bridge. We hypothesized that if dione binding potential could be increased, then dione activity could be improved.

3.3 Docking Studies with Topoisomerase IV and Tricyclic Fluoroquinolones and Diones

The investigation of tricyclic fluoroquinolones and diones began with docking studies of hypothetical compounds possessing an aryl conjugation on the 5,6- and 4,5-position, which is shown in Figure 3.3. Synthetic planning for the 5,6-phenyl quinolone led to the necessity of an 8-nitrogen. This realization led to the conceptualization of a 1,8-napthyridone structure as the basis for the 5,6-phenyl quinolone, hereafter called the 5,6-phenyl napthyridone. Using the SYBYL docking software, these compounds were docked into the 2XKK crystal structure of *A. baumannii* topoisomerase IV bound to the known clinical fluoroquinolone moxifloxacin. The composite score for binding affinity, termed CScore and referred to as "Score" in Figure 3.3, is the result of an algorithm that measures several parameters including steric clash, entropic advantage, hydrophobic interactions, potential for H-bond donating and accepting, and potential for pi-stacking interactions. Higher scores represent increased binding affinity. Overall, all compounds were found to dock comparably well to known fluoroquinolone and dione structures.

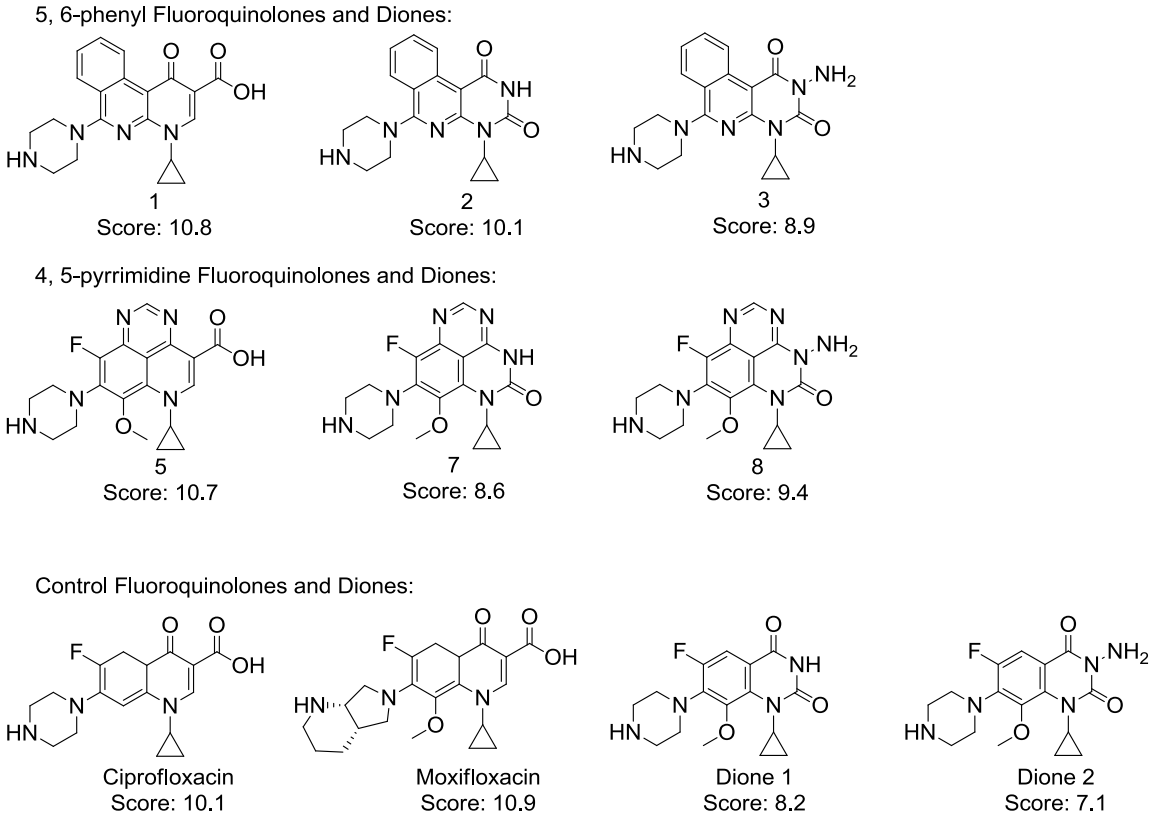

Figure 3.3: Docking scores of hypothetical fluoroquinolone and dione skeletons with aryl extensions of their core structure in order to form intercalative/ π-stacking interactions with nucleoside bases, along with known fluoroquinolone and dione structures as controls. Each compound was docked into the 2XKK crystal structure. The "Score" is a composite CScore generated by SYBYL.

Though advantageous pi-stacking interactions were not strongly reflected in the docking scores of the 4,5-pyrimidine or 5,6-phenyl napthyridones, the fact that they were able to dock with comparable affinity to the fluoroquinolone-binding pocket as known fluoroquinolone and diones validated the concept of extending the fluoroquinolone and dione skeletons to an aryl-tricyclic center as a novel modification that could be accommodated in the ternary complex. Furthermore, the diones containing aryl extensions of the core structure were found to have slightly improved binding affinity. With this knowledge in hand, attempts were undertaken to synthesize the respective core structures shown in Figure 3.4.

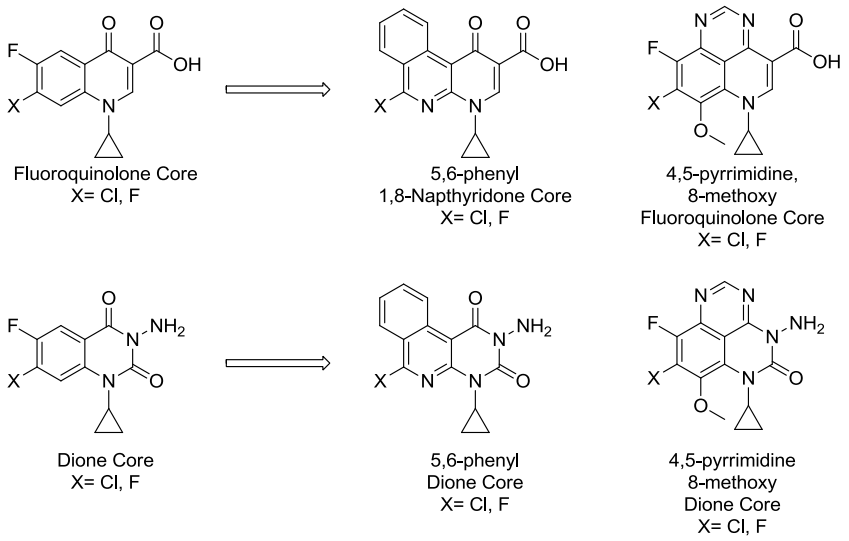

Figure 3.4: Proposed modifications to fluoroquinolone and dione drug skeletons. Once core structures had been made it was believed that side chains would be facile to attach and thus the compounds could be diversified as required.

3.4: Attempts to Synthesize 5,6-phenyl Napthyridone, 4,5-Pyrimidine Fluoroquinolone, and 5,6-phenyl Dione Cores

The efforts to synthesize a 5,6-phenyl napthyridone core began with analyzing established methods for creating fluoroquinolones. Shown in Scheme 1 is the conventional synthetic route to a basic fluoroquinolone core structure.[107] In this methodology 2,4,5-trifluorobenzoic acid is converted to an acyl chloride **2** and then acylated with ethyl lithium malonate to generate a β-ketoester **3**, which will later form the crucial 3,4 β-ketoacid of the fluoroquinolone skeleton. The acidic methylene of the β-ketoester then undergoes aldol condensation with triethylorthoformate to form **4** with a bridging ethylene between carbonyls. The ethylene ethoxide of **4** is then substituted with an appropriate amine; in the case of this fluoroquinolone cyclopropylamine is used. The extended head group undergoes base-mediated ring closure to complete the fluoroquinolone "head group" in **5** and the ester is subsequently removed with strong acid

and heat, thus completing the fluoroquinolone core structure that can then be functionalized at the C7-position with an appropriate side chain.

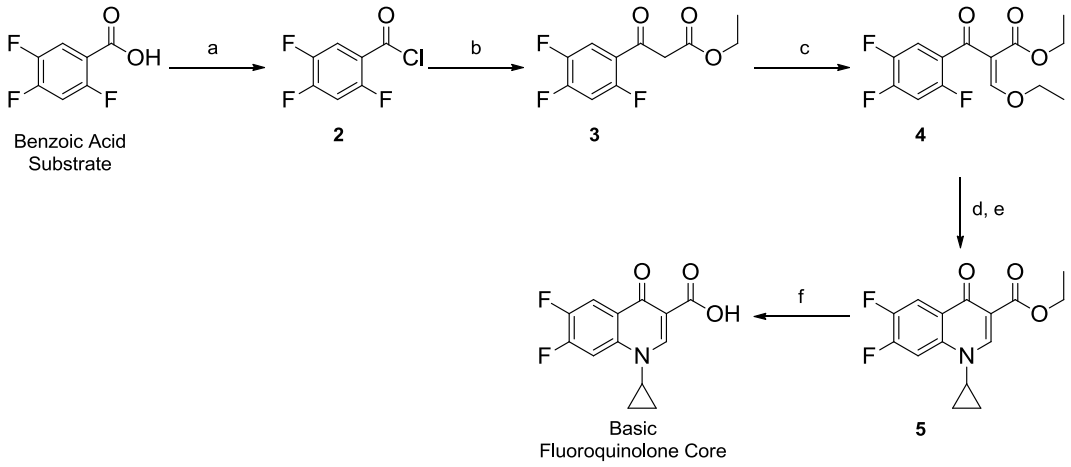

Reagents and Conditions: (a) $(COCl)_2$, DMF, CH_2Cl_2; (b) $(CO_2Et)_2CH_2Li_2$, THF; (c) $HC(OEt)_3$, Ac_2O; (d) cyclopropylamine, t-BuOH; (e) t-BuOK, t-BuOH; (f) 6M HCl, heat

Scheme 3.1: Typical synthesis of basic fluoroquinolone core structure prior to side chain addition.[107]

It was believed that an appropriate bicyclic acid could be purchased or synthesized and then established methodology to generate fluoroquinolones would provide the core structure for a new set of 5,6-phenyl fluoroquinolones diversified at the C7-position as desired. A search of the literature furnished a three-step, single-flask process to convert commercially available homophthallic acid to 1,3-dichloroisoquinolone.[108] Some experimentation with this procedure eventually produced methodology to quickly generate the dichloroisoquinolone that could then be selectively acylated with very high efficiency. The process for this route is depicted in Scheme 3.2, which also shows the divergent synthetic methodology planned to generate the 5,6-phenyl napthyridone compounds and later the dione compounds.

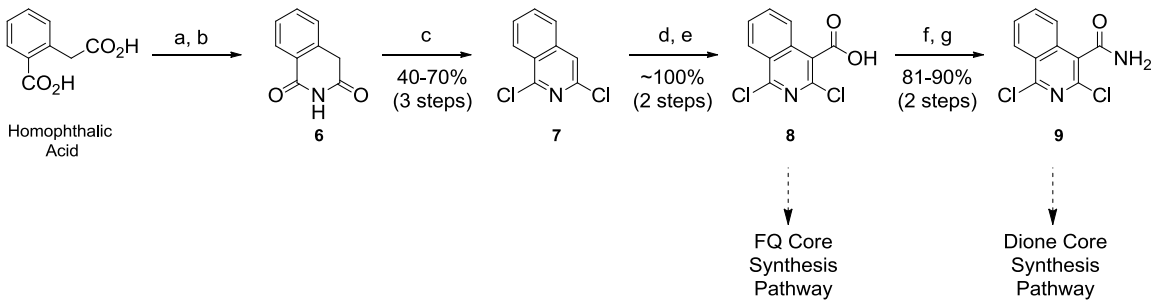

Reagents and Conditions: (a) NH_4OH, heat; (b) 1,2-dichlorobenzene, 200°C; (c) $PhP(O)Cl_2$, 160°C; (d) LDA, THF/hexanes, -78°C; (e) CO_2, THF/hexanes, -78°C - 25°C; (f) $SOCl_2$, DMF, Toulene 80°C; (g) NH_4OH, CH_2Cl_2, 0°C - 25°C

Scheme 3.2: Synthesis of 5,6-phenyl napthyridone and dione precursors.

Synthesis of both the 5,6-phenyl napthyridone and dione precursors began with amidation of homophthalic acid in heated ammonium hydroxide. The amides were then cyclized to the isoquinolone dione **6** in 1,2-dichlorobenzene at 200°C. In a second reaction in 160°C phenylphosphonic dichloride, the imide carbonyls were dually substituted with chlorine and the ring became aromatic to give the dichloroisoquinolone **7**. Yields for these initial three steps were moderate and the process did not require any chromatographic purification. Carboxylation of the C4-position was carried out in a two-step process adapted from work by Laeckmann et. al.[109] The C4-position of the isoquinolone was selectively lithiated using lithium diisopropylamide at -78°C. This allowed C4 to serve as a nucleophilic attachment point for a carboxylate provided in the form of carbon dioxide gas in the subsequent step. Through many iterations of this reaction it was found that quantitative yields of the isoquinolone-carboxylate **8** could be reproducibly achieved. Thus providing the nicotinic acid derivative upon which the fluoroquinolone head group could theoretically be built, as shown in Scheme 3.3. It was anticipated that the C4-carboxylate could be converted to the β-ketoester **10**, the methylene of which could then undergo substitution to form the 2,3-dicarbonylethylene system of the head group in **11**. The ethoxide could then be replaced with an

appropriately substituted amine, in this case cyclopropylamine, and the head group could then be closed with strong base to form **12**. Hydrolysis of **13** with strong acid would furnish the 5,6-phenyl napthyridone core **14**, which could then be substituted appropriately at the C7-position. In both the case of the head-group closure and substitution of the C7-position it was believed that the nitrogen *ortho* to the isoquinolone ring chlorines would facilitate the S_NAr reaction required in the subsequent synthetic steps. This has been demonstrated in established synthetic methodology to produce previous 1,8-napthyridones.

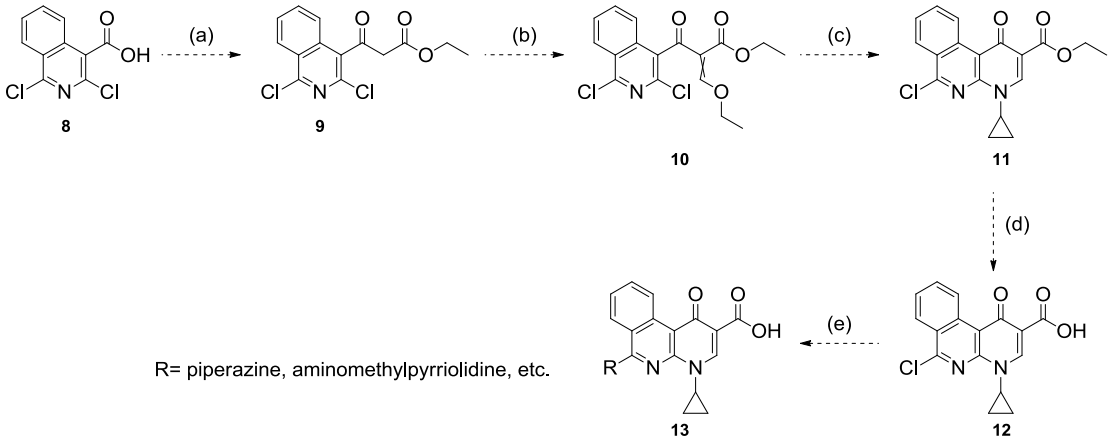

Reagents and Conditions: (a) oxalyl chloride, ethyl potassium malonate, triethylamine; CH_2Cl_2 (b) triethylorthoformate, acetic anhydride (c) cyclopropylamine, strong base (d) conc. HCl (e) side chains, TEA or DIPEA; DMSO

Scheme 3.3: Proposed synthesis of 5,6-phenyl napthyridone derivatives, following established methodology for creating many fluoroquinolone cores.

Unfortunately, functionalization of the 4-carboxylate in **8** was not achieved as planned using established protocols. Repeated attempts to form a 4-malonate system in one step from **8** with ethyl potassium malonate or diethyl malonate elicited either no reaction or highly complex inseparable product mixtures. Eventually a different four-step, two-pot path to the C4 β-ketoester **10** via aldol coupling through the methyl ketone intermediate **15** was employed, as depicted in Scheme 3.4. However, synthetic methods

to progress from the C4 β-ketoester to the completed napthyridone core were not discovered. It was hypothesized that the synthetic dead end was caused by steric hindrance of the ketoester methylene position. In the C4-β-ketoester **10**, the ketoester methylene is sterically blocked by both the conjugated phenyl system of the isoquinolone and by the chlorine *ortho*- to the ketoester. Attempts to functionalize the methyl ketone **15** with more advanced carbonyls resulted in no reactions. Though other methodology was available for synthesis of the 5,6-phenyl napthyridone core, it was decided that research efforts should be redirected towards the second route to novel fluoroquinolone scaffold, the 4,5-pyrimidine fluoroquinolone core.

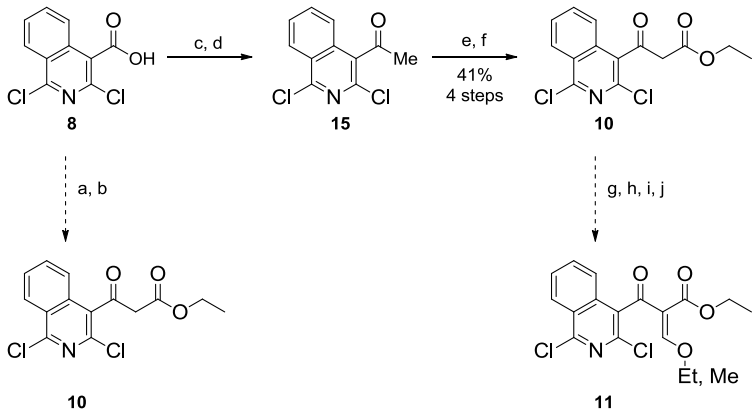

8 **15** **10** **10** **11**

Reagents and Conditions: (a) oxalyl chloride, ethyl potassium malonate with TEA or (b) diethyl malonate and TEAor DIPEA; CH_2Cl_2 (c) Thionyl chloride, DMF; toluene,80°C (d) MeLi, NaI; CH_2Cl_2, -80°C (e) LiHMDS; THF, -78°C (f) Ethyl chloroformate; THF, -78°C - room temp.(g) triethylorthoformate; acetic anhydride 90-150°C or (h) NaH; THF 0°C - room temp. or LiHMDS; THF 0°C-room temp. followed by triethylorthoformate or (i) triethylorthoformate 80-130°C or (j) formaldehyde, TEA, water, methanol 0°C - room temp.

Scheme 3.4: Attempts to progress in the synthesis of the 5, 6-phenyl napthyridone core from the C4 β-ketoester dichloroisoquinolone.

Attempts to extend the fluoroquinolone aromatic center through the 4,5-position by generating the 4,5-pyrimidine fluoroquinolone core **25** began with a known synthetic

pathway to generate a C5-amino fluoroquinolone core **23** as shown in Scheme 3.5. In this methodology, a commercially available N1-cyclopropyl, C8-methoxy fluoroquinolone core is nitrated in the 5-position using potassium nitrate in cold sulfuric acid to produce **21**. The C3-carboxylic acid is then protected as the methyl ester to give **22** using dimethylsulfate in refluxing acetone. The C5-nitro group is then reduced to an aniline **23** under a hydrogen atmosphere using palladium in charcoal as a catalyst. It was believed that a C5-aniline and C4-carbonyl carbon could be cyclized by undergoing condensation with formamide to create the desired 4,5-pyrimidine in **24**. After several attempts this indeed was moderately successful by using formamide and sulfuric acid in heated dimethylacetamide to cyclize the C4-carbonyl to the C5-aniline, thereby forming the extended aromatic core in **24**. This was a very encouraging result as it was the first successful iteration of an extended fluoroquinolone aromatic system produced by our efforts. However, the 4,5-pyrimidine ring proved to be too unstable and was hydrolyzed in the strongly acidic or basic conditions required to remove the 3-methyl ester from **24**. Strangely, all attempts to generate the 4,5-ring with the C3-acid proved unsuccessful. At this point, the next steps to overcome this problem would have been to employ a more labile carboxylate protecting group to facilitate subsequent removal. However, another issue is that the S_NAr conditions usually employed to attach the C7-side chain are very nucleophilic and may also have compromised the stability of the 4,5-pyrimidine linkage. Because of these concerns at the time, this portion of the project was abandoned.

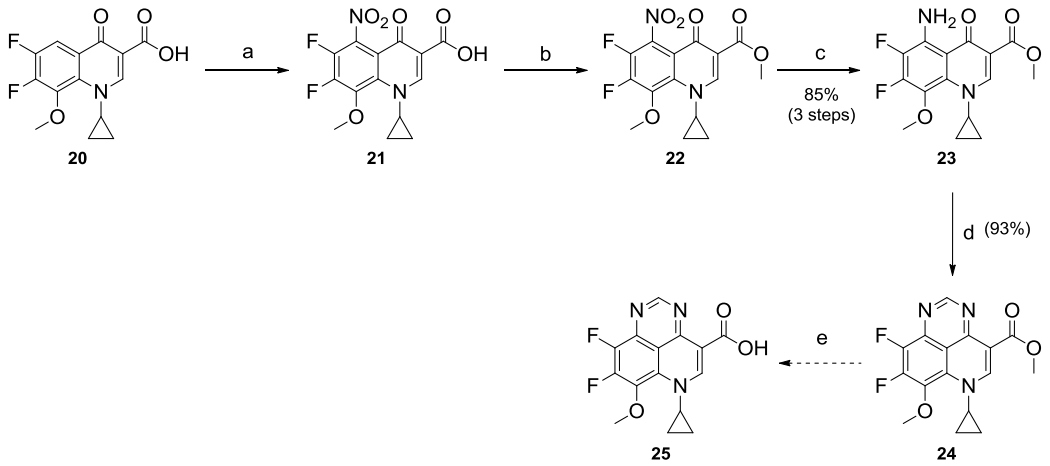

Reagents and Conditions: (a) potassium nitrate; H_2SO_4, 0°C (b) dimethylsulfate, potassium carbonate; acetone, reflux (c) hydrogen atmosphere, Pd/C; ethanol:benzene 2:1 (d) formamide, H_2SO_4; toulene or DMA, 80°C (e) HCl or LiOH; water:MeCN 1:1

Scheme 3.5: Synthesis of the 4,5-pyrimidine fluoroquinolone core.

A series of 5,6-phenyl dione derivatives was pursued as an extension of this study because diones are topoisomerase inhibitors that are distinct from fluoroquinolones in that dione binding is inherently not affected by Helix-4 substitutions that disrupt the formation of the Mg-water bridge. Previous studies with diones possessed equipotent activity against wild-type and fluoroquinolone-resistant DNA gyrase and topoisomerase IV, albeit with 10-fold or lower efficacy than fluoroquinolones.[110 26 79] Therefore, diones were promising lead structures, and the 5,6-phenyl modification was expected to increase intercalative or pi-stacking binding within the ternary complex which would translate into increased equipotent inhibition of wild-type and fluoroquinolone-resistant type-II bacterial topoisomerases. Unable to find a successful path to the 5,6-phenyl napthyridone core **14**, efforts were then focused on synthesis of the 5,6-phenyl dione cores **18** and **19**. In the proposed methodology, as shown in Scheme 3.6, the C4-amido-1,3-dichloroisoquinolone **9** is converted to a C4-carbonyl-isocyanate **16**. The carbon center of the isocyanate then undergoes nucleophilic substitution with cyclopropylamine to

generate an imide-amine chain in **17**, which is then cyclized to form the dione head group in **18**. This provides the first dione core in which the 3-nitrogen can then undergo amination to provide the second dione core **19**. In this way, it was proposed that analogs of the N3-hydrogen and N3-amine dione cores could be provided. The cores could then be modified with C7-side chains as required.

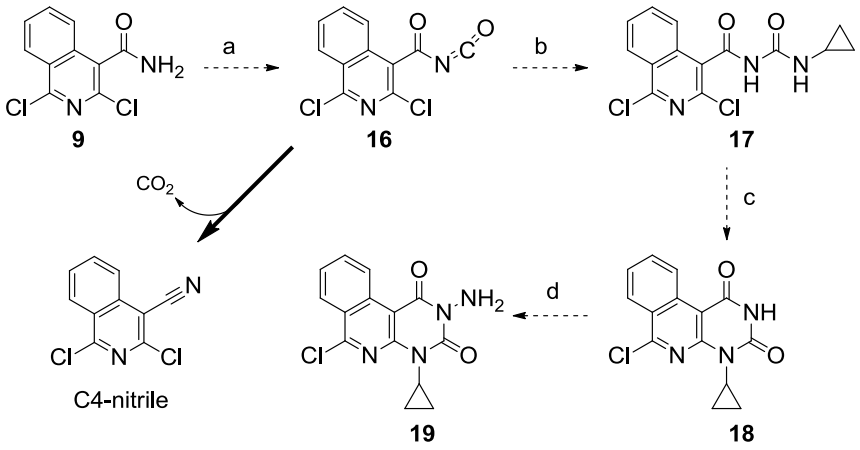

Reagents and Conditions: (a) oxalyl chloride, TEA; CH_2Cl_2, 0°C (b) cyclopropylamine, TEA; CH_2Cl_2, 0°C (c) NaH; THF, 0°C - room temp. (d) 2, 4-dintitrophenylhydroxylamine, TEA or DIPEA, CH_2Cl_2

Scheme 3.6: Proposed synthesis of the 5,6-phenyl dione cores and the C4-nitrile product resulting from the unfavorable rearrangement of the carbonyl isocyanate.

In the case of the diones, problems arose with generation of isocyanate **16**. Traditionally, synthesis of the isocyanate is accomplished through the reaction of a benzylamide precursor with oxalyl chloride as an electrophilic carbonyl source. In the case of isoquinolone precursor **9**, this procedure resulted in the immediate formation of a C4-nitrile. This unfortunate trend was repeated under a variety of conditions with other carbonyl sources: phosgene, triphosgene, and carbonyldiimidazole. This was later attributed to an unfavorable rearrangement of the carbonyl isocyanate to the nitrile, releasing carbon dioxide (Scheme 3.6). A second method was employed in order to

generate the imide-amine head group precursor **17** in which the acid-chloride of the isoquinolone **8** is reacted at high temperatures with urea to furnish the closed dione head group in a single step. The N1-group could then be added in a subsequent step. Unfortunately this methodology also resulted in the 4-nitrile product. Attempts to generate a cyclopropyl isocyanate were successful and several attempts were made to couple this product to the isoquinolone amide **9**, however without success.

Other methodology was available to generate each of the three iterations of the tricyclic napthyridones, fluoroquinolones and diones, however it was at this time that new discoveries with the potential of the C7-aminomethylpyrrolidine side chain to overcome fluoroquinolone resistance had started to come to fruition. Therefore, it was decided to focus research efforts towards exploring this new discovery. Unfortunately this required that the goal of extending the aromatic character of the fluoroquinolone and dione cores as a possible way of overcoming bacterial resistance be set aside in favor of a more promising direction in research.

3.5: Conclusions and Future Directions

A substantial amount of time, effort, and resources was expended to construct three novel iterations of tricyclic fluoroquinolone-like cores: 5,6-phenyl napthyridones, 4,5-pyrimidine fluoroquinolones, and 5,6-phenyl diones. Unfortunately, no synthetic routes to any of these compounds were ever discovered. These efforts, however, have resulted in the application of two interesting reactions: The cyclization of substituents at the C5-position with the C4-carbonyl of the fluoroquinolone core to give a bridged 4,5-pyrimidine fluoroquinolone core structure was demonstrated to be possible, and in fact could likely, with modifications, be useful in future efforts. Perhaps the greatest success of these efforts was found in the selective acylation of the 1,3-dichloroisoquinolone to give the carboxylic acid **8**, which was found to provide nearly quantitative results in every successful attempt of the reaction. This may also serve in future attempts to

functionalize the C5-position of the fluoroquinolone core or the generation of novel precursors to fluoroquinolone cores. Regardless, these efforts were highly useful in the exploration of novel synthetic methodology and training in the proper rigor and practice of synthetic chemistry.

CHAPTER IV: EFFECT OF AMINOMETHYLPYRROLIDINE SIDE CHAIN ON FLUOROQUINOLONE ANTIMUTANT ACTIVITY

4.1: Introduction

Fluoroquinolones are broad-spectrum antimicrobials that target bacterial type II bacterial topoisomerases, DNA gyrase and topoisomerase IV, by forming reversible ternary complexes composed of drug, enzyme, and double-strand nicked DNA. These reversible complexes block transcription,[111] replication,[112 113] and growth of bacteria.[112 114] DNA gyrase and topoisomerase IV are composed of two subunits: GyrA in DNA gyrase (ParC in topoisomerase IV) is the site of DNA nicking and religation, and GyrB in DNA gyrase (ParE in topoisomerase IV) is the site of ATP binding and hydrolysis, which provides energy to drive the action of the enzyme.[50]

The interface region between the two topoisomerase subunits is the site of fluoroquinolone binding. X-ray crystallography of cleaved complexes revealed that within the fluoroquinolone binding site the 3-carboxylate of the drug skeleton is oriented to form a Mg-water bridge (see Figures 1.2 and 1.7). This Mg-water bridge anchors the C3,4 β-ketoacid moiety of the fluoroquinolone to Helix-4 through coordination with conserved serine and acidic residues, for example Ser83 and Asp87 in *E. coli* GyrA.[58 57b] Mutations to these two Helix-4 residues of GyrA and/or ParC are found in the majority of clinical fluoroquinolone-resistant isolates.[74 75] Previous studies have demonstrated the importance of the Mg-water bridge and that disruption of this interaction causes loss of fluoroquinolone activity.[115] Fluoroquinolones containing a C7-aminomethylpyrrolidine side chain and similar derivatives have been known for some time;[116 117] however, fluoroquinolones in clinical use have different C7 ring structures.

Quinazolinediones, a class of agents similar to fluoroquinolones, have been shown to retain activity against fluoroquinolone-resistant bacteria, including those resistant to fluoroquinolones through having Helix-4 resistance substitutions.[118] In a

previous study we demonstrated that fluoroquinolones possessing a C7-aminomethylpyrrolidine side chain are also able to maintain activity against fluoroquinolone-resistant Helix-4 mutants in *B. anthracis,* as shown in Figure 4.1.[26]

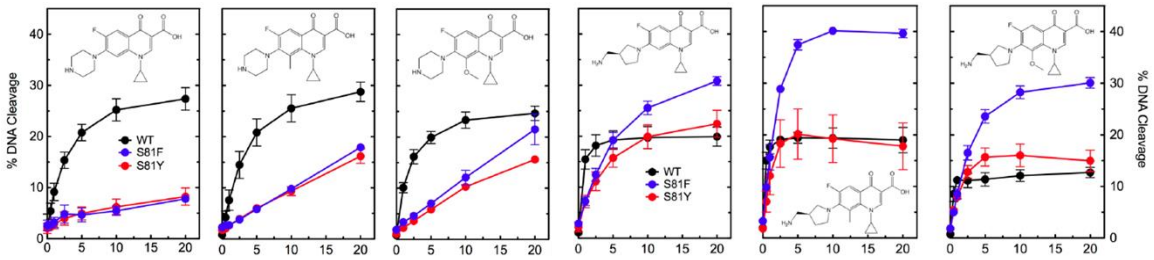

Figure 4.1: DNA cleavage activity with *B. anthracis* TopoIV as a result of the binding of fluoroquinolones containing a C7 piperazine, diazabicyclononane, or aminomethylpyrrolidine group. The wild-type activities (black lines) observed with the C7 piperazine and diazabicyclononane fluoroquinolones are lost when serine 81 is substituted with phenylalanine (blue lines) or tyrosine (red lines). In *B. anthracis* serine 81 is a key residue that coordinates the Mg-water bridge to Helix-4. The C7-aminomethylpyrrolidine fluoroquinolones are able to either maintain or have improved activity with these substitutions. Adapted from previous work by Schwanz and colleagues.[26]

To explain the ability of the C7-aminomethylpyrrolidine group to preserve activity against Helix-4 mutants resistant to other fluoroquinolones, subsequent docking studies were performed using the 2XKK crystal structure and a previously studied C7-aminomethylpyrrolidine fluoroquinolone UING-05-249 and potential interactions between the C7-aminomethylpyrrolidine and GyrB/ ParE regions in the fluoroquinolone binding pocket were demonstrated.[110] Specifically, a crucial binding interaction between a conserved glutamate residue in GyrB/ ParE (E466 in *E. coli*) and the basic primary amine of the aminomethylpyrrolidine side chain was observed as shown in Figure 4.2. This novel interaction is believed to function as an alternative anchor-point for fluoroquinolones within the ternary complex, thus diminishing the importance of the Mg-water bridge. This binding in turn diminishes the effect of resistance-causing mutations

of the serine and acidic residues on Helix-4. Other interactions have also been observed. Of the 20 poses used in docking the fluoroquinolones bearing the C7-aminomethylpyrrolidine side chain, five possible binding contacts were observed for the primary basic amine: interaction with conserved glutamate in GyrB/ParE (Glu437), interactions with a DA-20 ribose oxygen of the bound DNA, interactions with the backbone carbonyl of an arginine residue (Arg418), interactions with a guanidine ring nitrogen of the bound DNA, and a possible divalent interaction between the Glu437 and Arg418 carbonyl, as shown in Figure 4.2.

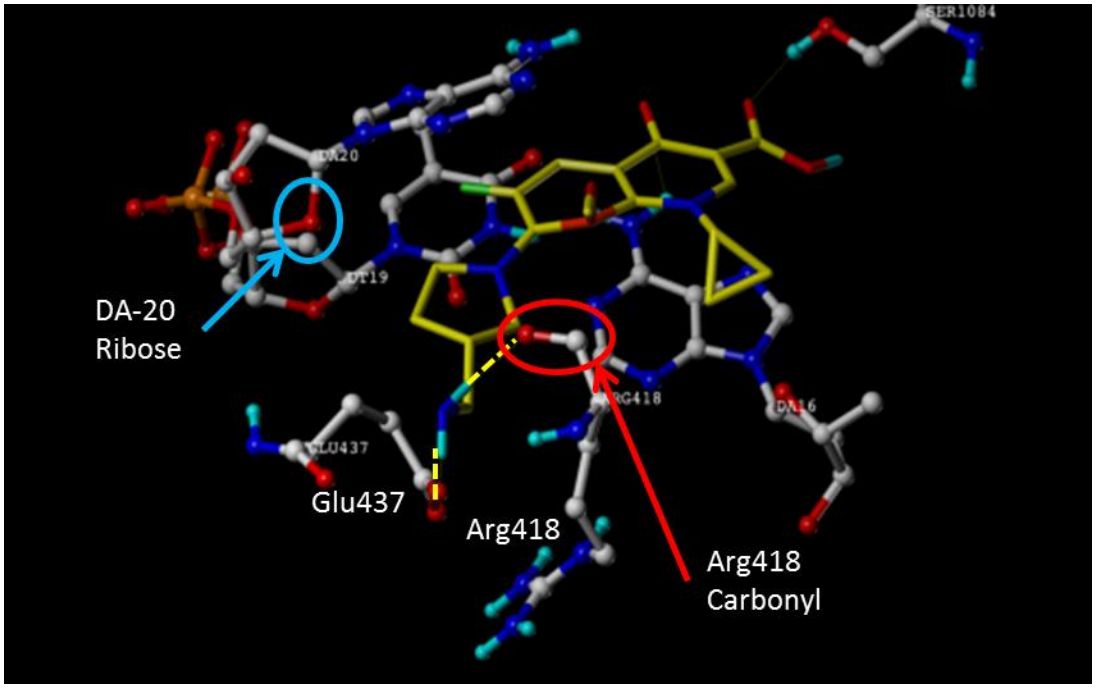

Figure 4.2: Docking studies with UING-05-249 in *A. baumannii* topoisomerase IV structure (2XKK). The highest scoring pose is depicted and consists of a bridging interaction of the primary amine of the C7- aminomethylpyrrolidine between the Glu437 side chain of ParE and a backbone carbonyl of R418 (orange circle). In other docking poses it is also possible for the C7-aminomethylpyrrolidine chain to twist around and interact with the ribose oxygen of DA-20 (blue circle), mimicking the binding of the moxifloxacin diazabicyclononane C7-side chain or the C7-piperazine of ciprofloxacin.

4.2: Goals of the Study

The demonstrated ability of a C7-aminomethylpyrrolidine side chain to preserve the activity of fluoroquinolones with Helix-4 serine substitutions, which imparts resistance to currently used fluoroquinolones, is an important step forward in designing fluoroquinolones that can dually target topoisomerase in wild-type and resistant-mutant bacteria. As shown in previous studies,[79] the extent of the ability of a C7-aminomethylpyrrolidine to preserve activity varies with the structure at the C8-position (Figure 4.1). This was evidence that the ability of the C7-aminomethylpyrrolidine group to preserve activity against fluoroquinolone-resistant enzyme is affected by fluoroquinolone core-structure. Thus I set out in this study to explore and understand the effect of structural changes to the fluoroquinolone-core structure on the ability of a C7-aminomethylpyrrolidine group to preserve activity against fluoroquinolone-resistant type-II topoisomerases and bacteria. To accomplish this, a series of fluoroquinolones with a wide variety of core structures-each possessing a C7-aminomethylpyrrolidine side chain-where synthesized and tested for the ability to inhibit the action of purified type-II topoisomerases, to poison purified type-II topoisomerases, and to inhibit the growth of both wild-type bacteria and Helix-4 resistant mutants.

Previous studies have shown that some fluoroquinolones with a C7-aminomethylpyrrolidine cross over and poison human topoisomerase IIα. In those same studies, it was demonstrated that selectivity for bacterial type-II topoisomerases over human type-II topoisomerase can be altered by the substituent present at the C8-position on the fluoroquinolone core.[58] The ability of some C7-aminomethylpyrrolidine compounds to act on to human topoisomerase IIα can be partially explained: human topoisomerase IIα lacks the serine and acidic residues on Helix-4 that coordinate the Mg-water bridge. Therefore, human topoisomerase IIα is structurally comparable to a fluoroquinolone-resistant form of bacterial topoisomerase IV or DNA gyrase, which is why many clinically used fluoroquinolones are highly selective for inhibition of bacterial

type-II topoisomerases over human type-II topoisomerases. It is believed that both bacterial and human type-II topoisomerases possess a glutamate residue in the GyrB/ParE region, of which the C7-aminomethylpyrrolidine is able to bind. Thus the binding contact that allows the C7-aminomethylpyrrolidine side chain to bestow retention of activity against fluoroquinolone-resistant mutants is conserved in human type-II topoisomerase. As such, exploring the utility of the C7- aminomethylpyrrolidine and similar moieties included testing the specificity of targeting of the fluoroquinolones for bacterial type-II topoisomerases over human type-II topoisomerases. The objective of the current study was to understand structural features of the fluoroquinolone core and C7-aminomethylpyrrolidine that are required for: 1) acting on both wild-type and Helix-4 resistant mutants and 2) acting on bacterial type-II topoisomerases without crossing over to human topoisomerase IIα.

4.3: Synthesis of Core-Diverse C7-Aminomethylpyrrolidine Fluoroquinolone Series

A panel of structurally-diverse C7-aminomethylpyrrolidine fluoroquinolones, as shown in Figure 4.3, was synthesized using nucleophilic aromatic substitution of a C7-aryl fluorine or chlorine on the precursor fluoroquinolone core structure, as shown in Scheme 4.1. All substitution reactions were performed in dimethylsulfoxide with heat (60-100^{o}C), using varying equivalents of diisopropylethylamine or triethylamine. Reactions were then treated with trifluoroacetic acid to remove the Boc-protecting group after C7- side chain addition. In most cases the reactions produced singular products and progressed to completion. Detailed synthetic methods are listed in the Experimental Section. Core structures were selected to test a variety of N1 and C8 structures of known clinical fluoroquinolones in conjunction with the C7- aminomethylpyrrolidine moiety. The C5-methyl and C5-amino variations to the core were generated in previous work, as was the N1-isopropyl system of the UITT-03-245 compound. The compound UIBW-04-236,

while not from a developed clinical core, shares a C2-thioether moiety with similar positioning to the N1-C2 thiobutyl structure in the known clinical fluoroquinolone ulifloxacin.

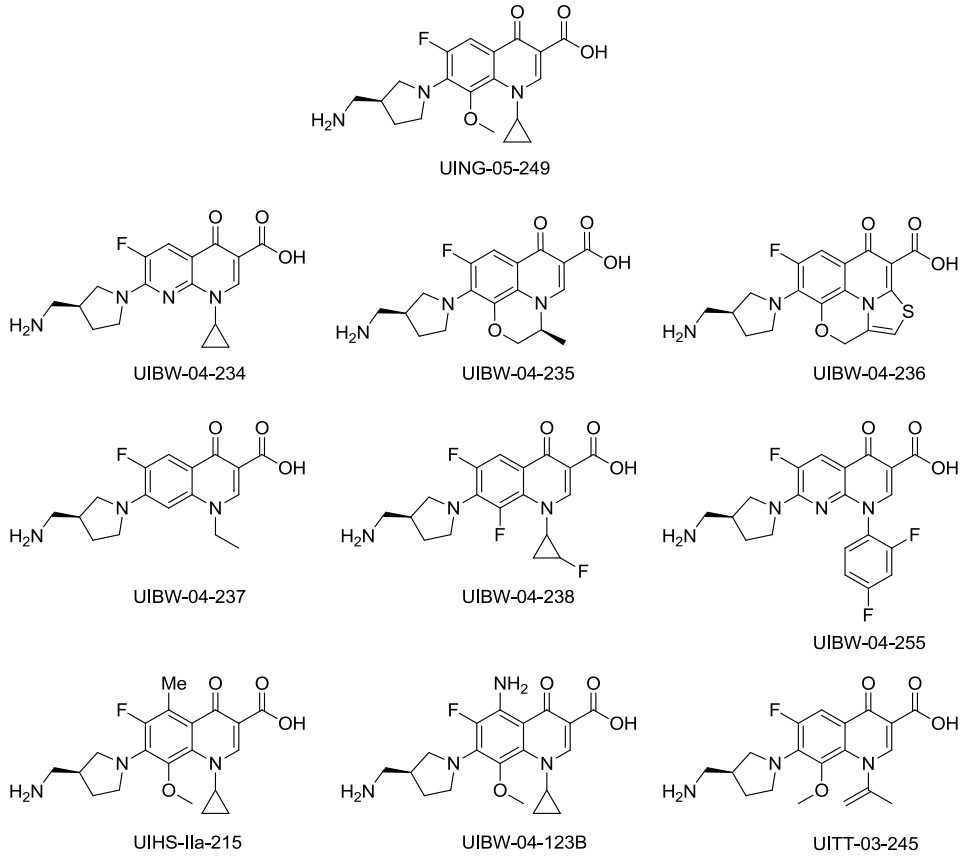

Figure 4.3: The panel of core-diverse C7-aminomethylpyrrolidine fluoroquinolones

Scheme 4.1: General methodology used to perform nucleophilic aromatic substitution of the C7-position on a variety of structurally diverse fluoroquinolone cores possessing either a C7-chlorine or fluorine.

4.4: Docking Studies with Core-Diverse C7-Aminomethylpyrrolidine Fluoroquinolones

Each of the C7-aminomethylpyrrolidine fluoroquinolones synthesized for this study was docked into the 2XKK crystal structure of *A. baumannii* topoisomerase IV using SYBYL molecular modeling and simulation software. Initial studies with wild-type topoisomerase revealed that all compounds were able to dock with comparable affinity to each other and to the clinical fluoroquinolones ciprofloxacin and moxifloxacin, as shown in Figure 4.4. It was also observed that binding orientation for all compounds is conserved in wild-type topoisomerase IV, as shown in Figure 4.5. All compounds are able to bind through the Mg-water bridge.

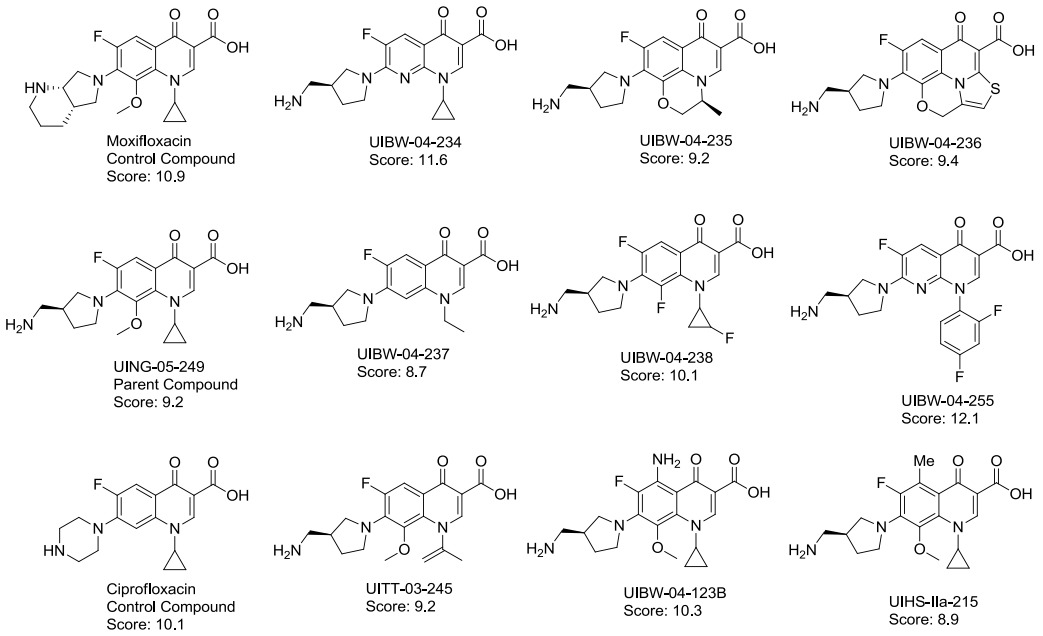

Figure 4.4: C7-aminomethylpyrrolidine fluoroquinolones with the control compounds ciprofloxacin, moxifloxacin, and UING-05-249. Beneath each compound is its SYBYL-generated docking score for docking into a crystal structure of a ternary complex of *A. baumannii* topoisomerase IV (PDB:2XKK). Higher scores represent increased binding affinity. All compounds dock with comparable affinity into the fluoroquinolone binding-pocket with the Mg-water bridge as the main binding contact.

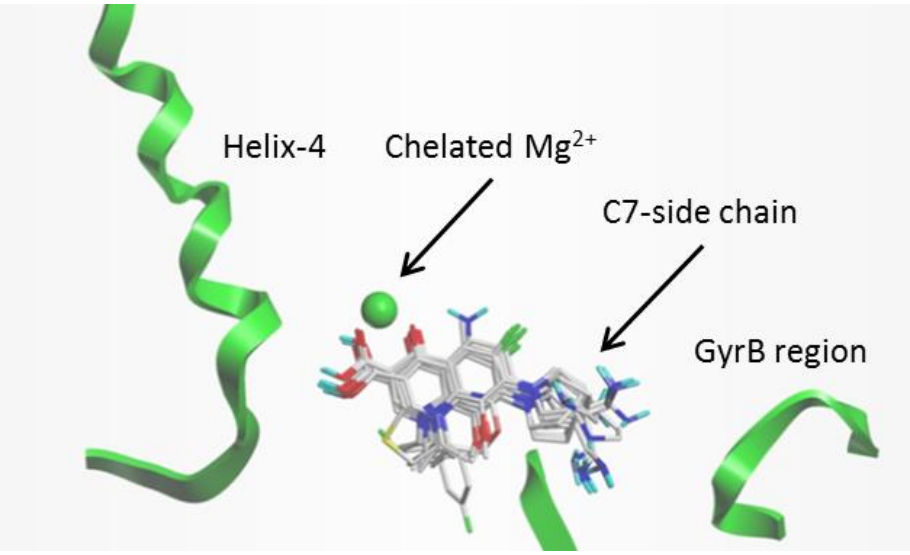

Figure 4.5: Simplified depiction of *in silico* docking of the core-diverse C7-aminomethylpyrrolidine fluoroquinolones and moxifloxacin in *A. baumannii* topoisomerase IV crystal structure 2XKK. The binding orientation is conserved across all compounds.

4.5: Enzyme Inhibition Activity by C7-Aminomethylpyrrolidine Fluoroquinolones

Each of the core-diverse, C7- aminomethylpyrrolidine fluoroquinolones was tested for the ability to inhibit the supercoiling activity of wild-type *E. coli* DNA gyrase and the decatenation activity of Topoisomerase IV in two separate assays: a supercoiling inhibition assay and a DNA decatenation assay, respectively. In the supercoiling inhibition assay, DNA gyrase was incubated with plasmid DNA, and to this mixture was added increasing concentrations of each fluoroquinolone. The amount of negatively supercoiled DNA produced as a result of enzyme function was then measured by gel electrophoresis to determine the overall potency of each fluoroquinolone to inhibit the function of *E. coli* DNA gyrase. The concentration of each fluoroquinolone required to prevent 50% of DNA gyrase supercoiling activity was determined, as shown in Table 4.1. Comparisons of supercoiling inhibition IC_{50} to the IC_{50} of the parent C7-

aminomethylpyrrolidine fluoroquinolone, UING-05-249, are also shown. In the DNA decatenation assay, *E. coli* Topoisomerase IV was incubated with catenated (linked) kinetoplast DNA, and to this mixture was added increasing concentration of each fluoroquinolone. The amount of decatenated (separated) DNA produced as a result of enzyme function was then measured by gel electrophoresis to determine the overall potency of each fluoroquinolone to inhibit the function of *E. coli* Topoisomerase IV.[119] None of the core-diverse, C7-aminomethylpyrrolidine fluoroquinolones exhibited inhibition of DNA decatenation in *E. coli* Topoisomerase IV up to a concentration of 2 μM. This suggests that DNA gyrase in *E. coli* (and possibly other Gram-negative bacteria) is the primary target for these fluoroquinolones.

Supercoiling Inhibition Compounds	IC_{50} (μM) [a] Mean ± SD (n=3 or 4)	IC_{50} compound/ IC_{50} UING-05-249
UING-05-249	0.177 ± 0.004	
UIBW-04-123B	0.387 ± 0.093	2.2
UIBW-04-234	0.189 ± 0.034	1.1
UIBW-04-235	0.175 ± 0.034	1
UIBW-04-236	0.100 ± 0.017	0.6
UIBW-04-237	0.644 ± 0.076	3.6
UIBW-04-238	0.103 ± 0.031	0.6
UIBW-04-255	0.427 ± 0.050	2.4
UIHS-IIa-215	0.355 ± 0.068	2
UITT-03-245	0.821 ± 0.146	4.6

Table 4.1: Supercoiling inhibition with wild-type *E. coli* DNA gyrase by core-diverse, C7- aminomethylpyrrolidine fluoroquinolones. The fold-difference between IC_{50} of each compound and the IC_{50} of a previously studied C7-aminomethylpyrrolidine compound, UING-05-249 is listed in the right column.

When tested for supercoiling inhibition of wild-type *E. coli* purified DNA gyrase, few compounds showed a substantial improvement in activity over the parent C7-aminomethylpyrrolidine fluoroquinolone, UING-05-249. Compound UIBW-04-123B, which has an N1-cyclopropyl C5-amino C8-methoxy core, compound UIBW-04-255, which has an N1-difluorophenyl 8-napthyridone core, and compound UIHS-IIa-215, which has an N1-cyclopropyl C5-methyl C8-methoxy core, suffered a 2-fold increase in IC_{50}. Compound UIBW-04-234, which has an N1-cyclopropyl 8-napthyridone core, and compound UIBW-04-235, which has an N1-C8 2-methylmorpholone core, had similar activity to UING-05-249. Interestingly, compound UIBW-04-236, which has an N1-C2 thiazole N1-C8 morpholine core, and compound UIBW-04-238, which has an N1-fluorocyclopropyl C8-fluoro core, had slightly more potent supercoiling inhibition compared to UING-05-249. Of the core-diverse series, compound UIBW4-237, which has an N1-ethyl core, and compound UITT-03-245, which has an N1-isopropene C8-methoxy core, showed the most dramatic losses of activity, each having a 4- to 5-fold increase in IC_{50}. To summarize, many of the core-diverse, C7-aminomethylpyrrolidine fluoroquinolones displayed similar ability (within 3-fold IC_{50}) to inhibit the supercoiling activity of purified wild-type *E. coli* DNA gyrase compared to the parent compound UING-05-249. Indeed, the largest margin of difference was a five-fold increase in IC_{50} of UITT-03-245 compared to the parent compound UING-05-249.

Having determined the relative ability of the core-diverse, C7-aminomethylpyrrolidine fluoroquinolones to inhibit supercoiling activity in *E. coli* DNA gyrase, the next assay would be used to determine the ability of these compounds to specifically poison DNA gyrase by blocking religation of nicked DNA. The poisoning activity of the core-diverse, C7-aminomethylpyrrolidine fluoroquinolones was determined with a DNA cleavage assay that measured the extent of cleaved DNA complex formation as a result of ternary complex formation with the fluoroquinolones. Cleaved complex formation as a result of fluoroquinolone binding was determined by

measuring the formation of cleaved (linear) DNA released from a ternary complex upon treatment with the detergent sodium dodecyl sulfate, which dissociates the ternary complex. This assay was performed by incubating *E. coli* DNA gyrase with plasmid DNA. The complex composed of DNA gyrase and DNA was then treated with increasing concentrations of test fluoroquinolone in order to form the ternary complex. After incubation, the ternary complex was treated with sodium dodecyl sulfate to dissociate the ternary complex and release the cleaved DNA. The amount of cleaved (linear) DNA was then measured by gel electrophoresis.[110] The amount of cleaved DNA that was released indicated the stability of the ternary complex with the test fluoroquinolone, which in turn was indicative of the extent to which the test fluoroquinolones were capable of poisoning *E. coli* DNA gyrase. The poisoning-fold stimulation is the fold-increase in cleaved DNA observed above baseline at the test compound supercoiling inhibition IC_{50}. The CC_3 value is the test fluoroquinolone concentration required to triple the amount of released cleaved (linear) DNA. The results of these assays are shown in Table 4.2.

Cleaved Complex Formation of C7-AMP series

Compounds	Poisoning Fold-stimulation (S.C. $IC_{50,}$ μM)	CC_3 (μM)
UING-05-249	18.4 ± 0.3	0.0090 ± 0.0010
UIBW-04-123B	22.1 ± 0.6	0.022 ± 0.0010
UIBW-04-234	21.1 ± 3.6	0.018 ± 0.0070
UIBW-04-235	29.2 ± 8.9	0.013 ± 0.0010
UIBW-04-236	22.3 ± 7.5	0.0080 ± 0.0020
UIBW-04-237	21.1 ± 4.0	0.052 ± 0.021
UIBW-04-238	21.3 ± 4.1	0.0070 ± 0.0010
UIBW-04-255	15.1 ± 0.7	0.017 ± 0.0020
UIHS-IIa-215	14.8 ± 1.4	0.036 ± 0.0010
UITT-03-245	20.5 ± 0.2	0.039 ± 0.0050

Table 4.2: Cleaved complex formation and poisoning activity measured by formation of linear DNA complexes as a result of incubation with core-diverse series of fluoroquinolones. Poisoning activity is listed at supercoiling IC_{50}. CC_3 is the concentration of fluoroquinolone required to triple the amount of released cleaved complexes.

Of the core-diverse, C7-aminomethylpyrrolidine fluoroquinolones, UIBW-04-235 and UIBW-04-236 were found to have the highest-fold poisoning activity. However, because of the relatively high uncertainty associated with the fold stimulation of UIBW-04-235 and UIBW-04-236, they should be considered to have comparable poisoning activity to UIBW-04-234, UIBW-04-237, and UIBW-04-238. The lowest-fold poisoning activity was found with UIHS-IIa-215. Though there are substantial variations in activity between the core-diverse, C7-aminomethylpyrrolidine fluoroquinolones, an important result of these DNA cleavage assays is that all test compounds are capable of poisoning *E. coli* DNA gyrase.

At higher test fluoroquinolone concentrations than CC_3 in the supercoiling inhibition assay, enough of the wild-type *E. coli* DNA gyrase in the incubation solution is

bound into a ternary complex to lead to an inhibition of supercoiling activity in DNA gyrase. The IC_{50} of supercoiling inhibition for each fluoroquinolone (Table 4.1) can interpreted as catalytic inhibition. Catalytic inhibition by fluoroquinolones of type-II bacterial topoisomerases is distinct from the poisoning of type-II bacterial topoisomerases by fluoroquinolones. Type-II bacterial topoisomerases poisoning by a fluoroquinolone specifically refers the ability of the fluoroquinolone to bind into the double-strand nicks within the bound DNA and inhibit DNA religation. Catalytic inhibition, alternatively, refers to the ability of a fluoroquinolone to inhibit the function of type-II bacterial topoisomerases via a different mechanism than binding into the ternary complex and inhibiting DNA religation. An important comparison can be drawn between the supercoiling inhibition IC_{50} values for the core-diverse C7-aminomethylpyrrolidine fluoroquinolones and their CC_3 values: The fact that supercoiling inhibition IC_{50} and CC_3 values across the panel of core-diverse, C7-aminomethylpyrrolidine fluoroquinolones have a mostly consistent pattern suggests that supercoiling inhibition strongly relates to ternary complex formation. Therefore unlike true catalytic inhibitors of DNA gyrase, which inhibit the supercoiling activity of the enzyme without poisoning, the core-diverse C7-aminomethylpyrrolidine fluoroquinolones function as poisoners of wild-type *E coli* DNA gyrase.

The goal of this study was to understand structural requirements of the C7-aminomethylpyrrolidine group to improve activity against fluoroquinolone-resistant Helix-4 mutants. Previous studies have demonstrated that it is possible for the C7-aminomethylpyrrolidine group to not only bestow the ability to fluoroquinolones to inhibit *B. anthracis* Topoisomerase IV containing fluoroquinolone-resistant Helix-4 amino acid substitutions, but also that the C7-aminomethylpyrrolidine group can bestow the ability to fluoroquinolones to inhibit human topoisomerase IIα.[26] Therefore, the C7-variant compounds were tested for inhibition of purified human topoisomerase IIα in a DNA decatenation assay similar to the previously described DNA decatenation assay

performed with wild-type *E. coli* Topoisomerase IV, the results of which are shown in Table 4.3. Only compound UIBW-04-236 was found to have detectable inhibition of human topoisomerase IIα at 100 μM.

Inhibition activity of Core-Diverse C7-AMP fluoroquinolones with human Topoisomerase IIα

Compounds	% Inhibition (100 μM)	IC_{50} (μM)	Poisoning (fold-stimulation at IC_{50})
UING-05-249	< 5		
UIBW-04-123B	< 5		
UIBW-04-234	< 5		
UIBW-04-235	< 5		
UIBW-04-236	100	29.3 ± 0.8	5.15 ± 0.15
UIBW-04-237	< 5		
UIBW-04-238	< 5		
UIBW-04-255	< 5		
UIHS-IIa-215	< 5		
UITT-03-245	< 5		

Table 4.3: Supercoiling inhibition activity by core-diverse, C7-aminomethylpyrrolidine fluoroquinolones with human topoisomerase IIα. Poisoning fold-stimulation is measured at supercoiling IC_{50}.

4.6: Growth Inhibition Activity by Core-Diverse C7-Aminomethylpyrrolidine Fluoroquinolones

Having characterized the ability of the core-diverse, C7-aminomethylpyrrolidine fluoroquinolones to inhibit DNA gyrase supercoiling function and their ability to form cleaved complexes in purified *E. coli* DNA gyrase, the compounds were then tested for their ability to inhibit growth in *E. coli* bacteria. To mitigate common forms of drug efflux, of all *E. coli* strains used in this study were *tolC* knock-out (KO) strains. This was done by measuring the minimum inhibitory concentration (MIC), which is the minimum

concentration of test compound required to block visible growth in overnight culture, in a series of broth-dilution assays. The results are shown below in Table 4.4.

MIC of Core-Diverse C7-AMP fluoroquinolones with *E. coli*

Compound	MIC (μM)	MIC compound/ MIC UING-05-249
UING-05-249	0.0037	
UIBW-04-234	0.006 ±0.002	1.6
UIBW-04-235	0.032 ±0.005	8.6
UIBW-04-236	0.007 ±0.001	2
UIBW-04-237	0.180 ±0.046	48.5
UIBW-04-238	0.007 ±0.001	2
UIBW-04-255	0.009 ±0.002	2.5
UIBW-04-123B	0.006 ±0.002	1.6
UIHS-IIa-215	0.004 ±0.003	1.1
UITT-03-245	0.032 ±0.005	8.6

Table 4.4: Minimum inhibitory concentrations of core-diverse, C7-aminomethylpyrrolidine fluoroquinolones with *tolC* KO *E. coli* cells. The fold-difference between MIC's of each compound are compared to the MIC of UING-05-249.

With *tolC* KO *E. coli*, compound UIBW-04-234, which has an N1-cyclopropyl 8-napthyridone core, and compound UIHS-IIa-215, which has an N1-cyclopropyl C5-methyl C8-methoxy core, had MIC's comparable to that of the parent fluoroquinolone UING-05-249. Compound UIBW-04-238, which has an N1-fluorocyclopropyl C8-fluoro core, compound UIBW-04-236, which has an N1-C2 thiazole N1-C8 morpholine core, and compound UIBW-04-255, which has an N1-difluorophenyl 8-napthyridone core, had less potent growth inhibition activity, as shown by a 2-fold increase in MIC. Compound UIBW-04-235, which has N1-C8 2-methylmorpholone core, and the compound UITT-03-245, which has an N1-isopropene C8-methoxy core, both had dramatically less potent growth inhibition activity with a nearly 9-fold increase in MIC compared to compound

UING-04-249. However, the weakest growth inhibition potency was found in compound UIBW-04-237, which had a 49-fold increase in MIC compared to compound UING-04-249. Overall however, many compounds (6 out of 9) displayed comparable MIC (within 3-fold MIC) in *E. coli* cultures compared to UING-05-249. The scale of variation (up to ~50-fold difference in MIC values) within the core-diverse, C7-aminomethylpyrrolidine fluoroquinolones was intriguing as the core-diverse compounds exhibited markedly different MIC's compared to the IC_{50} results obtained from purified DNA gyrase. In a second bacteriostatic assay compounds were tested for growth inhibition activity in *M. smegmatis*. The results and comparison to *E. coli* MIC's are shown in Table 4.5.

MIC of Core-Diverse C7-AMP fluoroquinolones with *M. Smegmatis c*ultures

Compound	MIC	MIC compound/ MIC UING-05-249	MIC *M. Smeg/* MIC *E.coli*
UING-05-249	0.047 ±0.013		12.8
UIBW-04-234	0.157 ±0.032	3.3	26.1
UIBW-04-235	0.188 ±0.044	4.0	5.9
UIBW-04-236	0.379 ±0.089	8.0	51.5
UIBW-04-237	3.96 ±0.778	84.1	22.1
UIBW-04-238	0.028 ±0.004	0.6	3.9
UIBW-04-255	0.220 ±0.031	4.7	23.3
UIBW-04-123B	0.16 ±0.06	3.5	27.1
UIHS-IIa-215	0.418 ±0.073	8.9	107.5
UITT-03-245	0.238 ±0.098	5.1	7.5

Table 4.5: Bacteriostatic activities of C7-variant fluoroquinolones in wild-type *M. smegmatis* cells. The fold-difference between compound MIC and the MIC of UING-05-249 is listed to in the center-right column. The fold-difference between compound MIC in wild-type *M. smegmatis* cells ($MIC_{M.\ smeg}$) and MIC in *tolC* KO *E. coli* cells is listed in the far right column.

Bacteriostatic activities against *M. smegmatis* for core-diverse, C7-aminomethylpyrrolidine fluoroquinolones were overall weaker compared to the MIC's found in *E. coli*. As a whole, the pattern of MIC's across the series core-diverse, C7-

aminomethylpyrrolidine fluoroquinolones relative to each other also varied differently in comparison to the MIC's in *E.coli*. This is to say that core-diverse, C7-aminomethylpyrrolidine fluoroquinolones with relatively impressive growth inhibition activity in *E.coli* did not always also possess relatively impressive activity in *M. smegmatis* compared to other fluoroquinolones of this series. In particular, UIBW-04-236 and UIHS-IIa-215 showed 8- and 9-fold higher MIC's compared to UING-05-249. Compounds UIBW-04-235, UIBW-04-255, and UITT-03-245 had 4 to 5-fold higher MIC's compared to UING-05-249. Compounds UIBW-04-234 and UIBW-04-123B had more comparable activity, with only 3.3 and 3.7-fold higher MIC's than UING-05-249, respectively. Of all compounds, UIBW-04-238 showed the most potent MIC, having a slightly lower MIC than UING-05-249. Interestingly, this compound also had the most similar MIC between *M. smegmatis* and *E. coli* cell cultures. The least potent activity was seen in compound UIBW-04-237, with an 84-fold higher MIC compared to UING-05-249. Poor bacteriostatic activity observed for UIBW-04-237 with wild-type *M. smegmatis* cells is consistent with the assay *tolC* KO *E. coli*, in which UIBW-04-237 also displayed the least potent cell growth inhibition. The inconsistency of patterns in MIC's for core-diverse, C7-aminomethylpyrrolidine fluoroquinolones between *M. smegmatis* and *E. coli* suggests that cell penetration and off-target effects contribute to the unique activity of each compound.

4.7: Antimutant Activity Profiles of Core-Diverse C7-Aminomethylpyrrolidine Fluoroquinolones

A primary goal of this investigation is to understand structural modifications to the fluoroquinolones that enable equipotent targeting of wild-type and current fluoroquinolone-resistant strains of bacteria. As previously stated, target-mediated resistance is the most common form of clinically observed fluoroquinolone resistance. Specifically, point mutations that lead to alterations of the Helix-4 serine and acidic

residues, the residues observed *in silico* to coordinate the Helix-4 Mg-water bridge, account for 90% of clinical isolates that are fluoroquinolone-resistant.[74] [75]

As previously stated in Chapter 1.5, a major factor contributing to emerging fluoroquinolone resistance is the mutant selection window, which is a range of dosing between the minimum inhibitory concentration and the mutant prevention concentration. The minimum inhibitory concentration is the concentration of drug treatment required to prevent visible growth of bacteria colonies, resulting in bacteriostasis. The mutant prevention concentration is a higher concentration of treatment that is sufficient to prevent the selection of random resistant mutant within the cell colony. However, this concentration is often above safety thresholds for clinical utility. Clinical practice places dosing regimens within this window.[3] Though dosing within the mutant selection window is sufficient to suppress the predominantly wild-type bacterial load and treat infection, the practice gives rise to drug-resistant subpopulations of bacteria.[4] Therefore, to combat the emergence of fluoroquinolone resistance, it is imperative that fluoroquinolones with a very narrow mutant selection window be discovered. Such fluoroquinolones would display equipotent minimum inhibitory concentrations against both wild-type and cognate mutants that can arise and would otherwise be resistant to fluoroquinolones.

To test the ability of the core-diverse, C7-aminomethylpyrrolidine fluoroquinolones to overcome resistance, the compounds were tested for growth inhibition with several mutant strains of *E.coli* in order to determine their antimutant activity. In the context of this thesis, the term "antimutant activity" refers to a ratio of a given fluoroquinolone's minimum inhibitory concentration with bacteria possessing known fluoroquinolone resistance causing substitutions and the minimum inhibitory concentration with wild-type bacteria. A fluoroquinolone equipotent against both wild-type and resistant bacteria strains would show an antimutant activity of ~1 against bacteria with a known fluoroquinolone-resistant mutation. There are several known

mutations to Helix-4 that correlate to fluoroquinolone resistance, which are diagramed in Figure 4.6.

- **G81C, D82A, A84P:** Alters orientation of Helix-4 serine and acidic residues; may affect Mg-water bridge formation
- **S83L, D87N:** Compromises Mg-water bridge formation
- **S83W, D87Y:** Compromises Mg-water bridge formation and may sterically block Helix-4 binding region
- **D426N, K447E:** Theoretical GyrB region binding contact for basic 1°-amine in C7-aminomethylpyrrolidine; replacement should be reduce or enhance capability for GyrB binding, respectively.

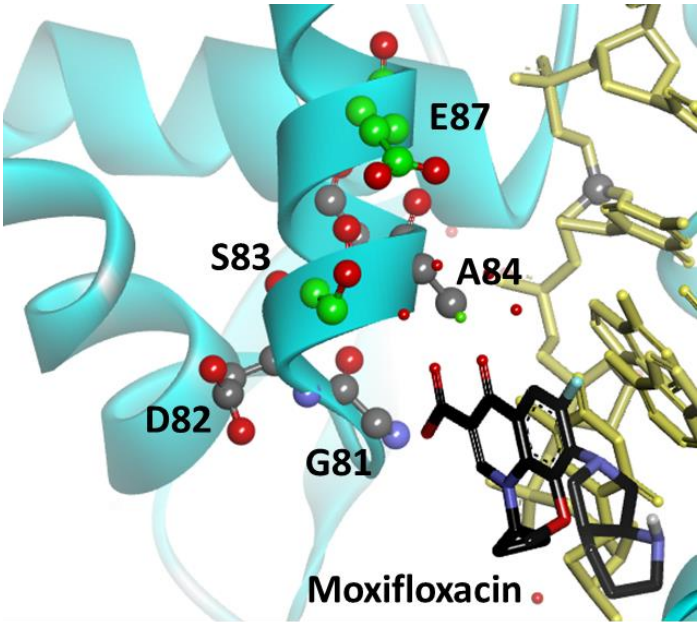

Figure 4.6: *In silico* depiction of Helix-4 residues (*E. coli* numbering) of Topoisomerase IV. Moxifloxacin (black stick) is bound to Helix-4 through the Mg-water bridge (green and red spheres) and is oriented into the DNA (gold stick) nicked site. The serine and aspartate residues that coordinate the Mg-water bridge are highlighted in green. Other Helix-4 residues of note are G81, D82 and A84. D426 and K447 (not shown) are GyrB/ParE residues that may interact with the C7-aminomethylpyrrolidine.

A series of bacterial cultures of *E. coli* were subjected to broth dilution assays in order to measure the MIC of the compounds with mutant strains and determine their antimutant activity. *In silico* modeling studies have led to predictions for the effect of each mutation, as listed above Figure 4.6. The antimutant activities of the core-diverse, C7-aminomethylpyrrolidine fluoroquinolones are shown below in Tables 4.6-10 and summarized in Figure 4.7 and Figure 4.8. In each of the Tables 4.6-10, "MIC" refers to the average minimum inhibitory concentration calculated for the test fluoroquinolone with the *E. coli* mutant. The far-right column "mut/wt" lists the calculated antimutant activity, which is the ratio of the determined compound MIC in the *E. coli* strain possessing the listed Helix-4 or GyrB substitution over the MIC of the compound with wild-type *E. coli.* It is important to compare the antimutant activity values for each of the core diverse, C7-aminomethylpyrrolidine fluoroquinolones within the context of the absolute MIC values obtained for the each of the compounds with *E. coli* mutant strains. This consideration is important because it is possible for a fluoroquinolone to possess an antimutant activity that is close or equal to 1 for a given *E. coli* strain, however the reason that the fluoroquinolone possesses such antimutant activity is because the compound MIC is near the upper limit of detection for MIC with both *tolC* KO *E.coli* and *tolC* KO *E.coli* strain possessing a Helix-4 or GyrB substitution. Thus, it is possible for a compound to possess an antimutant activity that is close to 1 with an *E. coli* strain possessing a Helix-4 or GyrB substitution because the compound has low-potency bacteriostatic activity in that strain as well as the wild-type *E. coli* strain.

Bacteriostatic Activity of Compounds against KD2862 (S83L) cells

Compound	MIC (μM)	mut/wt S83L
UING-05-249	0.014 ±0.002	3.88
UIBW-04-234	0.070 ±0.019	11.551
UIBW-04-235	0.143 ±0.017	4.481
UIBW-04-236	0.070 ±0.019	9.456
UIBW-04-237	1.75 ±0.25	9.75
UIBW-04-238	0.041 ±0.009	5.578
UIBW-04-255	0.114 ±0.014	12.085
UIBW-04-123B	0.029 ±0.004	4.685
UIHS-IIa-215	0.029 ±0.004	7.327
UITT-03-245	0.143 ±0.017	4.481

Bacteriostatic Activity of Compounds against KD2876 (S83W) cells

Compound	MIC (μM)	mut/wt S83W
UING-05-249	0.0214 ±0.008	5.819
UIBW-04-234	0.114 ±0.014	18.947
UIBW-04-235	0.1738 ±0.046	5.4638
UIBW-04-236	0.057 ±0.007	7.7551
UIBW-04-237	2.5 ±0.5	13.928
UIBW-04-238	0.057 ±0.007	7.7551
UIBW-04-255	0.1695 ±0.059	17.968
UIBW-04-123B	0.0428 ±0.015	7.0274
UIHS-IIa-215	0.057 ±0.007	14.653
UITT-03-245	0.205 ±0.045	6.4465

Table 4.6: Average MIC values, standard deviations, and antimutant activities of core-diverse C7-aminomethylpyrrolidine fluoroquinolones *E. coli* strains containing serine 83 mutations

Bacteriostatic Activity of Compounds against KD2880 (D87N) cells

Compound	MIC (μM)	mut/wt D87N
UING-05-249	0.017 ±0.005	4.730
UIBW-04-234	0.057 ±0.007	9.474
UIBW-04-235	0.214 ±0.076	6.722
UIBW-04-236	0.043 ±0.015	5.816
UIBW-04-237	1.25 ±0.25	6.964
UIBW-04-238	0.043 ±0.015	5.816
UIBW-04-255	0.070 ±0.019	7.367
UIBW-04-123B	0.021 ±0.008	3.514
UIHS-IIa-215	0.021 ±0.005	5.270
UITT-03-245	0.174 ±0.046	5.464

Bacteriostatic Activity of Compounds against KD2866 (D87Y) cells

Compound	MIC (μM)	mut/wt D87Y
UING-05-249	0.014 ±0.002	3.879
UIBW-04-234	0.041 ±0.009	6.814
UIBW-04-235	0.214 ±0.076	6.722
UIBW-04-236	0.070 ±0.019	9.456
UIBW-04-237	2.5 ±0.5	13.9
UIBW-04-238	0.043 ±0.015	5.816
UIBW-04-255	0.114 ±0.014	12.085
UIBW-04-123B	0.043 ±0.015	7.027
UIHS-IIa-215	0.029 ±0.004	7.327
UITT-03-245	0.174 ±0.046	5.464

Table 4.7: Average MIC values, standard deviations, and antimutant activities of core-diverse C7-aminomethylpyrrolidine fluoroquinolones *E. coli* strains containing aspartic acid 87 mutations

As shown in Tables 4.6 and 4.7, compound UIBW-04-237, which has an N1-ethyl core, consistently has the highest absolute MIC values with each of the S83 and D87 fluoroquinolone resistant strains tested. Compared to the other core-diverse, C7-

aminomethylpyrrolidine fluoroquinolones, UIBW-04-237 is relatively inactive as an inhibitor of cell growth across the entire panel of *E. coli* mutant strains tested. As the single exception, compound UIBW-04-237 does however have moderate bacteriostatic activity with the *E. coli* strain possessing the GyrB D426N substitution, compared to the other fluoroquinolones. Compound UIBW-04-235, which has N1-C8 2-methylmorpholone core, and UITT-03-245 which has an N1-isopropene C8-methoxy core, tend to have greater than 10-fold higher MIC's with S83 and D87 fluoroquinolone resistant strains compared to UING-05-249. With few exceptions, the new core-diverse C7-aminomethylpyrrolidine fluoroquinolones have inferior antimutant activity profiles compared to UING-05-249 across all tested fluoroquinolone resistant strains (Figure 4.7).

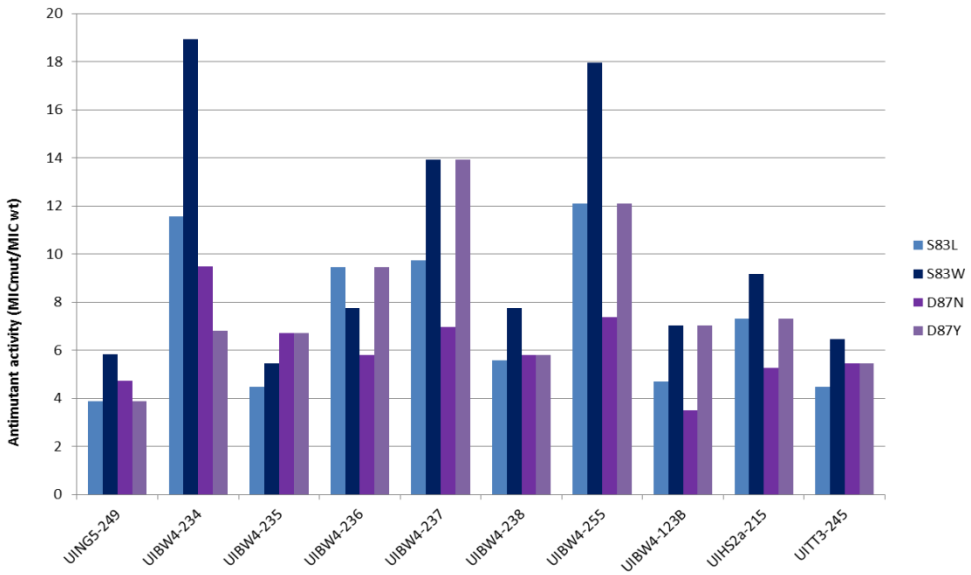

Figure 4.7: Bar-graph representation of antimutant activities of core-diverse C7-aminomethylpyrrolidine fluoroquinolone series *E. coli* strains possessing mutations of the S83L(blue), S83W (dark blue), D87N (purple), and D87Y (light purple). The residues S83 and D87 coordinate the Mg-water bridge and mutations to these residues are highly correlative to fluoroquinolone resistance. Lower antimutant activity represents greater retention of compound activity.

As shown in Figure 4.7, all four mutations to S83 and D87 raise the MIC for all core-diverse compounds, resulting in a 3.5 to 19-fold increase in MIC. The S83W mutation has the most detrimental effect on compound MIC across the panel of core-diverse compounds, exceptions being UIBW-04-235 and UIBW-04-236. The MIC of compound UIBW-04-123B is equally raised by both S83W and D87Y.

Bacteriostatic Activity of Compounds against KD2882 (G81C) cells

		mut/wt
Compound	**MIC (μM)**	**G81C**
UING-05-249	0.010 ±0.002	2.790
UIBW-04-234	0.029 ±0.004	4.737
UIBW-04-235	0.071 ±0.009	2.241
UIBW-04-236	0.029 ±0.004	3.878
UIBW-04-237	0.625 ±0.125	3.482
UIBW-04-238	0.029 ±0.004	3.878
UIBW-04-255	0.057 ±0.007	6.042
UIBW-04-123B	0.014 ±0.002	2.342
UIHS-IIa-215	0.007 ±0.001	1.832
UITT-03-245	0.071 ±0.009	2.241

Bacteriostatic Activity of Compounds against KD2956 (D82A) cells

		mut/wt
Compound	**MIC (μM)**	**D82A**
UING-05-249	0.0036	0.9800
UIBW-04-234	0.007 ±0.001	1.184
UIBW-04-235	0.036 ±0.004	1.119
UIBW-04-236	0.007 ±0.001	0.969
UIBW-04-237	0.144 ±0.107	0.799
UIBW-04-238	0.007 ±0.001	0.969
UIBW-04-255	0.014 ±0.002	1.511
UIBW-04-123B	0.007 ±0.001	1.171
UIHS-IIa-215	0.0036	0.9151
UITT-03-245	0.036 ±0.004	1.120

Table 4.8: Average MIC values, standard deviations, and antimutant activities of core-diverse C7-aminomethylpyrrolidine fluoroquinolones *E. coli* strains containing glycine 81 and aspartic acid 82 mutations.

Bacteriostatic Activity of Compounds against KD2864 (A84P) cells

Compound	MIC (μM)	mut/wt A84P
UING-05-249	0.00713 ±0.00088	1.93966
UIBW-04-234	0.007 ±0.001	1.184
UIBW-04-235	0.103 ±0.023	3.223
UIBW-04-236	0.029 ±0.004	3.878
UIBW-04-237	0.625 ±0.125	3.482
UIBW-04-238	0.014 ±0.002	1.939
UIBW-04-255	0.021 ±0.005	2.173
UIBW-04-123B	0.007 ±0.001	1.171
UIHS-IIa-215	0.007 ±0.001	1.832
UITT-03-245	0.103 ±0.023	3.223

Table 4.9: Average MIC values, standard deviations, and antimutant activities of core-diverse C7-aminomethylpyrrolidine fluoroquinolones *E. coli* strains containing adenine 84 mutations

Bacteriostatic Activity of Compounds against KD2932 (D426N) cells

Compound	MIC (μM)	mut/wt D426N
UING-05-249	0.00356 ±0.00044	0.96915
UIBW-04-234	0.0071 ±0.0008	1.1842
UIBW-04-235	0.05125 ±0.01125	1.61164
UIBW-04-236	0.01025 ±0.00225	1.39456
UIBW-04-237	0.156 ±0.031	0.869
UIBW-04-238	0.0285 ±0.0035	3.8776
UIBW-04-255	0.03525 ±0.02725	3.73675
UIBW-04-123B	0.00356 ±0.00044	0.58521
UIHS-IIa-215	0.00256 ±0.00056	0.6581
UITT-03-245	0.05125 ±0.01125	1.61164

Bacteriostatic Activity of Compounds against KD2934 (K447E) cells

Compound	MIC (μM)	mut/wt K447E
UING-05-249	0.0018	0.4846
UIBW-04-234	0.0036	0.5917
UIBW-04-235	0.0513 ±0.011	1.6116
UIBW-04-236	0.0036	0.4844
UIBW-04-237	0.0543 ±0.008	0.3022
UIBW-04-238	0.0353 ±0.027	4.7959
UIBW-04-255	0.0176 ±0.014	1.8657
UIBW-04-123B	0.0036	0.5852
UIHS-IIa-215	0.0036	0.9151
UITT-03-245	0.0513 ±0.011	1.6116

Table 4.10: Average MIC values, standard deviations, and antimutant activities of core-diverse C7-aminomethylpyrrolidine fluoroquinolones *E. coli* strains containing GyrB/ParE-region mutations D426N and K447E

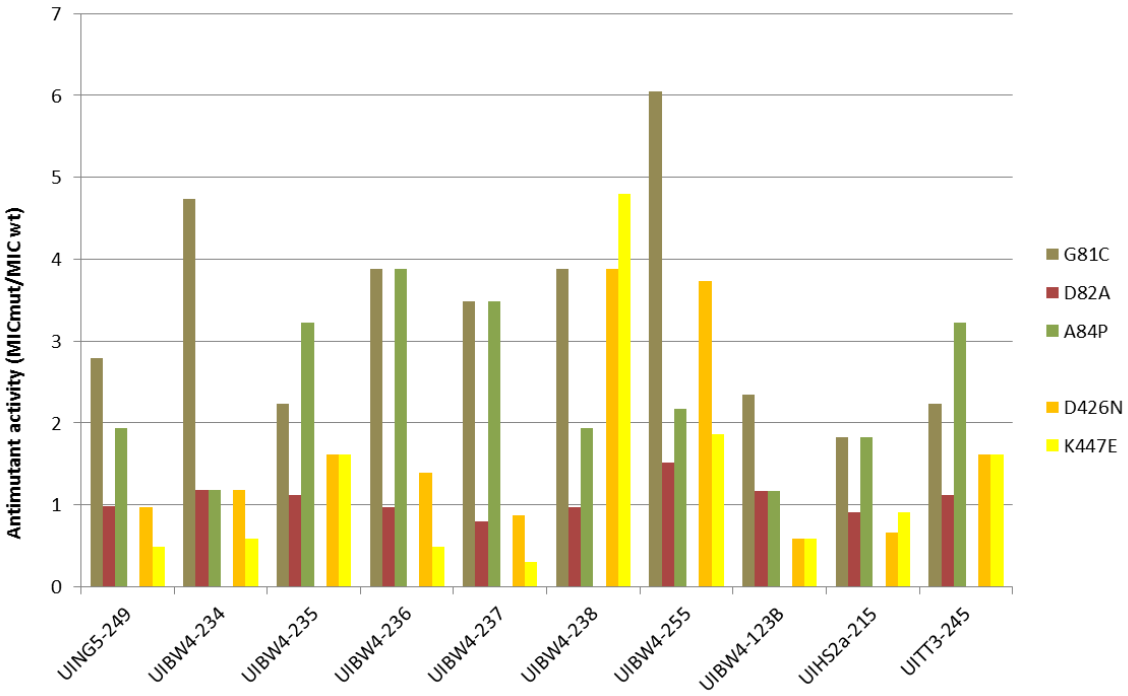

Figure 4.8: Antimutant activities of core-diverse C7-aminomethylpyrrolidine fluoroquinolones with *E. coli* strains containing the Helix-4 mutations G81C (olive), D82A (brown), and A84P (green) as well as strains with the GyrB mutations D426N (orange) and K447E (yellow).

As shown in Figure 4.8, the *tolC* KO *E.coli* strains possessing the Helix-4 D82A substitution does not affect the MIC of most core-diverse compounds; the antimutant activity of UIBW-04-255 with the D82A strain is largest antimutant activity observed with that strain, with an antimutant activity of ~1.5. The effect of the GyrB D426N mutation is inconsistent across the core-diverse series with either reduced or relatively unaltered MIC's for UING-05-249, UIBW-04-234, UIBW-04-237, UIBW-04-123B, UIHS-IIa-215. This substitution does raise the MIC of UIBW-04-235, UIBW-04-236, and UITT-03-245 with antimutant activities of 1.6, 1.4, and 1.6 respectively. The D426N mutation also raised the MIC of UIBW-04-238 and UIBW-04-255 to a greater extent, affording antimutant activities of 3.9 and 3.7, respectively. The GyrB K447E mutation was expected to improve antimutant activity by facilitating binding of the C7-

aminomethylpyrrolidine to the GyrB subunit, and this is true for most compounds. Notable exceptions are UIBW-04-235, UIBW-04-255, and UITT-03-245 whose MIC are raised by this mutation to give antimutant activities of 1.6-1.9 and UIBW-04-238 whose MIC is more dramatically raised with an antimutant activity of 4.8.

It is possible to make some considerable observations from the perspective of structure-activity relations with this data. The MIC of C5-position variants UING-05-249 (C5-hydrogen), UIBW-04-123B (C5-amine), and UIHS-IIa-215 (C5-methyl), is not affected to any great extent by the Helix-4 mutations G81C, D82A, or A84P. The antimutant activity of each compound is within 2-fold of other C5-variant compounds. These derivatives also have similar MIC values with resistant strains bearing the GyrB mutations D426N and K447E. Each of these three derivatives has an antimutant activity of 1 or <1 with both GyrB mutants. The Helix-4 S83W mutation is the most damaging to MIC across this entire panel of compounds: UIBW-04-237 (8-hydrogen; ~14 fold higher MIC) and more so by UIBW-04-234 and UIBW-04-255 (8-nitrogen heteroatom; ~20 fold higher MIC). The MIC of the three compounds UIBW-04-237, UIBW-04-234, and UIBW-04-255 are also raised by the Helix-4 S83L mutation, with antimutant activities of 9.7, 11.5, and 12.1 respectively. To a lesser extent the MIC of these three compounds are raised by the D87N and D87Y mutations, however the pattern is less consistent. This could suggest that lower steric character at C8 is disfavored against the S83 and D87 mutations. An exception to both observations is that the MIC of UIBW-04-238 (8-fluoro) is consistently less affected by S83 and D87 mutations than UIBW-04-237, UIBW-04-234, and UIBW-04-255. The MIC the compounds bearing a C8-N1 morpholone moiety, UIBW-04-235 and UIBW-04-236 and compound UITT-03-245, which has a similar C8-methoxy moiety, are raised by the D426N mutation. Other C8-methoxy compounds are inconsistently affected. The D426N mutation appears to be most detrimental to the MIC of compounds UIBW-04-238 and UIBW-04-255, where both of these compounds have fluorinated N1 groups and antimutant activities of 3.9 and 3.7 respectively. Mutations at

the Helix-4 S83 and D87 do not seem to differentiate based on steric character at N1 as the MIC of both UIBW-04-237 (N1= ethyl) and UIBW-04-255 (N1= *o*-difluorophenyl) are similarly increased by mutations in either position. Specifically, the antimutant activities of compound UIBW-04-237 against the S83/D87 mutants are S83L-9.7, S83W-13.9, D87N-7.0, D87Y-13.9. This pattern is very similar to the antimutant activities of compound UIBW-04-255 against the S83/D87 mutants, which are S83L-12.1, S83W-18.0, D87N-7.4, and D87Y-12.1.

A few miscellaneous observations were also made from these data. The compound UIBW-04-235 had potent supercoiling inhibition activity with wild-type *E. coli* DNA gyrase and also had the highest poisoning fold-stimulation, and the antimutant activities of UIBW-04-235 across many of the *E. coli* mutant strains tested compares favorably to the antimutant activities calculated for parent compound UING-05-249. This is also true for compound UIBW-04-238, which has potent supercoiling inhibition IC_{50} against *E.coli* DNA gyrase. An important consideration must be made in the context of this data. If the antimutant profiles of non-aminomethylpyrrolidine-containing fluoroquinolones such as the clinical drug moxifloxacin or a current fluoroquinolone like PD160788 are compared to this series, it is observed that most of the C7-aminomethylpyrrolidine fluoroquinolones have superior antimutant activity profiles. These comparisons are shown in Figure 4.9.

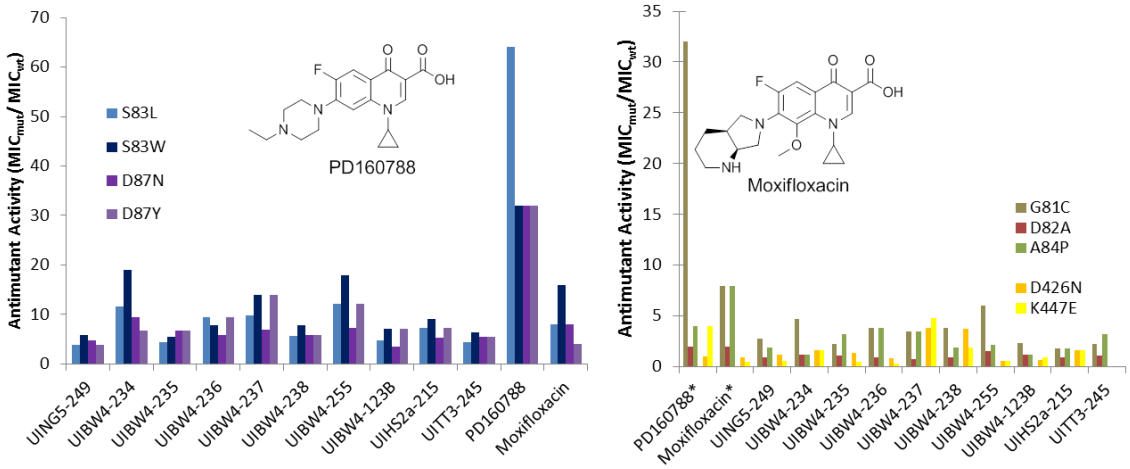

Figure 4.9: Bar graph of antimutant activities of C7-aminomethylpyrrolidine-containing fluoroquinolones with data for current fluoroquinolones PD160788 (left structure) and moxifloxacin (right structure). Antimutant profiles against S83/D87 substitutions are shown in the left graph and other Helix-4 and GyrB/ParE substitutions are shown in the right graph. The antimutant activities for PD160788 and moxifloxacin were adapted from previous studies.[120 121]

CHAPTER V: THE EFFECT OF MODIFICATIONS TO THE C7-AMINOMETHYLPYRROLIDINE SIDE CHAIN

5.1: Introduction

The previous chapter establishes that structural diversity of the fluoroquinolone core has a substantial effect on antimutant activity of C7-aminomethylpyrrolidine fluoroquinolones. However, relative to clinical fluoroquinolones such as moxifloxacin and ciprofloxacin, most C7-aminomethylpyrrolidine fluoroquinolones have better retention of bacteriostatic activity against fluoroquinolone-resistant *E. coli* Helix-4 mutants. The introduction of Chapter 4 describes in detail the observations made from SYBYL docking studies with the C7-aminomethylpyrrolidine fluoroquinolone UING-05-249. To summarize, there are four features of the GyrB/ParE region and within bound DNA that are observed binding contacts for the C7-aminomethylpyrrolidine side chain. The E437 residue can form a binding contact with the basic primary amine of the side chain. The backbone carbonyl oxygen of R418 can form a binding interaction through the primary amine of the side chain. As shown in Figure 5.1 (Panel A), it is also possible for the side chain amine to form a divalent binding pose between the E437 and the backbone carbonyl of R418. The aminomethylpyrrolidine group is flexible enough to twist around and form a binding contact with ribose oxygen of DA-20. Drug binding through this ribose oxygen is predicted to mimic the binding configuration of the moxifloxacin C7-group and other current fluoroquinolones (Figure 5.1-Panel B). Finally, it is possible for the aminomethyl moiety to form a binding contact with nucleoside base cyclic nitrogen of DA-16.

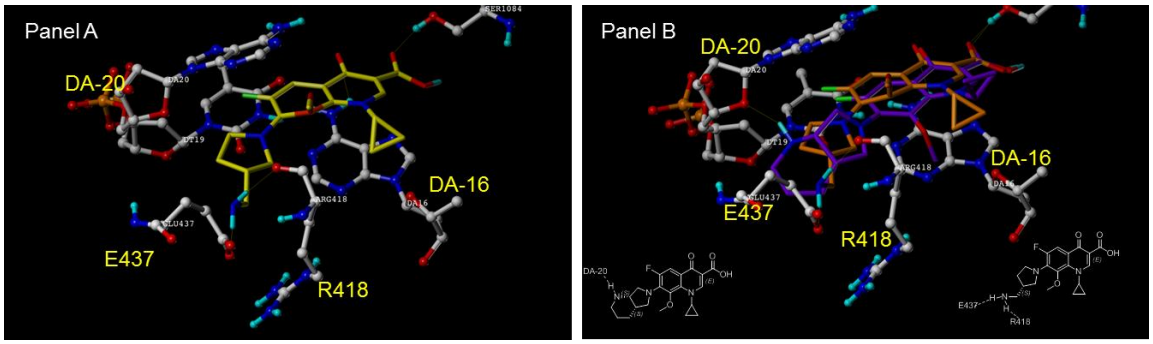

Figure 5.1: Panel A- Binding pose of UING-05-249 with the C7-aminomethylpyrrolidine primary amine forming a divalent binding pose between E437 and the backbone carbonyl of R418 in the 2XKK crystal structure. Panel B- Overlay of moxifloxacin and UING-05-249 binding poses in the 2XKK DNA nicked site. The DA-20 ribose oxygen binding contact of the moxifloxacin C7-group 2°-amine is shared by a binding pose of the C7-aminomethylpyrrolidine group of UING-05-249 (not shown).

With these observations, the investigation of the effect of C7-groups on fluoroquinolone activity with fluoroquinolone-resistant Helix-4 mutants led to exploring structural diversification of the aminomethylpyrrolidine ring of UING-05-249 in an effort to understand the structural requirements of the C7-aminomethylpyrrolidine group to impart activity against Helix-4 mutants that are poorly inhibited by current fluoroquinolones. To this end, four modifications to the C7-aminomethylpyrrolidine group of UING-05-249 were conceived as depicted in Figure 5.2. This series was designed to test the need for the primary basic amine in a C7-aminomethylpyrrolidine group for overcoming resistance, which led to the design and synthesis of compounds UIBW04-259, which has a rigid, non-basic amide side chain, and UIBW04-263, which has a hydroxyl side chain. To test the importance of the positioning of the primary amine of the C7-aminomethylpyrrolidine group, compound UIBW04-261 was designed to possess a primary amine on a shortened side chain that was predicted to reduce interactions with GyrB residues and maintain potential for binding with DA-20 or DA-16. *In silico* modeling of UIBW-04-261 led to the expectation that the aminopyrrolidine

side chain of UIBW-04-261 would closely mimic the binding orientation of the moxifloxacin side chain. The compound UIBW04-267 was designed with a *N*-methyl-aminomethylpyrrolidine side chain. This modification of the C7-aminomethylpyrrolidine side chain prevents the ability of the side chain to form a divalent binding interaction between E437 and the backbone carbonyl of R418 (Figure 5.1-Panel A) while retaining the flexibility of the aminomethylpyrrolidine side chain.

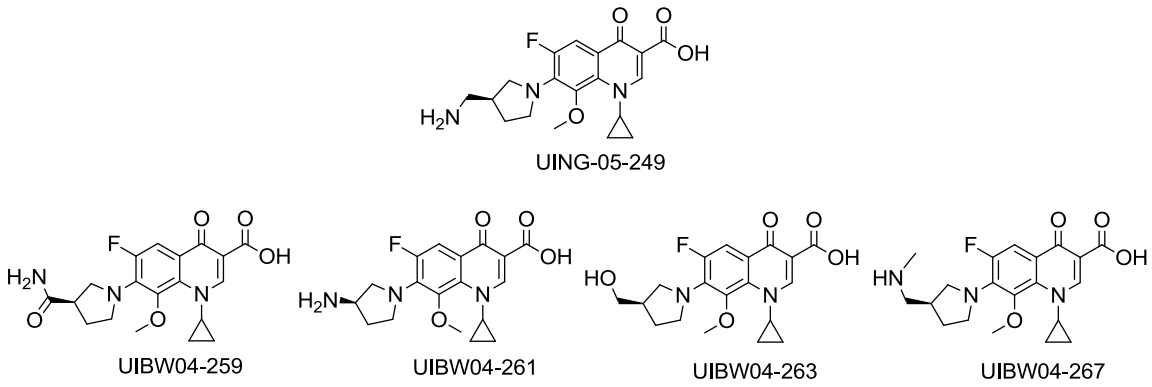

Figure 5.2: The C7-variant fluoroquinolone series, structurally based on the original C7-aminomethylpyrrolidine fluoroquinolone UING-05-249.

5.2: Goals of the Study

The goal of this study was to understand the structural requirements of the C7-aminomethylpyrrolidine side chain to bestow activity to fluoroquinolones against fluoroquinolone-resistant Helix-4 mutants. It is believed that GyrB/ParE-region binding interactions as a way of overcoming fluoroquinolone resistance caused by mutations of the Helix-4 region of DNA gyrase and topoisomerase IV. A secondary goal of this study was to understand the structural requirements of the C7-aminomethylpyrrolidine group to bestow activity with human topoisomerase IIα to fluoroquinolones. In this endeavor, fluoroquinolones were generated with C7-groups that are structural analogs of the

aminomethylpyrrolidine group were designed to vary the C7-group rigidity, positioning of the amine, group basicity, and steric character of the aminomethylpyrrolidine group, and hereafter are referred to as "C7-variant fluoroquinolones". These fluoroquinolones were evaluated for binding affinity in cleaved complexes with docking studies with SYBYL software. The C7-variant fluoroquinolones were also tested in supercoiling inhibition and cleaved complex formation assays with wild-type *E. coli* DNA gyrase and in DNA decatenation assays with wild-type *E. coli* topoisomerase IV. Bacteriostatic assays were also performed in order to test minimum inhibitory concentration in *tolC* KO *E. coli* cells, wild-type *M. smegmatis* cells, and *E. coli* bacteria strains containing fluoroquinolone-resistant Helix-4 mutations to calculate antimutant activities for the compounds.

5.3: Synthesis of C7-Variant Fluoroquinolones

The series of fluoroquinolones with structural variations to the C7-aminomeyhylpyrrolidine group were created by using nucleophilic aromatic substitution to add pyrrolidines, featuring structural diversification of the 3-position, to the C7-position of an N1-cyclopropyl C8-methoxy fluoroquinolone core, as shown in Scheme 5.1. As before, all reactions were performed in dimethylsulfoxide and used 3-10 equivalents of either diisopropylethylamine for the synthesis of UIBW-04-259, UIBW-04-261, and UIBW-04-267, or triethylamine for the synthesis of UIBW-04-263. In the synthesis of UIBW-04-261, following C7-addition the reaction was treated with trifluoroacetic acid to remove the Boc-protecting group. In most cases the reactions produced single products. The C7-addition of the *N*-methyl-aminomethylpyrrolidine to the N1-cyclopropyl C8-methoxy fluoroquinolone core resulted in two regioisomers, however the desired regioisomer UIBW-04-267 was the major product. Detailed synthetic methods are listed in the Experimental Section.

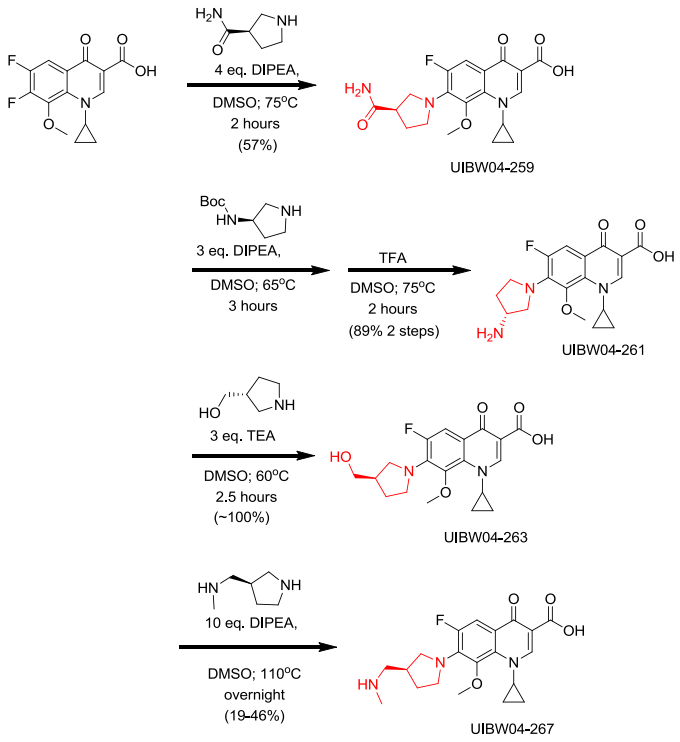

Scheme 5.1: Synthesis of C7-variant fluoroquinolones. Nucleophilic aromatic substitution is used to add the four C7-side chains to an N1-cylcopropyl, C8-methoxy fluoroquinolone core.

5.4: Docking Studies with C7-Variant Fluoroquinolones

The C7-variant fluoroquinolones were docked into the 2XKK crystal structure of *A. baumannii* topoisomerase IV using SYBYL software. Initial studies with wild-type topoisomerase revealed that all compounds were able to dock with comparable affinity to each other and to moxifloxacin, as shown in Figure 5.3. It was also observed that binding orientation for all compounds is conserved in wild-type topoisomerase IV, as shown in Figure 5.4. All compounds are able to bind through the Mg-water bridge. Interestingly, the side chains of the C7-variant fluoroquinolones do not bind through E437 in their highest ranking binding poses. It may be that this contact is only exploited in the case of fluoroquinolone binding without the Mg-water bridge.

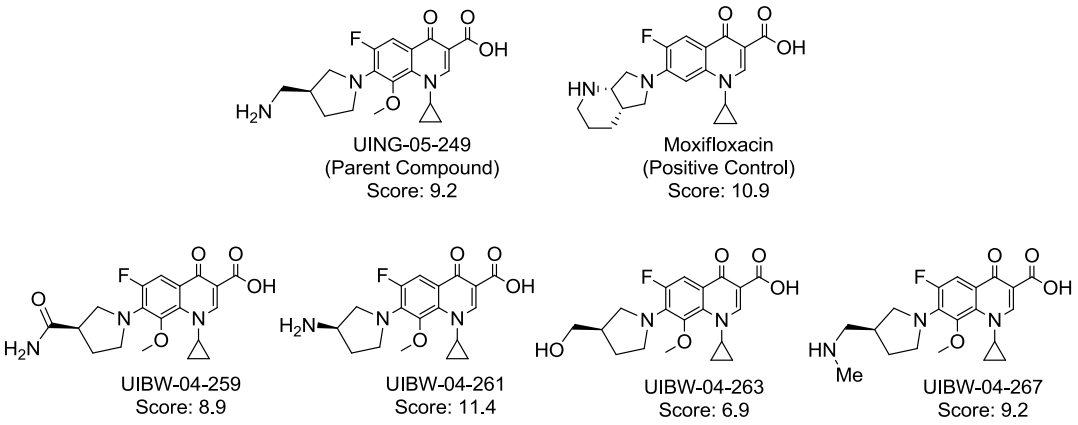

Figure 5.3: The C7-variant fluoroquinolones with SYBYL-generated docking scores as a composite measurement of binding affinity. All C7-variant fluoroquinolones, UING-05-249 and moxifloxacin are able to dock with comparable affinity to each other. All compounds dock into the fluoroquinolone binding-pocket with the Mg-water bridge as the main binding contact.

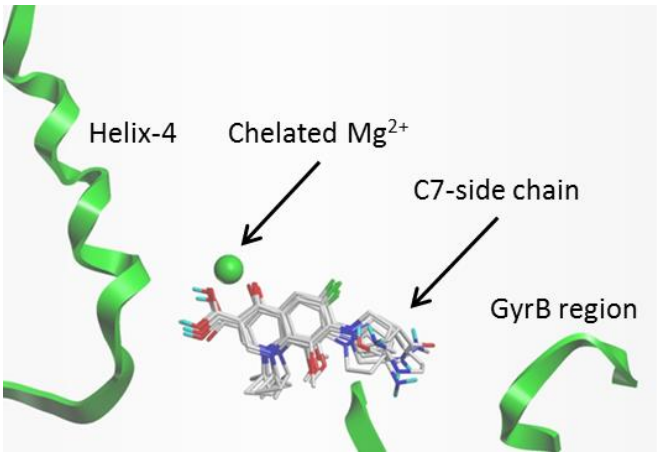

Figure 5.4: Simplified picture of C7-variant fluoroquinolones and UING-05-249 binding into *A. baumannii* crystal structure 2XKK. The highest scoring binding pose of each of the C7-variant fluoroquinolones uses the Mg-water bridge as the major binding contact in wild-type topoisomerase IV.

5.5: Enzyme Inhibition by C7-Variant Fluoroquinolones

Each of the C7-variant fluoroquinolones was tested for the ability to inhibit the supercoiling activity of wild-type *E. coli* DNA gyrase and the decatenation activity of topoisomerase IV in two separate assays: a supercoiling inhibition assay and a DNA decatenation assay, respectively. In the supercoiling inhibition assay, DNA gyrase was incubated with plasmid DNA and to this mixture was added increasing concentrations of each fluoroquinolone. The amount of negatively supercoiled DNA produced as a result of enzyme function was then measured by gel electrophoresis to determine the overall potency of each fluoroquinolone to inhibit the function of *E. coli* DNA gyrase. The concentration of each C7-variant fluoroquinolone required to prevent 50% of DNA gyrase supercoiling activity was determined, as shown in Table 5.1. Comparisons of supercoiling inhibition IC_{50} to the IC_{50} of the parent C7-aminomethylpyrrolidine fluoroquinolone, UING-05-249, are also shown. In the DNA decatenation assay, *E. coli* topoisomerase IV was incubated with catenated (linked) kinetoplast DNA, and to this mixture was added increasing concentration of each fluoroquinolone. The amount of decatenated (separated) kinetoplast DNA produced as a result of topoisomerase IV function was then measured by gel electrophoresis to determine the overall potency of each fluoroquinolone to inhibit the function of *E. coli* topoisomerase IV.[119] As before in Chapter 4.5 with the core-diverse, C7-aminomethylpyrrolidine fluoroquinolones, none of the C7-variant fluoroquinolones exhibited inhibition of DNA decatenation in *E. coli* topoisomerase IV up to a concentration of 2 μM.

Activity against E. coli gyrase (wild type)		
Compounds	IC_{50} (μM) Mean ± SD (n=3 or 4)	IC_{50} Compound/ IC_{50} UING-05-249
UING-05-249	0.177 ± 0.003	
UIBW-04-259	1.45 ± 0.31	8.19
UIBW-04-261	0.386 ± 0.037	2.18
UIBW-04-263	1.29 ± 0.14	7.29
UIBW-04-267	0.347 ± 0.082	1.96

Table 5.1: Inhibition of supercoiling activity of purified wild-type *E. coli* DNA gyrase by C7-variant fluoroquinolones. In the right column is a comparison between the activity of each C7-variant fluoroquinolone and the parent C7-aminomethylpyrrolidine fluoroquinolone, UING-05-249, listed as a ratio of their respective IC_{50} values.

When the supercoiling assay was performed with the C7-variant fluoroquinolones it was found that none of the compounds showed an advantage for inhibition of wild-type *E. coli* DNA gyrase compared to UING-05-249. Indeed, both UIBW-04-261, which has an aminopyrrolidine C7-group, and UIBW-04-267, which has an *N*-methyl-aminomethylpyrrolidine C7-group, had approximately 2-fold higher IC_{50} values compared to UING-05-249. The compound UIBW-04-263, which has a hydroxymethylpyrrolidine C7-group, was considerably less active against wild-type *E. coli* DNA gyrase with a 7.3-fold higher IC_{50} compared to UING-05-249. The compound UIBW-04-259, which has a carbamoylpyrrolidine C7-group, was found to have an 8-fold higher IC_{50} compared to UING-05-249.

A DNA cleavage assay was used to determine the ability of each of the C7-variant fluoroquinolones to poison wild-type *E. coli* DNA gyrase. This assay was performed with each C7-variant fluoroquinolone by measuring the amount of cleaved (linear) complexes of DNA that were released from incubations of the ternary complex upon treatment with the detergent sodium dodecyl sulfate. Briefly, wild-type *E. coli* DNA gyrase was

incubated with circular plasmid DNA. The complex composed of DNA gyrase and DNA was then treated with fluoroquinolone in order to form the ternary complex. The concentration of each fluoroquinolone used was the previously determined wild-type *E. coli* DNA gyrase supercoiling inhibition IC_{50} of the test fluoroquinolone. After incubation, the ternary complex was treated with sodium dodecyl sulfate to dissociate the ternary complex and release the DNA. The amount of cleaved (linear) DNA was then measured by gel electrophoresis.[110] The amount of cleaved DNA that was released indicated of the stability of the ternary complex with the test fluoroquinolone, which in turn was indicative of the extent to which the test fluoroquinolones were capable of poisoning wild-type *E. coli* DNA gyrase. The poisoning-fold stimulation, listed in Table 5.2, is the fold-increase in cleaved DNA observed above baseline at the test compound wild-type *E. coli* DNA gyrase supercoiling inhibition IC_{50}. The CC_3 value, which is listed for each fluoroquinolone in Table 5.2 is the concentration of test fluoroquinolone required to triple the amount of released cleaved complexes.

Cleaved Complex formation in *E. coli* wild-type DNA gyrase		
Compounds	Poisoning (μM) fold-stimulation at IC_{50}	CC_3 (μM)
UING-05-249	18.4 ± 0.3	0.0090 ± 0.0010
UIBW-04-259	18.9 ± 2.8	0.056 ± 0.012
UIBW-04-261	20.8 ± 1.8	0.024 ± 0.001
UIBW-04-263	15.9 ± 2.8	0.055 ± 0.013
UIBW-04-267	13.7 ± 2.7	0.021 ± 0.003

Table 5.2: Poisoning activity measured by formation of cleaved (linear) complexes of DNA as a result of ternary complex formation with C7-variant fluoroquinolones. Poisoning activity was determined as the supercoiling inhibition IC_{50} of each compound, which are listed in Table 5.1.

In the DNA cleavage assay, it was observed that the only C7-variant fluoroquinolone that exhibited higher poisoning activity than the parent compound UING-05-249 was UIBW-04-261, which has an aminopyrrolidine C7-group. The compound UIBW-04-259, which has a carbamoylpyrrolidine C7-group, was found to have similar poisoning activity to UING-05-249. The compound UIBW-04-263, which has a hydroxymethylpyrrolidine C7-group, and UIBW-04-267, which has an *N*-methyl-aminomethylpyrrolidine C7-group, had lower poisoning activity than UING-05-249.

At higher test fluoroquinolone concentrations than CC_3 in the supercoiling inhibition assay, enough of the wild-type *E. coli* DNA gyrase in the incubation solution is bound into a ternary complex to lead to an inhibition of supercoiling activity in DNA gyrase. The IC_{50} of supercoiling inhibition for each fluoroquinolone (Table 5.1) can be interpreted as catalytic inhibition by the fluoroquinolones. To reiterate, catalytic inhibition by fluoroquinolones of type-II bacterial topoisomerases is distinct from the poisoning of type-II bacterial topoisomerases by fluoroquinolones. Type-II bacterial topoisomerases poisoning by a fluoroquinolone specifically refers the ability of the

fluoroquinolone to bind into the double-strand nicks within the bound DNA and inhibit DNA religation. Catalytic inhibition, alternatively, refers to the ability of a fluoroquinolone to inhibit the function of type-II bacterial topoisomerases via a different mechanism than binding into the ternary complex and inhibiting DNA religation. As observed with the core-diverse, C7-aminomethylpyrrolidine fluoroquinolones, comparing the supercoiling inhibition IC_{50} values for the C7-variant fluoroquinolones and their CC_3 values shows a consistent pattern that suggests that supercoiling inhibition strongly relates to ternary complex formation. Therefore the C7-variant fluoroquinolones, like the core-diverse, C7-aminomethylpyrrolidine fluoroquinolones, are able to inhibit the function of wild-type *E coli* DNA gyrase by forming the ternary complex. In other words, the C7-variant fluoroquinolones are not true catalytic inhibitors of wild-type *E coli* DNA gyrase but are instead wild-type *E coli* DNA gyrase poisons.

A goal of this study was to understand structural requirements of the C7-aminomethylpyrrolidine group to improve activity against fluoroquinolone-resistant Helix-4 mutants. Previous studies have demonstrated that it is possible for the C7-aminomethylpyrrolidine group to not only bestow the ability to fluoroquinolones to inhibit *B. anthracis* topoisomerase IV containing fluoroquinolone-resistant Helix-4 amino acid substitutions, but also that the C7-aminomethylpyrrolidine group can bestow the ability to fluoroquinolones to inhibit human topoisomerase IIα.[26] Therefore, the C7-variant compounds were tested for inhibition of purified human topoisomerase IIα in a DNA decatenation assay similar to the previously described DNA decatenation assay performed with wild-type *E. coli* topoisomerase IV. As shown in Table 5.3, of the C7-variant fluoroquinolones, only compound UIBW-04-261 was found to inhibit human enzyme (IC_{50}= 74.4 ± 4.3 μM). Also, UIBW-04-261 inhibits human topoisomerase with 50% the efficacy as UIBW04-236, the only core-diverse, C7-aminomethylpyrrolidine fluoroquinolone to exhibit activity in human topoisomerase IIα.

Activity with Human Topoisomerase IIα			
Compounds	% Inhibition at 100 μM	IC_{50} (μM)	Poisoning (fold-stimulation at IC_{50})
UING-05-249	< 5		
UIBW-04-259	< 5		
UIBW-04-261	50	74.4 ± 4.3	3.95 ± 0.55
UIBW-04-263	< 5		
UIBW-04-267	< 5		

Table 5.3: Decatenation inhibition and poisoning fold-stimulation activity of C7-variant fluoroquinolones with human topoisomerase IIα. Poisoning fold-stimulation by was determined at decatenation inhibition IC_{50}.

5.6: Growth Inhibition Activity by C7-Variant Fluoroquinolones

The C7-variant compounds were found to possess substantial differences in supercoiling inhibition with wild-type *E. coli* DNA gyrase. As with the core-diverse fluoroquinolones, none of the C7-variant fluoroquinolones were found to inhibit decatenation function in wild-type *E. coli* topoisomerase IV. The C7-variant fluoroquinolones were tested for bacteriostatic activity in *tolC* knock-out (KO) *E. coli* and wild-type *M. smegmatis* cultures. This was done by measuring the minimum inhibitory concentration (MIC), which is the minimal concentration of fluoroquinolone required to block visible growth in cultures during an overnight incubation in a series of broth-dilution assays. The results are shown in Table 5.4. *TolC* KO *E. coli* strains were used in order to prevent a reduction in bacteriostatic activity of the C7-variant fluoroquinolones by common efflux pump mechanisms.

Bacteriostatic Activity in wild-type *E. coli* cells

Compound	MIC	Compound MIC/ UING-05-249 MIC
Moxifloxacin	0.0078	2.2
UING-05-249	0.004	
UIBW-04-259	0.002	0.5
UIBW-04-261	0.006 ±0.003	1.6
UIBW-04-263	0.001	0.4
UIBW-04-267	0.005 ±0.001	1.3

Table 5.4: Bacteriostatic activities of C7-variant fluoroquinolones in *tolC* KO *E. coli* cells. The MIC value for Moxifloxacin in *tolC* KO *E. coli* cells was obtained from a separate study.[122]

When C7-variant fluoroquinolones were tested for bacteriostatic activity in *tolC* KO *E. coli,* UIBW-04-261, which has an aminopyrrolidine C7-group, and UIBW-04-267, which has an *N*-methyl-aminomethylpyrrolidine C7-group, were found to have slightly lower activity than UING-04-249 with 1.6-fold and 1.3-fold higher MIC values, respectively. Interestingly, UIBW-04-259, which has a carbamoylpyrrolidine C7-group, had more potent bacteriostatic activity with an MIC that was 2-fold lower than that of UING-05-249. Similarly, UIBW-04-263, which has a hydroxymethylpyrrolidine C7-group, was also found to have increased bacteriostatic activity with an MIC 2.5-fold lower than that of UING-05-249. This was a surprising result as the compounds UIBW-04-259 and UIBW-04-263 performed poorly compared to the other C7-variant fluoroquinolones and UING-05-249 in the supercoiling inhibition assay with wild-type *E. coli* DNA gyrase. The MIC of moxifloxacin with *tolC* KO *E.coli* , which was obtained in a separate study,[122] is higher than the MIC determined for each of the C7-varient fluoroquinolones. This indicates that all of the C7-varient fluoroquinolones have bacteriostatic activity in *tolC* KO *E.coli* that compares favorably to at least one clinical

fluoroquinolone. The bacteriostatic activities of C7-variant fluoroquinolones with wild-type *M. smegmatis* cells are listed in Table 5.5.

Bacteriostatic Activity in wild-type *M. smegmatis* cells

Compound	MIC	MIC Compound/ MIC UING-05-249	$MIC_{M. smeg}$/ $MIC_{E.coli}$
UING-05-249	0.047 ±0.013		12.813
UIBW-04-259	0.078 ±0.034	1.66	44.007
UIBW-04-261	0.058 ±0.007	1.22	9.742
UIBW-04-263	0.14 ±0.04	2.89	106.51
UIBW-04-267	0.022 ±0.003	0.47	4.611

Table 5.5: Bacteriostatic activities of C7-variant fluoroquinolones in wild-type *M. smegmatis* cells. The fold-difference between compound MIC and the MIC of UING-05-249 is listed to in the center-right column. The fold-difference between compound MIC in wild-type *M. smegmatis* cells ($MIC_{M. smeg}$) and MIC in *tolC* KO *E. coli* cells ($MIC_{E.coli}$) is listed in the far right column.

Each of the C7-variant fluoroquinolones was found to possess lower bacteriostatic potency in *M. smegmatis* cells compared to *tolC* KO *E.coli*. The range of MIC values for C7-variant fluoroquinolones obtained in wild-type *M. smegmatis* cells was slightly wider than the range of MIC values obtained in *tolC* KO *E. coli* cells. Compound UIBW-04-259, which has a carbamoylpyrrolidine C7-group, and compound UIBW-04-261, which has an aminopyrrolidine C7-group, were found to have slightly lower bacteriostatic activity than UING-05-249, with MIC's 1.7 and 1.2-fold higher than UING-05-249, respectively. Compound UIBW-04-263, which has a hydroxymethylpyrrolidine C7-group, had the lowest bacteriostatic activity in wild-type *M. smegmatis* cells, with a 3-fold higher MIC than that of UING-05-249. The most potent bacteriostatic activity was seen with UIBW04-267, which has an *N*-methyl-aminomethylpyrrolidine C7-group, with an MIC of 2-fold lower that of UING-05-249. An important trend is also the disconnection in MIC profiles with *E. coli* cells and supercoiling inhibition in *E. coli*

DNA gyrase. In the *E. coli* growth inhibition assay, UIBW-04-259 and UIBW-.04-263 have the lowest MIC's, exhibiting better activity than UING-05-249. However in the *M. smegmatis* growth inhibition assay, only compound UIBW-04-267 possesses a lower MIC than UING-05-249.

5.7: Antimutant Activity of C7-Variant Fluoroquinolones

This study sought to understand the structural requirements of the C7-aminomethylpyrrolidine group to bestow the ability to fluoroquinolones to overcome fluoroquinolone resistance caused by Helix-4 mutations of DNA gyrase and topoisomerase IV. It is believed C7-aminomethylpyrrolidine group is able to bind through GyrB/ParE in the fluoroquinolone binding site within ternary complex, and thus exploit binding interactions separate from the Mg-water bridge. In theory, a fluoroquinolone that has a binding orientation through the Mg-water bridge in wild-type bacterial type-II topoisomerases and possible alternative binding confirmations such as binding through GyrB/ParE contacts or others in the case of being unable to bind through the Mg-water bridge would have increased ability to bind and inhibit the function of bacterial type-II topoisomerases with resistance-causing Helix-4 mutations. In theory this would mean that such a fluoroquinolone would have comparable growth-inhibition activity against wild-type bacteria (by binding through the Mg-water bridge) and fluoroquinolone-resistant bacteria (by binding through GyrB/ParE region). This would result in a fluoroquinolone with a narrow or closed mutant selection window, as explained in Chapter 4.7. The growth inhibition activity of the C7-variant fluoroquinolones was measured in broth dilution assays with the same series of *tolC* KO *E. coli* cells and *tolC* KO *E. coli* strains possessing resistance-causing Helix-4 substitutions used in Chapter 4.7. The term "antimutant activity," in the contest of this thesis, refers to a ratio of C7-variant fluoroquinolone MIC against *tolC E. coli* Helix-4 mutant over MIC of *tolC E. coli* cells without Helix-4 alterations. The following tables

(Table 5.6-9) show the absolute MIC values determined for each of the C7-variant fluoroquinolones as an average of replicate bacteriostatic assays with each *E. coli* mutant strain. The calculated antimutant activities of each of the C7-variant fluoroquinolones are also listed in the far-right column as "mut/wt." The antimutant activities for each compound are also summarized as a bar graph in Figure 5.5. Comparison of the antimutant activity values for each of the C7-variant fluoroquinolones without the context of the absolute MIC's obtained for the each of the compounds with *E. coli* mutant strains can mask the possibility of a compound possessing a very high MIC, and thus very poor bacteriostatic activity, with both *tolC* KO *E.coli* and *tolC* KO *E.coli* possessing Helix-4 or GyrB mutations. Therefore the antimutant activities of the compounds by themselves can be misleading because it is possible for a relatively inactive compound to have antimutant activities close to 1.

Bacteriostatic Activity of Compounds against KD2862 (S83L) cells

Compound	MIC (μM)	mut/wt S83L
UING-05-249	0.014 ±0.002	3.879
UIBW-04-259	0.00869 ±0.00231	4.88062
UIBW-04-261	0.057 ±0.007	9.657
UIBW-04-263	0.006 ±0.008	4.785
UIBW-04-267	0.0205 ±0.0045	4.3158

Bacteriostatic Activity of Compounds against KD2876 (S83W) cells

Compound	MIC (μM)	mut/wt S83W
UING-05-249	0.02138 ±0.00764	5.81897
UIBW-04-259	0.02138 ±0.00764	12.0084
UIBW-04-261	0.0695 ±0.0185	11.7747
UIBW-04-263	0.01225 ±0.00284	9.57031
UIBW-04-267	0.0285 ±0.0035	6.0000

Table 5.6: Average MIC values and standard deviations of C7-variant fluoroquinolones with *E. coli* mutant strains containing serine 83 mutations. The calculated antimutant activity of each compound in the serine 83 mutant strain is listed in the far-right column as "mut/wt."

Bacteriostatic Activity of Compounds against KD2880 (D87N) cells

Compound	MIC (μM)	mut/wt D87N
UING-05-249	0.017 ±0.005	4.730
UIBW-04-259	0.009 ±0.002	4.880
UIBW-04-261	0.057 ±0.007	9.657
UIBW-04-263	0.005 ±0.002	4.174
UIBW-04-267	0.017 ±0.005	3.658

Bacteriostatic Activity of Compounds against KD2866 (D87Y) cells

Compound	MIC (μM)	mut/wt D87Y
UING-05-249	0.014 ±0.002	3.879
UIBW-04-259	0.00713 ±0.00088	4.00281
UIBW-04-261	0.057 ±0.007	9.657
UIBW-04-263	0.00356 ±0.00044	2.78125
UIBW-04-267	0.01425 ±0.00175	3.00000

Table 5.7: Average MIC values and standard deviations of C7-variant fluoroquinolones with *E. coli* mutant strains containing aspartic acid 87 mutations. The calculated antimutant activity of each compound in the aspartic acid 87 mutant strain is listed in the far-right column as "mut/wt."

Bacteriostatic Activity of Compounds against KD2882 (G81C) cells

Compound	MIC (μM)	mut/wt G81C
UING-05-249	0.010 ±0.002	0.719
UIBW-04-259	0.009 ±0.002	1.000
UIBW-04-261	0.029 ±0.004	0.500
UIBW-04-263	0.0036	0.5812
UIBW-04-267	0.010 ±0.002	0.500

Bacteriostatic Activity of Compounds against KD2956 (D82A) cells

Compound	MIC (μM)	mut/wt D82A
UING-05-249	0.0036	0.2526
UIBW-04-259	0.0018	0.2049
UIBW-04-261	0.008 ±0.004	0.145
UIBW-04-263	0.006 ±0.001	1.000
UIBW-04-267	0.007 ±0.001	0.348

Bacteriostatic Activity of Compounds against KD2864 (A84P) cells

Compound	MIC (μM)	mut/wt A84P
UING-05-249	0.00713 ±0.00088	1.93966
UIBW-04-259	0.0036	2.0000
UIBW-04-261	0.029 ±0.004	4.828
UIBW-04-263	0.0018	1.3906
UIBW-04-267	0.010 ±0.002	2.158

Table 5.8: Average MIC values and standard deviations of C7-variant fluoroquinolones with *E. coli* mutant strains containing Helix-4 mutations separate from residues that coordinate the Mg-water bridge. The calculated antimutant activity of each compound in the listed mutant strain in each subsection of the table is listed in the far-right column as "mut/wt."

Bacteriostatic Activity of Compounds against KD2932 (D426N) cells

Compound	MIC (uM)	mut/wt D426N
UING-05-249	0.0036	0.9692
UIBW-04-259	0.0013	0.7191
UIBW-04-261	0.007 ±0.001	1.207
UIBW-04-263	0.0007	0.5078
UIBW-04-267	0.0036	0.7495

Bacteriostatic Activity of Compounds against KD2934 (K447E) cells

Compound	MIC (uM)	mut/wt K447E
UING-05-249	0.0018 ±0.0004	0.4846
UIBW-04-259	0.0018	1
UIBW-04-261	0.0018	0.3016
UIBW-04-263	0.0018	1.3916
UIBW-04-267	0.0018	0.3747

Table 5.9: Average MIC values and standard deviations of C7-variant fluoroquinolones with *E. coli* mutant strains containing GyrB-region mutations. The calculated antimutant activity of each compound with the given mutant strain of each subsection of the table is listed in the far-right column as "mut/wt"

A broad trend in the absolute MIC values determined for the C7-variant fluoroquinolones, across all of the *E. coli* mutant strains in which they were tested for bacteriostatic activity, is that all C7-variant fluoroquinolones have comparable bacteriostatic activity to UING-05-249 in that all compounds have MIC's that are within 5-fold difference of the MIC of UING-05-249 in each *E. coli* mutant strain. This trend lends credibility to the antimutant activities that were determined for each of the C7-variant fluoroquinolones because this trend removes the possibility for a compound to demonstrate promising antimutant activity which in fact masks the fact that the compound simply possesses high MIC values with both *tolC* KO *E.coli* and *tolC* KO *E.coli* strain possessing Helix-4 or GyrB mutations. The absolute MIC data from the C7-variant fluoroquinolones also shows that the compounds UIBW-04-259 and UIBW-04-

263 almost consistently possess either lower MIC values than UING-05-249 or very similar MIC values to UING-05-249 with each of *tolC* KO *E.coli* strain possessing Helix-4 or GyrB mutations. The single exception is the MIC of UIBW-04-263 with the *tolC* KO *E.coli* strain possessing the D82A mutation, which is 1.7-fold higher than the MIC determined for UING-05-249 with that strain. Otherwise, the compounds UIBW-04-259 and UIBW-04-263 demonstrate consistently more potent or equipotent inhibition of cell growth in of *tolC* KO *E.coli* strains possessing Helix-4 or GyrB mutations compared to UING-05-249. As shown in Figure 5.5, the trend of the superior or equipotent bacteriostatic activity of UIBW-04-259 and UIBW-04-263 does not translate into these compounds possessing superior antimutant activity profiles compared to UING-05-249.

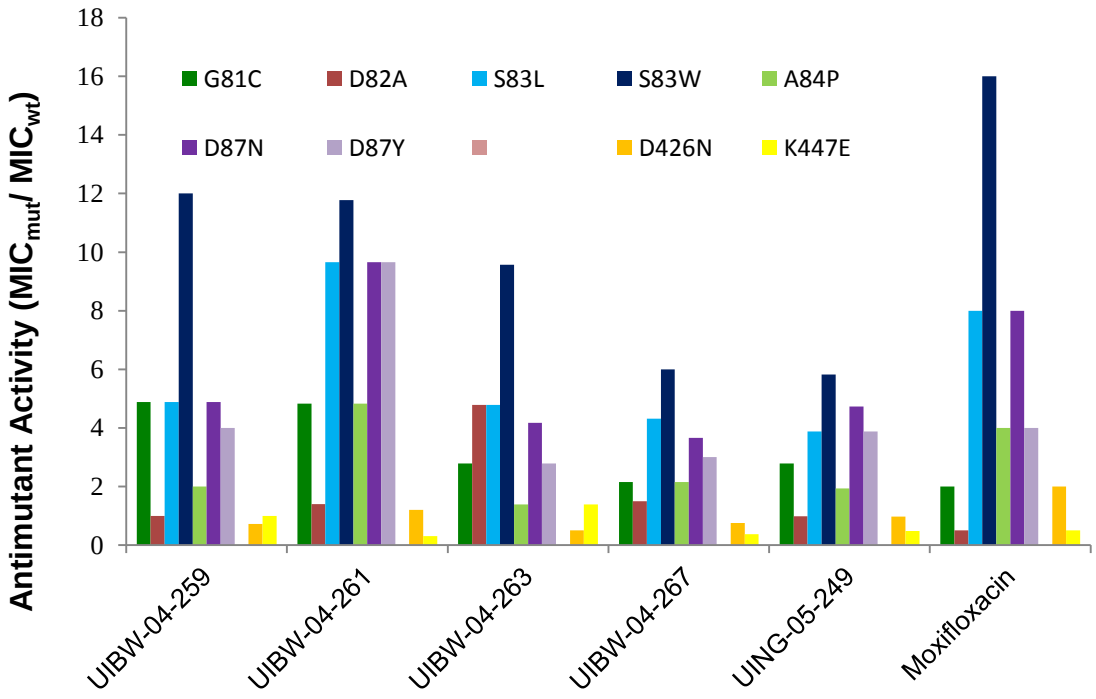

Figure 5.5: Antimutant activities (y-axis) for each of the C7-variant fluoroquinolones (x-axis) with *E. coli* Helix-4 mutants (G81C- dark green, D82A- brown, S83L- blue, S83W- dark purple, A84P-light green, D87N- purple, D87Y- gray) and *E. coli* GyrB mutants (D426N- orange, K447E- yellow). The antimutant activities shown for moxifloxacin were adapted from a previous study.[122]

Though the MIC values of the C7-variant fluoroquinolones compare reasonably well to the MIC of UING-05-249 in the growth inhibition assays, none of the compounds were found to possess substantially superior antimutant activity across the panel of *E. coli* mutant strains. Interestingly, UIBW-04-263, which has a hydroxymethylpyrrolidine C7-group, is uniquely affected by the D82A Helix-4 substitution and possesses an antimutant activity of 4.8 with the *tolC* KO *E.coli* strain possessing that substitution. This effect of the Helix-4 D82A substitution is not only unique among the C7-variant fluoroquinolones but this effect is absent in the core-diverse, C7-aminomethylpyrrolidine fluoroquinolones as well. The highest antimutant activities determined for the C7-variant fluoroquinolones are observed with the *tolC* KO *E.coli* strains possessing Helix-4 mutations to the S83 and D87 residues, which is not surprising because these residues coordinate the Mg-water bridge. Of the *tolC* KO *E.coli* strains possessing Helix-4 substitutions to the residues that coordinate the Mg-water bridge, the antimutant activities determined for all C7-variant fluoroquinolones are highest with the *tolC* KO *E.coli* strain possessing the Helix-4 S83W substitution. The MIC of the UIBW-04-263 compound is slightly higher with the *tolC* KO *E.coli* strains possessing the GyrB K447E substitution, with an antimutant activity of 1.4. Interestingly, the antimutant activity of UIBW-04-263 is lower against the *tolC* KO *E.coli* strains possessing the GyrB D426N mutation with antimutant activity of 0.5. The antimutant activity of UIBW-04-259 is 0.7 with the *tolC* KO *E.coli* strains possessing the Helix-4 D426N substitution. The antimutant activity of UIBW-04-267 also has an antimutant activity of 0.7 with the *tolC* KO *E.coli* strains possessing the Helix-4 D426N substitution. The antimutant activities observed for UIBW-04-261, which has an aminopyrrolidine C7-group, are higher with *tolC* KO *E.coli* strains possessing any of the Helix-4 substitutions to the S83 and D87 residues, which may be reflective of the diminished ability of the C7-aminopyrrolidine side chain to bind to GyrB compared to other C7-variant fluoroquinolones. Surprisingly, UIBW-04-261 and moxifloxacin have similar antimutant activity of 0.3 and ~0.5, respectively, with *tolC* KO *E.coli* strains

possessing the GyrB K447E substitution, which is similar to the antimutant activity of 0.5 determined for UING-05-249 with that *tolC* KO *E.coli* strain. This was not expected because neither UIBW-04-261 nor moxifloxacin is expected to make binding contact with GyrB and therefore the antimutant activities of both compounds with *tolC* KO *E.coli* strains possessing either the D426N or K447E GyrB substitutions should be approximately 1. The UIBW-04-259 compound is equipotent with *tolC* KO *E.coli* and *tolC* KO *E.coli* strains possessing the GyrB K447E substitution, which suggests that the carbamoylpyrrolidine C7-group of UIBW-04-259 does not make binding contact through acidic GyrB residues. The antimutant activity of UIBW-04-263 is 1.4, which suggests that the hydroxymethylpyrrolidine C7-group also does not make binding contact through acidic GyrB residues. Interestingly, a broad trend in antimutant activity profiles of C7-vairant fluoroquinolones is that all compounds possess inferior profiles to UING-05-249. The single exception to this is UIBW-04-267, which has equivalent or lower antimutant activity with most *tolC* KO *E.coli* strains possessing either Helix-4 or GyrB substitutions. Only the antimutant activity of UIBW-04-267 with *tolC* KO *E.coli* strains possessing the Helix-4 D82A substitution is substantially higher than the antimutant activity of UING-05-249 with the same strain. As with the studies with the core-diverse fluoroquinolones, it is important to consider the antimutant activity profiles of these C7-variant fluoroquinolones in reference to the antimutant activity profile for moxifloxacin, which was obtained in a previous study.[122] As shown in Figure 5.5, all C7-variant compounds and UING-05-249 have overall superior antimutant activity to moxifloxacin across the *tolC* KO *E.coli* mutant strains tested.

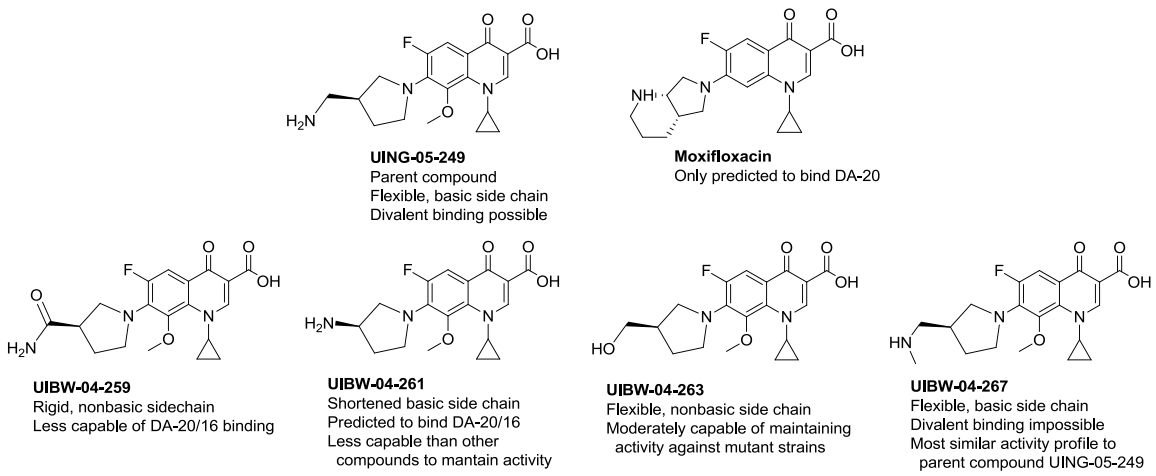

Figure 5.6: Summary of global observations from antimutant activities determined for C7-variant fluoroquinolones, comparing their overall abilities to maintain activity with fluoroquinolone-resistant *E. coli* mutant strains.

CHAPTER VI: EXPERIMENTAL SECTION

6.1: General Methods

All reagents were purchased from commercial sources and used without further purification. Semi-preparative HPLC separations to purify final compounds were carried out with a Restek-Luna 5µm PFP (150 mm×21.2 mm) column for all other compounds connected to a Shimadzu system that was equipped with two LC-10AT pumps (one for solvent A and one for solvent B), SPD-M10Avp photodiode array detector, and SCL-10Avp system controller. The system was connected to a Dell Optiplex 755 and controlled by Shimadzu EZ-Start Version 7.4 software.

H^1-NMR and Mass Spectrometry Data: All synthetic derivatives were characterized by nuclear magnetic resonance (NMR) and mass spectrometry. Routine NMR spectra were obtained for 1H and 19F using a Bruker Ultrashield 300 MHz instrument at ambient temperature. Chemical shifts are reported in parts per million from low to high field and referenced to residual solvent. Standard abbreviations indicating multiplicity are used as follows: br s = broad singlet, d = doublet, m = multiplet, s = singlet, and t = triplet. In all cases $CDCl_3$ or d-DMSO were used as the solvent unless otherwise noted. Low resolution mass spectrometry (LRMS) was determined using a Thermo LCQ Deca mass spectrometer with electrospray ionization (ESI) and quadrupole ion trap mass analyzer.

HPLC Methodology: All final compounds were purified >95%, as determined by analytical high-performance liquid chromatography (HPLC). The analytical HPLC analysis was determined using a Shimadzu system equipped with LC-20AT pump, DGU-14A degasser, CBM-20A system controller, and SPD-M10Av photodiode array detector. The system was connected to a Dell Optiplex GX400 PC and controlled by Shimadzu Client/Server Version 7.4 software. A Restek Allure PFP Propyl (150mm x 4.6 mm) 5um column was used as stationary phase, while mobile phase consisted of solvent A (water,

buffered 0.1% trifluoroacetic acid) and solvent B (acetonitrile, buffered 0.1% trifluoroacetic acid). Gradient elution used the following program: from t=0 min [solvent A (0.95mL/min), solvent B (0.05mL/min)] to t =30min [solvent A (0.05mL/min), solvent B (0.95mL/min)], to t=35 min [solvent A (0.05mL/min), solvent B (0.95mL/min)], to t =40 [solvent A (0.95mL/min), solvent B (0.05mL/min)]. Analytical HPLC was used to monitor reactions, as well as to determine purity for final products.

6.2: Synthesis of Intermediates to Obtain 5, 6-phenyl Fluoroquinolone and Dione Cores (Chapter 3)

6.2.1: Preparation of Isoquinolone-1, 3 (2*H*, 4*H*)-dione (**6**) (**UIBW01-236**)

Commercially available homophthalic acid (10.0 g, 55.6 mmol) was stirred to suspension in 28% NH_4OH solution (7.5 mL) in a 100 mL round-bottom flask. The gold-colored mixture with visible precipitate was stirred for an additional 30 min, and then the solvent was removed *in vacuo*. The resulting dark gel was then dissolved in a second volume of NH_4OH (7.5 mL) and stirred for 30 minutes. The solvent was removed *in vacuo* and the resultant dark gel was then dissolved in *o*-dichlorobenzene (20 mL) and heated, uncovered, to 200^oC. During this time the solution became very dark orange. After 3 hours an argon stream was directed into the flask to facilitate solvent evaporation. Once the solvent was removed and the yellow solid had completely dried, the yellow solid was cooled to room temperature, then suspended in MeOH (20 mL) and allowed to stand overnight at room temperature. The resulting white precipitate was filtered via a Buchner funnel, washed with volumes of cold MeOH (3*20 mL), and dried (7.05 g; 78.8 %). The product was used in the subsequent reaction without purification. ^{1}H-NMR (300 MHz, $CDCl_3$): 8.25 ppm (dd, 1H, J_1=7.5 Hz, J_2=1.2 Hz), 7.66 ppm (dt, 1H, J_1= 7.5 Hz, J_2= 1.8 Hz), 7.50 ppm (t, 1H, J_1=7.8 Hz), 7.35 ppm (d, 1H, J_1=7.2 Hz), 7.29 ppm (s, solvent),

4.06 ppm (s, 2H), 1.56 ppm (m, H_2O). LRMS (ESI) calculated for (M+H+) 161.05, found 324.92 [2M+2H].

6.2.2: Preparation of 1, 3-dichloroisoquinolone (**7**) (**UIBW01-239**)

The dried yellow solid of BW01-236 (7.05 g, 43.7 mmol) was suspended in phenylphosphonic dicholoride (12.4 mL) with gentle stirring. The yellow slurry was then heated to 160^{o}C for 3 hours, during which time the solution darkened. The dark-colored mixture was then allowed to cool overnight with continued stirring. The resulting waxy orange material was then diluted with THF (200 mL) and treated with H_2O (60 mL). The THF was removed *in vacuo* and the water was neutralized with 28% aq. NH_4OH (15 mL). The cream-colored precipitate that evolved was then extracted with ethyl acetate (3*100 mL). The organic phases were combined, washed with brine (~30 mL), dried over Na_2SO_4, and concentrated *in vacuo* to produce a yellow-cream powder (88.9%). This yellow-cream powder was used in subsequent reactions without further purification. ^{1}H-NMR (300 MHz, DMSO-d_6): 8.30 ppm (d, 1H, J_1= 8.7 Hz), 8.17 ppm (s, 1H), 8.09 ppm (d, 1H, J_1= 7.8 Hz), 7.96 ppm (dt, 1H, J_1= 6.9 Hz, J_2= 1.2 Hz), 7.81 ppm (dt, 1H, J_1= 6.9 Hz, J_2= 1.2 Hz), 3.33 ppm (s, H_2O), 4.10 ppm (q), 2.00 ppm (s), 1.20 ppm (t); EtOAc, 2.50 ppm (m, DMSO). ^{13}C-NMR (300 MHz, d-DMSO): 150.106 ppm, 142.070 ppm, 139.663 ppm, 133.274 ppm, 130.268 ppm, 127.358 ppm, 126.187 ppm, 125.491 ppm, 120.935 ppm. LRMS (ESI) calculated for ($M+H^+$) 198.05; found 221.03 (M+Na). HPLC retention measured as 23.02 minutes on 5-95%. MeCN:H_2O 30 minute gradient.

6.2.3: Preparation of 1,3-dichloroisoquinoline-4-carboxylic acid (**8**) (**UIBW02-121**)

Lithium-diisopropylamine solution was freshly prepared by suspension of diisopropylamine (0.06 mL, 0.56 mmol) that had been freshly distilled over CaH_2 into dry THF (3 mL) in a flame-dried 10 mL flask under argon. This was cooled to -78^{o}C in a

dry ice/acetone bath. The n-butyllithium solution (1.6 M in hexanes, 0.35 mL, 0.51 mmol) was then added, and the solution was stirred at temperature for 10 minutes, warmed to 0°C with an ice water bath and stirred for 10 minutes, and chilled back to -78°C. This entire solution was then cannulated into a 25 mL flask containing thrice-benzene-dried 1,3 dichloroisoquinolone **8** (100.0 mg, 0.51 mmol) suspended in dry THF (5 mL) under argon. The mixture was then chilled to -78°C. The starting material solution changed from clear yellow to bright orange or red immediately. This mixture was stirred for 2 hours at -78°C. A separate 250mL flame-dried round-bottom flask was placed under vacuum for 5 minutes, then filled with CO_2, then placed under vacuum again and subsequently filled again with CO_2. This operation was repeated three times. The CO_2 from this round-bottom flask was then introduced into the flask containing the lithiated dichloroisoquinolone via cannula, with the tip of the cannula inserted beneath the surface of the THF. The reaction solution was then permitted to warm to room temperature and CO_2 was continuously pumped through the solution overnight with vigorous stirring. Immediately upon addition of the CO_2 into the reaction flask the clear, bright orange solution became canary-yellow slurry. The reaction was quenched by the addition of H_2O. The aqueous phase was adjusted to pH~1 with concentrated HCl. The precipitate was then separated via centrifuge, then taken up into MeOH and dried *in vacuo*. (Yield= 123 mg, ~100%). ^{1}H-NMR (300 MHz, $CDCl_3$): 8.429 ppm (d, 1H, J_1= 8.1 Hz), 8.039 ppm (d, 1H, J_1= 8.1 Hz), 7.906 ppm (dt, 1H, J_1= 7.2, Hz, J_2= 1.2 Hz), 7.788 ppm (dt, 1H, J_1= 7.2, Hz, J_2= 1.2 Hz), 7.29 ppm (s, $CHCl_3$), 2.10 ppm (s, acetone), 1.56 ppm (m, H_2O). LRMS (ESI) calculated for ($M\text{-}H^+$) 240.97, found 239.99 [M-H]. HPLC retention measured as 17.46 minutes on 5-95%. MeCN:H_2O 30 minute gradient.

6.2.4: Preparation of 1,3-dichloroisoquinoline-4-carboxamide (**9**) (**UIBW02-297**)

1,3-dichloroisoquinoline-4-carboxylic acid **8** (150 mg, 0.62 mmol) was dissolved in dry toluene (2 mL) in a flame-dried 25 mL 2-neck round-bottom flask fitted with a condenser and under argon atmosphere. To this yellow solution was dropwise added a catalytic amount of DMF (2 drops) and thionyl chloride (0.09 mL, 1.25 mmol). The reaction mixture was then heated to 85^{o}C for two hours and darkened to a brownish color over that time. Afterwards, the brown reaction slurry was cooled to room temperature and the solvent was removed *in vacuo*. To remove the unreacted thionyl chloride, the residual dark oil was dissolved in toluene (15 mL) and evaporated to dryness, then dissolved in CH_2Cl_2 (15 mL) and evaporated to dryness. The light-yellow powder was re-dissolved in CH_2Cl_2 (15 mL) and evaporated to dryness twice more. The residual light-yellow powder was then suspended in CH_2Cl_2 (3 mL) and cooled to 0^{o}C in an ice/ water bath. To this was then dropwise added aqueous ammonium hydroxide (28% solution, 0.6 mL, 9.3 mmol) and the reaction mixture was stirred for 1.5 hours, then poured over H_2O (3mL). The light-yellow precipitate was then extracted several times with ethyl acetate and CH_2Cl_2. The organic phases were combined, washed with water (5 mL) and brine (5 mL), then dried over Na_2SO_4 and concentrated *in vacuo*. Yield: 117 mg (77.6%, 2 steps). ^{1}H-NMR (300 MHz, $CDCl_3$): 8.40 ppm (ddd, 1H, J_1= 8.4 Hz, J_2= 0.6 Hz, J_3= 0.3 Hz), 8.03 ppm (ddd, 1H, J_1= 8.4 Hz, J_2= 0.6 Hz, J_3= 0.3 Hz), 7.88 ppm (dt, 1H, J_1= 7.2 Hz, J_2= 1.5 Hz), 7.77 ppm (dt, 1H, J_1= 8.4 Hz, J_2= 1.2 Hz), 7.29 ppm (s, $CHCl_3$), 6.18 ppm (bs, 1H), 6.02 ppm (bs, 1H), 1.56 ppm (s, H_2O), 1.50 ppm (solvent). LRMS (ESI) calculated for ($M+H^+$) 239.99, found 240.99 [M+1]. HPLC retention measured as 13.99 minutes on 5-95%. MeCN:H_2O 30 minute gradient.

6.2.5: Preparation of ethyl 3-(1,3-dichloroisoquinoline-4-yl)-3-oxopropanoate (**10**) (**UIBW02-299**)

1,3-dichloroisoquinoline-4-carboxylic acid **8** (500.0 mg, 2.1 mmol) was dissolved in dry toluene (20 mL) in a flame-dried 100 mL round-bottom flask under argon. To this yellow solution was dropwise added a catalytic amount of DMF (4-5 drops) and thionyl chloride (0.30 mL, 4.14 mmol). The yellow-orange reaction mixture was then heated to 85ºC for two hours and darkened to a brownish color over that time. Afterwards, the brown reaction solution was permitted to cool to room temperature and the solvent was removed *in vacuo*. To remove any unreacted thionyl chloride, the residual brown gel was dissolved in toluene (25 mL) and concentrated *in vacuo,* then re-dissolved in CH_2Cl_2 (25 mL) and evaporated to dryness twice. Over the course of this operation, the material lightened in color to a light yellow powder. The material was then re-dissolved in CH_2Cl_2 (25 mL) under argon and cooled to -78ºC in a dry ice/methanol bath. To the solution was then dropwise added methyllithium solution (1.6 M in ether, 3.9 mL, 6.21 mmol), and the solution was stirred at -78ºC for 1.5 hours then quenched with water and warmed to room temperature. The solution was extracted with ethyl acetate several times. The organic phases were combined, washed with water and brine, then dried over Na_2SO_4 and concentrated *in vacuo* to grant **15** as a yellow powder. The yellow powder **15** was then suspended in dry THF (25 mL) and cooled to -78ºC in a dry ice/methanol bath. To the solution was then dropwise added lithium bis-(trimethylsilyl)amide (1.0 M in THF, 3.1 mL, 3.11 mmol). The reaction mixture was stirred at -78ºC for 1 hour, then ethyl chloroformate (0.50 mL, 4.14 mmol) was dropwise added and the reaction was allowed to warm to room temperature as it stirred overnight. The reaction was then quenched with water (3mL) and extracted several times with ethyl acetate (2*30 mL) and CH_2Cl_2 (2*30 mL). The organic phases were combined, washed with water (5 mL) and brine (5 mL), then dried over Na_2SO_4 and evaporated to a cream-colored powder. The crude material was subjected to column chromatography (5:1 hexanes: ethyl acetate) to provide product

10 as a cream-colored powder. Yield: 262 mg (41% over 4 steps). ^{1}H-NMR (300 MHz, $CDCl_3$): 8.36 ppm (d, 1H, J_1= 8.7 Hz), 8.28 ppm (d, 1H, J_1= 8.4 Hz), 7.86 ppm (dt, 1H, J_1= 7.5 Hz, J_2= 1.2 Hz), 7.74 ppm (dt, 1H, J_1= 6.9 Hz, J_2= 1.5 Hz), 7.29 ppm (s, $CHCl_3$), 5.81 ppm (d, 1H, J_1= 2.7 Hz), 5.25 ppm (d, 1H, J_1= 2.7 Hz), 4.19 ppm (q, 2H, J_1= 6.9 Hz), 1.30 ppm (t, 3H, J_1= 6.9 Hz). LRMS (ESI) calculated for ($M+H^+$) 311.01, found 312.02 [M+H] and 314.02 [Cl isotope peak]. HPLC retention measured as 24.50 minutes on a 5-95%. MeCN:H_2O 30 minute gradient.

.

6.3: Synthesis of Intermediates to Obtain 4, 5-pyrimidine Fluoroquinolone Core (Chapter 3)

6.3.1: Preparation of 1-cyclopropyl-6,7-difluoro-8-methoxy-5-nitro-4-oxo-1,4-dihydroquinoline-3-carboxylic acid (**21**) (**UIBW02-067**)

Commercially available 1-cyclopropyl-6,7-difluoro-8-methoxy-4-oxo-1,4-dihydroquinoline-3-carboxylic acid (500.0 mg, 1.70 mmol) was dissolved in concentrated sulfuric acid (12 mL) and cooled to 0^{o}C in an ice water bath, forming an orange solution. To this was added potassium nitrate (240 mg, 2.37 mmol) as the mixture was stirred vigorously at 0^{o}C for 3 hours. The reaction mixture was then poured into ice water (300 mL), causing a white precipitate to form. This was separated via a Buchner funnel, washed with cold water (20 mL), and dried by dissolving into acetone (50 mL) then evaporating to give **21** as a canary-yellow powder. Yield: 567 mg (98.5%). ^{1}H-NMR (300 MHz, DMSO-d_6): 13.53 ppm (bs, 1H), 8.79 ppm (s, 1H), 4.23 ppm (m, 1H), 4.15 ppm (s, 3H), 3.33 ppm (s, H_2O), 2.50 ppm (m, DMSO), 1.13 ppm (m, 4H). ^{19}F-NMR (292 MHz, DMSO-d_6): -140.121 (dd, 1F), -148.614 (d, 1F). HPLC retention measured as 20.46 minutes on a 5-95%. MeCN:H_2O 30 minute gradient. This product had been made before

by our group and spectral data matched with previously characterized product. Therefore this material was not characterized beyond NMR and HPLC.

6.3.2: Preparation of methyl 1-cyclopropyl-6,7-difluoro-8-methoxy-5-nitro-4-oxo-1,4-dihydroquinoline-3-carboxylate (**22**) (**UIBW02-068**)

The canary-yellow powder **21** (567 mg, 1.67 mmol) was dissolved into acetone (35 mL), in which was also suspended oven-dried potassium carbonate (1.38 g, 8.35 mmol). To this mixture was dropwise added dimethyl sulfate (0.17 mL, 1.8 mmol), after which the reaction flask was fitted with a condenser and heated to 80^{o}C for 4 hours. The reaction was then cooled to room temperature and then quenched with saturated aqueous sodium bicarbonate (10 mL). The acetone was removed *in vacuo* and the murky aqueous solution was extracted several times with CH_2Cl_2 (6*50 mL). The organic phases were combined, washed with water (5 mL) and brine (5 mL), then dried over Na_2SO_4 and evaporated to give **22** as a light-yellow solid. Yield: 437 mg (73.9%) ^{1}H-NMR (300 MHz, $CDCl_3$): 8.67 ppm (s, 1H), 7.29 ppm (s, $CHCl_3$), 4.19 ppm (s, 3H), 4.06 ppm (m, 1H), 3.91 ppm (s, 3H), 1.56 ppm (s, H_2O), 1.25 ppm (m, 2H), 1.07 ppm (m, 2H). ^{19}F-NMR (292 MHz, $CDCl_3$): -141.603 (d, 1F), -147.576 (d, 1F). HPLC retention measured as 18.87 minutes on a 5-95%. MeCN:H_2O 30 minute gradient. This product had been made before by our group and spectral data matched with previously characterized product. Therefore this material was not characterized beyond NMR and HPLC.

6.3.3: Preparation of methyl 5-amino-1-cyclopropyl-6,7-difluoro-8-methoxy-4-oxo-1,4-dihydroquinoline-3-carboxylate (**23**) (**UIBW02-196**)

The light-yellow solid **22** (579 mg, 1.63 mmol) was suspended in of a 2:1 mixture of benzene: ethanol (30 mL) in a 75 mL conical flask. To this was added a small amount of palladium on charcoal (~10-20 mg). The flask was then fitted with a hydrogen gas

balloon via a three way valve. The reaction flask was purged of air, and then filled with hydrogen gas from the balloon. This was repeated 5-6 times to ensure complete removal of air. The reaction was then left open to the hydrogen balloon and stirred very vigorously for 4 days at room temperature. The resultant black slurry was then filtered through Celite, washed with 10:10:1 MeOH: CH_2Cl_2: aqueous 28% ammonium hydroxide (42 mL). The resultant dark gold solution was then dried over Na_2SO_4 and evaporated to dryness to produce **23** as bright yellow solid. Yield: 489 mg (89.1%). ^{1}H NMR (300 MHz, $CDCl_3$): 8.51 ppm (s, 1H), 7.29 ppm (s, $CHCl_3$), 6.92 ppm (bs, 2H), 3.95 ppm (m, 1H), 3.92 ppm (s, 3H), 3.88 ppm (s, 3H), 1.17 ppm (m, 2H), 0.96 ppm (m, 2H). ^{19}F-NMR (292 MHz, $CDCl_3$): -145.223 (d, 1F), -164.170 (d, 1F). HPLC retention measured as 17.09 minutes on a 5-95%. MeCN:H_2O 30 minute gradient. This product had been made before by our group and spectral data matched with previously characterized product. Therefore this material was not characterized beyond NMR and HPLC.

6.3.4: Preparation of methyl 6-cyclopropyl-8,9-difluoro-7-methoxy-6H-pyrido[4,3,2-de]quinazoline-4-carboxylate (**24**) (**UIBW02-157**)

The product **23** (25 mg, 0.084 mmol) was suspended in of toluene (4 mL) treated with dimethylacetamide (2 drops) to improve solubility. To this was dropwise added of concentrated sulfuric acid (3-4 drops, ~1.5 equ.). The yellow solution was then stirred for 30 minutes, and then formamide (4-5 drops, ~2 equ.) were added. The reaction flask was then fitted with a refluxing column and heated to 110^{o}C for 6 hours. The reaction was quenched with saturated aqueous sodium bicarbonate (3 mL). The toluene was removed *in vacuo* and the aqueous material was extracted several times with ethyl acetate (5*15 mL). The organic phases were combined then dried over Na_2SO_4 and concentrated to produce crude product **24** as a light-colored powder. The calculated percent yield was

105%, indicating an impurity that was later characterized on HPLC as a small amount of residual starting material. ^{1}H NMR (300 MHz, DMSO-d_6): 8.85 ppm (bs, 1H), 8.53 ppm (s, 1H), 4.09 ppm (m, 1H), 3.99 ppm (s, 3H), 3.76 ppm (s, 3H), 3.33 ppm (s, H_2O), 2.50 ppm (m, DMSO), 1.08 ppm (m, 2H), 0.98 ppm (m, 2H). ^{19}F-NMR (292 MHz, DMSO-d_6): -145.0 (d, 1F), -163.793 (d, 1F). LRMS (ESI) calculated for ($M+H^+$) 333.09, found 334.26 [M+H]. HPLC retention measured as 15.51 minutes on 5-95% aqu. MeCN over 30 minute gradient.

6.4 Synthesis of Core-Diverse 7-Aminomethylpyrrolidine Fluoroquinolones (Chapter 4)

6.4.1: Preparation of (S)-7-(3-(aminomethyl)pyrrolidin-1-yl)-1-cyclopropyl-6-fluoro-8-methoxy-4-oxo-1,4 dihydroquinoline-3-carboxylic acid (**UING-05-249/ UIHS-IIa-077**)

(*R*)-3-N-Boc-aminomethyl pyrrolidine (72.1 mg, 0.360 mmol) and 1-cyclopropyl-6,7-difluoro-8-methoxy-4-oxo-1,4-dihydroquinoline-3-carboxylic acid (51.1 mg, 0.169mmol) were added to DMSO (0.7 mL), heated to 85^{o}C, and stirred for 2 hours. Trifluoroacetic acid (0.5 mL) was then added and the reaction mixture was stirred at room temperature overnight. The resulting product solution was purified via semi-prep HPLC to give a yellow powder (51.1 mg, 84% yield). ^{1}H-NMR (300 MHz, DMSO-d_6): 1.040 ppm (m, 4H), 1.756 ppm (m, 1H), 2.144 ppm (m, 1H), 3.33 ppm (s, H_2O), 2.50 ppm (m, DMSO), 2.970 ppm (m, 2H), 3.459 ppm (m, 1H), 3.553 ppm (s, 3H), 3.668 ppm (m, 3H), 4.140 ppm (m, 1H), 7.689 ppm (d, J=13.8Hz, 1H), 7.860 ppm (s, 3H), 8.668 ppm (s, 1H), 15.161 ppm (s, 1H). ^{19}F-NMR (292 MHz, DMSO-d_6): -121.99 ppm (J=15.1)

6.4.2: Preparation of (S)-7-(3-(aminomethyl)pyrrolidin-1-yl)-1-cyclopropyl-6-fluoro-8-methoxy-5-methyl-4-oxo-1,4-dihydroquinoline-3-carboxylic acid (**UIHS-IIa-215**).

(*R*)-3-N-Boc-aminomethyl pyrrolidine (30.2 mg, 0.162 mmol), triethylmine, (0.02 mL) and 1-cyclopropyl-6,7-difluoro-8-methoxy-5-methyl-4-oxo-1,4-dihydroquinoline-3-carboxylic acid (21.2 mg, 0.646 mmol) were added to DMSO (0.3 mL) and stirred at 80^{o}C for 1 hour. Trifluoroacetic acid (1.0 mL) was added and the reaction mixture was aged for 1 hour at room temperature. The resulting product was purified via semi-prep HPLC to give a light yellow powder (18.4 mg, 69% yield). ^{1}H NMR (300 MHz, DMSO-d_6): 15.630 ppm (s, 1H), 8.648 ppm (s, 1H), 7.889 ppm (br s, 3H), 4.125 ppm (m, 1H), 3.671 ppm (m, 3H), 3.481 ppm (m, 3H), 3.460 ppm (m, 2H), 2.963 ppm (m, 2H), 2.684 ppm (d, J=34Hz, 3H), 3.33 ppm (s, H_2O), 2.50 ppm (m, DMSO), 2.142 ppm (m, 1H), 1.739 ppm (m, 1H), 0.980 ppm (m, 4H). ^{19}F-NMR (DMSO-d292 MHz, DMSO-d_6): -125.12 ppm, 1 trifluoroacetic acid. LRMS (ESI) calculated for ($M+H^+$) 390.18, found 390.13 (M+H).

6.4.3: Preparation of (S)-7-(3-(aminomethyl)pyrrolidin-1-yl)-6-fluoro-8-methoxy-4-oxo-1-(prop-1-en-2-yl)-1,4-dihydroquinoline-3-carboxylic acid (**UITT-03-245**).

Author's note: The amount of UITT-03-243 fluoroquinolone core starting material used in the following reaction was not listed in the UITT-03 research notebook. A previous reaction to produce this product used UITT-01-179 (25 mg, 0.081 mmol) as the fluoroquinolone core starting material and generated the C7-aminomethylpyrrolidine fluoroquinolone UITT-02-111, which is structurally identical to UITT-03-245, in 32% yield).

UITT-03-243 was dissolved in DMSO (1.5 mL). The reaction vessel was then heated with stirring to 50^{o}C and (*R*)-3-N-Boc-aminomethyl pyrrolidine (88.7 mg, 0.44

mol) was added. The reaction was allowed to proceed for 24 hours. Trifluoroacetic acid (0.5 mL) was then added and the reaction was stirred for 4 hours. The product was then purified by preparatory HPLC to give a yellow powder (71 mg yield). ^{1}H-NMR (300 MHz, DMSO-d_6): 8.420 ppm (s, 1H), 8.069 ppm (bs, 2H), 8.015 ppm (bs, 1H), 7.690 ppm (d, J=13.5Hz, 1H), 5.491 ppm (s, 1H), 5.250 ppm (s, 1H), 3.892 ppm (bs, 2H), 3.516 ppm (m, 2H), 3.365 ppm (s, 3H), 2.959 ppm (m, 2H), 3.33 ppm (s, H_2O), 2.50 ppm (m, DMSO), 2.457 ppm (bs, 1H), 2.185 ppm (bs, 1H), 2.070 ppm (s, 3H), 1.627 ppm (m, 1H). ^{19}F-NMR (DMSO-d_6): -120.562 ppm, J=14.3Hz. LRMS (ESI) calculated for ($M+H^+$) 376.17, found 376.18 (M+H).

6.4.4: Preparation of (S)-5-amino-7-(3-(aminomethyl)pyrrolidin-1-yl)-1-cyclopropyl-6-fluoro-8-methoxy-4-oxo-1,4-dihydroquinoline-3-carboxylic acid (**UIBW04-123B**).

To a stirred suspension of 5-amino-1-cyclopropyl-6,7-difluoro-8-methoxy-4-oxo-1,4-dihydroquinoline-3-carboxylic acid (21 mg, 0.066 mmol) in dry dimethylsulfoxide (0.5 mL) at room temperature was added (R)-3-N-boc-aminomethylpyrrolidine (32 mg, 0.161 mmol) followed by triethylamine (0.027 mL, 0.193 mmol). The reaction was then heated to 75^{o}C. The reaction was stirred for 7 hours then cooled to room temperature and under a stream of argon was treated with trifluoroacetic acid (2.0 mL), producing a white gas. The reaction was then heated to 70^{o}C and stirred for two hours. Once the reaction was observed to be complete by analytical HPLC, the solution was cooled to room temperature and drop-wise added to cold diisopropylether (2 mL) to precipitate the crude product. The precipitated yellow product was separated from the ether by centrifuge then taken up into methanol, dried, suspended in H_2O:MeCN (6 mL) and purified by semi-preparative HPLC with a 45 minute 5-95% MeCN (0.1% trifluoroacetic acid): H_2O (0.1% trifluoroacetic acid) linear gradient to give a yellow powder (25 mg, 77% yield) ^{1}H-NMR

(300 MHz, DMSO-d_6): 15.07 ppm (br s, 1H), 8.52 ppm (s, 1H), 7.86 ppm (br s, 3H), 7.12 (br s, 2H), 4.02 ppm (m, 1H), 3.65 ppm (m, 3H), 3.46 ppm (m, 1H), 3.41 ppm (s, 3H), 2.96 ppm (m, 2H), 3.33 ppm (s, H_2O), 2.50 ppm (m, DMSO), 2.45 ppm (m, 1H), 2.10 ppm (m, 1H), 1.73 ppm (m, 1H), 1.11-0.7 ppm (m, 2H). ^{19}F-NMR (292 MHz, DMSO-d_6): -73.75 ppm (trifluoroacetic acid salt), -150.37 ppm. LRMS (ESI) calculated for ($M+H^+$) 391.15, found 391.08.

6.4.5: Preparation of (S)-7-(3-(aminomethyl)pyrrolidin-1-yl)-1-cyclopropyl-6-fluoro-4-oxo-1,4-dihydro-1,8-naphthyridine-3-carboxylic acid (**UIBW04-234**).

To a stirred suspension of 1-cyclopropyl-6,7-difluoro-4-oxo-1,4-dihydro-1,8-naphthyridine-3-carboxylic acid (26 mg, 0.10 mmol) in dry dimethylsulfoxide (2.0 mL) was added (R)-3-N-boc-aminomethylpyrrolidine (90.4 mg, 0.451 mmol) at room temperature. To this was added diisopropylethylamine (0.125 mL, 0.68 mmol). The reaction was then heated to 70^{o}C. After 30 minutes the pyrrolidine coupling was observed to be complete by HPLC analysis and the reaction was cooled to room temperature. The reaction solution was then treated with trifluoroacetic acid (2.0 mL), producing a white gas that was removed with a stream of argon. The reaction was then heated to 85^{o}C and stirred overnight. The solution was then cooled to room temperature and added drop-wise into cold diisopropylether (2.0 mL) to precipitate the crude product. The white precipitate was separated from the ether by centrifuge and then taken up into methanol, dried, and purified by semi-preparative HPLC with a 45 minute 5-95% MeCN (0.1% trifluoroacetic acid): H_2O (0.1% trifluoroacetic acid) linear gradient to give a white powder (Yield: 37 mg, 83%). ^{1}H-NMR (300 MHz, DMSO-d_6): 15.43 ppm (br s= 1H), 8.58 ppm (s= 1H), 8.00 ppm (d= 1H, J= 12.9 Hz), 7.91 ppm (br s= 2H), 3.98 ppm (br d= 2H, J= 27Hz), 3.79 ppm (br s= 1H), 3.68 ppm (m= 1H), 3.56 ppm (br s= 1H), 3.33 ppm (s, H_2O), 2.50 ppm (m, DMSO), 2.98 ppm (m= 2H), 2.17 ppm (br s= 1H), 1.80 ppm (m= 1H), 1.21 ppm (m=

2H), 1.09 ppm (m= 2H). ^{19}F-NMR (292 MHz, DMSO-d_6): -73.63 ppm (s, trifluoroacetic acid salt), -134.18 ppm (dd). LRMS (ESI) calculated for ($M+H^+$) 347.14, found 347.01.

6.4.6: Preparation of (S)-10-((S)-3-(aminomethyl)pyrrolidin-1-yl)-9-fluoro-3-methyl-7-oxo-3,7-dihydro-2H-[1,4]oxazino[2,3,4-ij]quinoline-6-carboxylic acid (**UIBW04-235**).

To a suspension of (S)-9,10-difluoro-3-methyl-7-oxo-3,7-dihydro-2H-[1,4]oxazino[2,3,4-ij]quinoline-6-carboxylic acid (31 mg, 0.11 mmol) in dry dimethylsulfoxide (2.0 mL) at room temperature was added (R)-3-N-boc-aminomethylpyrrolidine (54.8 mg, 0.274 mmol), followed by triethylamine (0.05 mL, 0.358 mmol). The reaction was then heated to 70^{o}C. After 80 minutes the pyrrolidine coupling was observed to be complete by HPLC analysis. The reaction was then cooled to room temperature and under a stream of argon was treated with trifluoroacetic acid (2.0 mL), producing a colorless gas. The reaction was then heated to 50^{o}C and stirred overnight. The solution was then cooled to room temperature and dropwise added to cold diisopropylether (5 mL) to precipitate the crude product. The light-yellow precipitate was separated from the ether by centrifuge then taken up into methanol, dried, and purified by semi-preparative HPLC with a 45 minute 5-95% MeCN (0.1% trifluoroacetic acid): H_2O (0.1% trifluoroacetic acid) linear gradient to give a bright yellow powder (Yield 26 mg, 51%). ^{1}H-NMR (300 MHz, DMSO-d_6): 15.42 ppm (br s=1H), 8.93 ppm (s=1H), 7.85 ppm (br s=3H), 7.56 ppm (d=1H, J=12Hz), 4.89 ppm (dm=1H, J=6Hz), 4.53 ppm (dd=1H, J1=9Hz, J2=3Hz), 4.27 ppm (dd=1H, J1=12Hz, J2=3Hz), 3.77 ppm (qm=2H,J1=9Hz, J2=3Hz), 3.68 ppm (m=1H), 3.57 ppm (td=1H, J1=9Hz, J2=3Hz), 2.99-2.90 ppm (m=2H), 3.33 ppm (s, H_2O), 2.50 ppm (m, DMSO), 2.08 ppm (pm=1H), 1.68 ppm (ddm=1H), 1.45 ppm (d=3H, J=6Hz). ^{19}F-NMR (292 MHz, DMSO-d_6): -73.74 ppm (s= trifluoroacetic acid salt), -120.94 ppm (d=1F). LRMS (ESI) calculated for ($M+H^+$) 362.15, found 362.02.

6.4.7: Preparation of (S)-6-((S)-3-(aminomethyl)pyrrolidin-1-yl)-5-fluoro-8-oxo-3H,8H-4-Oxa-1-thia-9b-azacyclopenta[cd]phenalene-9-carboxylic acid (**UIBW04-236**).

To a suspension of 5,6-difluoro-8-oxo-3H,8H-4-Oxa-1-thia-9b-azacyclopenta[cd]phenalene-9-carboxylic acid (28 mg, 0.091 mmol) in dry dimethylsulfoxide (2.0 mL) at room temperature was added (R)-3-N-boc-aminomethylpyrrolidine (38.6 mg, 0.193 mmol) followed by diisopropylethylamine (0.05 mL, 0.286 mmol). The reaction was heated to 70^{o}C. After 60 minutes the pyrrolidine coupling was observed to be complete by HPLC analysis. The reaction was then cooled to room temperature and under a stream of argon was treated with trifluoroacetic acid (1.0 mL), producing a white gas. The reaction was then heated to 70^{o}C and stirred overnight. The solution was then cooled to room temperature and drop-wise added into cold diisopropylether to precipitate the crude product. The bright yellow precipitate was separated from the ether by centrifuge then taken up into methanol, dried, and purified by semi-preparative HPLC with a 45 minute 5-95% MeCN (0.1% trifluoroacetic acid): H_2O (0.1% trifluoroacetic acid) linear gradient to give a bright yellow powder (Yield: 36 mg, 79%). ^{1}H-NMR (DMSO-d_6): 15.80 ppm (br s=1H), 7.93 ppm (bs s=3H), 7.61 ppm (s=1H), 7.45 ppm (d=1H, J=12 Hz), 5.44 ppm (q=2H, J_1=27 Hz, J_2=15 Hz), 4.64-3.89 ppm (br s=3H), 3.83-3.67 (m=3H), 3.55 ppm (td=1H, J_1=9 Hz, J_2=3 Hz), 3.02-2.88 ppm (m=2H), 2.50 ppm (DMSO), 2.09 ppm (pm=1H), 1.72 ppm (dd=1H , J_1=12 Hz, J_2=6 Hz). ^{19}F-NMR (282 MHz, DMSO-d_6): -73.93 (s, trifluoroacetic acid salt), -120.19 (d=1F). LRMS (ESI) calculated for ($M+H^+$) 390.09, found 389.95.

6.4.8: Preparation of (S)-7-(3-(aminomethyl)pyrrolidin-1-yl)-1-ethyl-6-fluoro-4-oxo-1,4-dihydroquinoline-3-carboxylic acid (**UIBW04-237**).

To a suspension of 7-chloro-1-ethyl-6-fluoro-4-oxo-1,4-dihydroquinoline-3-carboxylic acid (30.5 mg, 0.113 mmol) in dry dimethylsulfoxide (2.0 mL) was (R)-3-N-boc-aminomethylpyrrolidine (100 mg, 0.501 mmol), followed by diisopropylethylamine (0.18 mL, 1.0 mmol). The reaction was then heated to 70^{o}C. After 16 hours the reaction was cooled to room temperature and under a stream of argon was treated with trifluoroacetic acid (2.0 mL), producing a white gas. The reaction was then heated to 70^{o}C and stirred overnight. The solution was then cooled to room temperature and drop-wise added into cold diisopropylether to precipitate the crude product. The white precipitate was separated from the ether by centrifuge then taken up into methanol, dried, and purified by semi-preparative HPLC with a 45 minute 5-95% MeCN (0.1% trifluoroacetic acid): H_2O (0.1% trifluoroacetic acid) linear gradient to give a yellow powder (Yield: 51.5 mg, 78%). ^{1}H-NMR (300 MHz, DMSO-d_6): 15.64 ppm (br s=1H), 8.87 ppm (s=1H), 7.96 ppm (br s=3H), 7.81 ppm (d=1H, J=15 Hz), 6.64 ppm (d=1H, J=9 Hz), 4.51 ppm (q=2H, J_1=9Hz, J_2=6 Hz), 3.78 ppm (m=1H), 3.64 ppm (m=2H), 3.43 ppm (tm=1H), 2.98 ppm (m=2H), 2.59 ppm (m=1H), 2.50 ppm (DMSO peak), 2.17 ppm (m=1H), 1.79 ppm (m=1H), 1.41 ppm. ^{19}F-NMR (292 MHz, DMSO-d_6): 19F-NMR: -73.92ppm (s, trifluoroacetic acid salt), -126.72ppm (d=1F). LRMS (ESI) calculated for ($M+H^{+}$) 334.16, found 334.01.

6.4.9: Preparation of 7-((S)-3-(aminomethyl)pyrrolidin-1-yl)-6,8-difluoro-1-(2-fluorocyclopropyl)-4-oxo-1,4-dihydroquinoline-3-carboxylic acid (**UIBW04-238**).

To a suspension of 6,7,8-trifluoro-1-(2-fluorocyclopropyl)-4-oxo-1,4-dihydroquinoline-3-carboxylic acid (25 mg, 0.083 mmol) was added (R)-3-N-boc-aminomethylpyrrolidine

(30 mg, 0.149 mmol) followed by diisopropylethylamine (0.05 mL, 0.29 mmol). The reaction was then heated to 70ºC. After 2.5 hours the pyrrolidine coupling was observed to be complete by HPLC analysis. The reaction was cooled to room temperature and under a stream of argon was treated with trifluoroacetic acid (1.5 mL), producing a white gas. The reaction was then heated to 70ºC and stirred overnight. The solution was then cooled to room temperature and drop-wise added to cold diisopropylether to precipitate the crude product. The precipitated product was separated from the ether by centrifuge then taken up into methanol, dried, and purified by semi-preparative HPLC with a 45 minute 5-95% MeCN (0.1% trifluoroacetic acid): H_2O (0.1% trifluoroacetic acid) linear gradient to give a yellow powder (Yield: 42 mg, 85%). ^{1}H-NMR (300 MHz, DMSO-d_6): 14.88 ppm (br s=1H), 8.67 ppm (d=1H, J=3.9 Hz), 7.98 ppm (br s=3H), 7.73 ppm (d=1H, J=13.5 Hz), 5.09 ppm (br d=1H, J=64.5 Hz), 4.11-4.02 ppm (pm=1H), 3.87-3.72 ppm (m=2H), 3.63-3.52 ppm (m=1H), 2.97 ppm (br s=2H), 2.50 ppm (DMSO peak), 2.12 ppm (m=1H), 1.85-1.56 ppm (m=3H). ^{19}F-NMR (300 MHz, DMSO-d_6): -73.836 ppm (s, trifluoroacetic acid salt), -120.326 ppm (dd=1F), -133.113 ppm (m=1F), -219.913 ppm (m=1F). LRMS (ESI) calculated for ($M+H^+$) 382.14, found 382.08.

6.4.10: Preparation of (S)-7-(3-(aminomethyl)pyrrolidin-1-yl)-1-(2,4-difluorophenyl)-6-fluoro-4-oxo-1,4-dihydro-1,8-naphthyridine-3-carboxylic acid (**UIBW04-255**).

To a stirred suspension 7-chloro-1-(2,4-difluorophenyl)-6-fluoro-4-oxo-1,4-dihydro-1,8-naphthyridine-3-carboxylic acid (29 mg, 0.081 mmol) was added 2.0 molar equivalents of (R)-3-N-boc-aminomethylpyrrolidine (34 mg, 0.17 mmol) followed by 6.8 molar equivalents of diisopropylethylamine (0.10 mL, 0.58 mmol). The reaction was then heated to 75ºC. After 90 minutes the pyrrolidine coupling was observed to be complete by HPLC analysis. The reaction was cooled to room temperature and under a stream of argon was treated with trifluoroacetic acid (1.5 mL), producing a white gas. The reaction

was then heated to 60°C and stirred overnight. The solution was then cooled to room temperature and drop-wise added to cold diisopropylether to precipitate the crude product. The light yellow precipitate was separated from the ether by centrifuge then taken up into methanol, dried, and purified by semi-preparative HPLC with a 45 minute 5-95% MeCN (0.1% trifluoroacetic acid): H_2O (0.1% trifluoroacetic acid) linear gradient to give a yellow powder (Yield= 35 mg, 78%). ^{1}H-NMR (300 MHz, DMSO-d_6): 15.19 ppm (br s, 1H), 8.82 ppm (s, 1H), 8.08 ppm (d, 1H, J=15 Hz), 7.82 ppm (m, 4H), 7.59 ppm (td, 1H, J_1= 9 Hz, J_2= 3 Hz), 7.34 ppm (td, 1H, J_1= 9 Hz, J_2= 3 Hz), 3.94 ppm (m, 1H), 3.50 ppm (m, 3H), 3.21 ppm (m, 1H), 2.88 ppm (br s, 2H), 2.50 ppm (DMSO peak), 2.45 ppm (s, 1H), 2.00 ppm (m, 1H), 1.67 ppm (m, 1H). ^{19}F-NMR (292 MHz, DMSO-d_6): -73.57 ppm (trifluoroacetic acid salt), -107.29 ppm, -114.99 ppm, -133.27 ppm. LRMS (ESI) calculated for ($M+H^+$) 419.14, found 418.92.

6.5: Synthesis of C7-Diverse Fluoroquinolones (Chapter 5)

6.5.1: Preparation of (R)-7-(3-carbamoylpyrrolidin-1-yl)-1-cyclopropyl-6-fluoro-8-methoxy-4-oxo-1,4-dihydroquinoline-3-carboxylic acid (**UIBW04-259**).

To a stirred suspension 1-cyclopropyl-6,7-difluoro-8-methoxy-4-oxo-1,4-dihydroquinoline-3-carboxylic acid (30 mg, 0.102 mmol) was added (R)-pyrrolidine-3-carboxamide (61 mg, 0.41 mmol) followed by excess triethylamine (0.25 mL, 1.8 mmol). The reaction was then heated to 60°C. The pyrrolidine coupling was observed to be complete by HPLC analysis after heating overnight. The reaction was cooled to room temperature and diluted with 1:1 H_2O:MeCN (6 mL), then purified by semi-preparative HPLC with a 45 minute 5-95% MeCN (0.1% trifluoroacetic acid): H_2O (0.1% trifluoroacetic acid) linear gradient to give a yellow powder (Yield: 23 mg, 57%). ^{1}H-NMR (300 MHz, DMSO-d_6): 15.18 ppm (br s=1H), 8.66 pm (s=1H), 7.68 ppm (d=1H. J=15Hz), 7.53 ppm (br s=1H), 7.02 ppm (br s=1H), 4.14 ppm (m=1H), 3.75 ppm

(dm=1H), 3.66 ppm (tm=2H), 3.55 ppm (m=1H), 3.01 ppm (t=1H), 2.44 ppm (m=1H), 2.09+2.06 ppm (2m=2H), 1.15 ppm (m=2H), 1.05 ppm (m=2H). ^{19}F-NMR (292 MHz, DMSO-d_6): -74.14ppm (s, residual trifluoroacetic acid- no extra acidic p+ in H-NMR), -121.12 ppm (m). LRMS (ESI) calculated for ($M+H^+$) 390.15, found 390.02.

6.5.2: Preparation of (R)-7-(3-aminopyrrolidin-1-yl)-1-cyclopropyl-6-fluoro-8-methoxy-4-oxo-1,4-dihydroquinoline-3-carboxylic acid (**UIBW04-261**).

To a stirred suspension 1-cyclopropyl-6,7-difluoro-8-methoxy-4-oxo-1,4-dihydroquinoline-3-carboxylic acid (30 mg, 0.10 mmol) was (R)-tert-butyl pyrrolidin-3-ylcarbamate (28 mg, 0.15 mmol) followed by excess triethylamine (0.05 mL, 0.31 mmol). The reaction was then heated to 60^{o}C. After 3 hours the pyrrolidine coupling was observed to be mostly complete by HPLC analysis. The reaction was cooled to room temperature then treated with trifluoroacetic acid (2 mL) under a stream or Ar. The reaction was the warmed to 75^{o}C and stirred for 2 hours. The reaction was cooled to room temperature and the trifluoroacetic acid was removed partially *in vacuo*. The remaining solvent was diluted with 1:1 H_2O:MeCN (8 mL), then purified by semi-preparative HPLC with a 45 minute 5-95% MeCN (0.1% trifluoroacetic acid): H_2O (0.1% trifluoroacetic acid) linear gradient to give a light yellow powder (Yield: 43 mg, 89%). ^{1}H-NMR (300 MHz, DMSO-d_6): 15.11 ppm (br s=1H), 8.68 ppm (s=1H), 8.14 ppm (br s=3H), 7.71 ppm (d=1H, J=15Hz), 4.15 ppm (m=1H), 3.84 ppm (dm=2H), 3.78 ppm (dm=2H), 3.58 ppm (s=3H), 2.44 ppm (m=1H), 2.29 ppm (dd=1H, J1=9Hz, J2=6Hz, J3=15Hz), 2.02 ppm (m=1H), 1.11 ppm (m=2H), 1.01 ppm (m=2H). ^{19}F-NMR (292 MHz, DMSO-d_6): -73.70 ppm (trifluoroacetic acid salt), -120.86 ppm (m=1F). LRMS (ESI) calculated for ($M+H^+$) 362.15, found 362.01.

6.5.3: Preparation of (R)-1-cyclopropyl-6-fluoro-7-(3-(hydroxymethyl)pyrrolidin-1-yl)-8-methoxy-4-oxo-1,4-dihydroquinoline-3-carboxylic acid (**UIB04-263**).

To a stirred suspension 1-cyclopropyl-6,7-difluoro-8-methoxy-4-oxo-1,4-dihydroquinoline-3-carboxylic acid (30 mg, 0.102 mmol) under Ar was added D-β-prolinol (50 mg, 0.49 mmol) followed by excess triethylamine (0.05 mL, 0.31 mmol). The reaction was then heated to 60^{o}C. After 2 hours the pyrrolidine coupling was observed to be mostly complete by HPLC analysis. The reaction was cooled to room temperature then diluted with 1:1 H_2O:MeCN (7 mL), then purified by semi-preparative HPLC with a 45 minute 5-95% MeCN (0.1% trifluoroacetic acid): H_2O (0.1% trifluoroacetic acid) linear gradient to give a bright yellow powder (Yield: 43.1 mg, 89%). ^{1}H-NMR (300 MHz, DMSO-d_6): 15.21 ppm (br s=1H), 8.65 ppm (s=1H), 7.66 ppm (d=1H, J=12Hz), 4.13 ppm (m=1H), 3.61 ppm (m=2H), 3.54 ppm (m=1H), 3.47 ppm (tm=3H), 2.44 ppm (m=2H), 2.01 ppm (m=1H), 1.71 ppm (m=1H), 1.18-0.92 ppm (2m=4H). ^{19}F-NMR (292 MHz, DMSO-d_6): -74.14 ppm (residual trifluoroacetic acid-not a salt peak), -121.01 ppm (d=1F). LRMS (ESI) calculated for ($M+H^{+}$) 377.15, found 377.02.

6.5.4: Preparation of (S)-1-cyclopropyl-6-fluoro-8-methoxy-7-(3-((methylamino)methyl)pyrrolidin-1-yl)-4-oxo-1,4-dihydroquinoline-3-carboxylic acid (**UIBW04-267**).

The (S)-tert-butyl 3-((methylamino)methyl)pyrrolidine-1-carboxylate (45 μL, 0.20 mmol) was drop-wise added to MeCN (0.5 mL) in a 10mL round-bottom flask. This solution was then treated with trifluoroacetic acid (1.0 mL) under a stream or Ar, and then stirred for 1 hour at room temperature. Once Boc-deprotection had been observed via TLC (10:1 MeOH: NH_4OH aqu.) the solution was partially concentrated by rotovap at 0^{o}C. The

remaining solution was then drop-wise added to diisopropylether (10mL), forming a fine, white precipitate that was separated via centrifuge. The precipitate was then dissolved in dimethylsulfate (10 mL) and moved to a 10 mL round bottom flask. To the solution was then added 1-cyclopropyl-6,7-difluoro-8-methoxy-4-oxo-1,4-dihydroquinoline-3-carboxylic acid (30.0 mg, 0.102 mmol) followed by diisopropylethylamine (1.0 mL), then the reaction was heated to 100^{o}C and stirred overnight, after which the pyrrolidine coupling was observed to be mostly complete by HPLC analysis. The reaction was cooled to room temperature then diluted with 1:1 H_2O:MeCN (7 mL), then purified by semi-preparative HPLC with a 5-30-32-95% MeCN (0.1% trifluoroacetic acid): H_2O (0.1% trifluoroacetic acid) over a 10-40-50 minute linear gradient to give a yellow powder (Yield: 9.7 mg, 19%). ^{1}H-NMR (300 MHz, DMSO-d_6): 15.16 ppm (br s=1H), 8.67 ppm (s=1H), 8.56 ppm (br s=2H), 7.68 ppm (d=1H, J=15Hz), 4.14 ppm (m=1H), (H_2O peak obscures 3.7 ppm m=3H), 3.55 ppm (s=3H), 3.47 ppm (m=1H), 3.08 ppm (m=2H), 2.62 ppm (t=3H, J1=6Hz, J2=6Hz), 2.16 ppm (m=1H), 1.76 ppm (m=1H), 1.13 ppm (m=2H), 1.05 ppm (m=2H), 0.97 ppm (m=1H). ^{19}F-NMR (292 MHz, DMSO-d_6): -74.93 ppm (trifluoroacetic acid salt peak), -121.01 ppm (d=1F). LRMS (ESI) calculated for ($M+H^+$) 390.19, found 390.08.

6.6: *In-silico* Docking Studies with SYBYL Software

Computer-aided docking was performed using a similar procedure to the method outlined in a previous study by Drlica et. al.[110] In these studies, SYBYL-X 1.3 was used to prepare 2XKK crystal structure (*A. baumannii* ParC of TopoIV bound to moxifloxacin and DNA) for ligand docking. Standard Tripos (St. Louis, MO) procedures were followed. Briefly, metal bonds were removed, atom types in the ligands were fixed, missing side chains were added, protein termini were charged, hydrogen atoms were added, and a staged minimization of the entire complex was performed. The force field used for the staged minimization was MMFF94s, and a gradient of 0.5 kcal/(mol•Å) was used with a

maximum of 1000 iterations. Prior to docking ligands with either wild-type or mutant structure, all water molecules were removed. The binding site was determined by instructing the program to probe the interactions surrounding one of the two bound moxifloxacin ligands (E/MFX or F/MFX). The Protomol algorithm in SYBYL-X 1.3 was used to generate the binding site, and the parameters used were threshold = 0.99 and a bloat = 0. The fluoroquinolone ligands were docked into this generated binding site using the Geom-X Surflex-Dock mode in the SYBYL-X 1.3 docking suite.

6.7: Analysis of Compound Activity

Two assays were used to determine compound activity in purified enzymes: a supercoiling inhibition assay to measure enzyme activity inhibition and a cleaved-complex formation assay to determine enzyme poisoning by compounds. Additionally, MIC values for the compound were determined in growth-inhibition assays with wild-type *E.coli* and *M. smegmatis* (*tolC*-knock out) cell cultures and various mutant strains of *E. coli*, as listed in Table 6.1. All activity characterization assays were performed as previously reported.

Supercoiling Inhibition Assays: Relaxed DNA was prepared by incubating the negatively supercoiled DNA with human topoisomerase I. The subunits of *E. coli* gyrase and *E. coli* Topo IV were expressed and purified, and the active enzymes were reconstituted as described previously.[119] The purified enzyme was incubated in buffer with relaxed DNA, ATP, and 10 μM of the test compound. Reaction mixtures were incubated at 37°C for 15 min and terminated by adding EDTA to release the supercoiled DNA. The DNA products were analyzed by gel electrophoresis. Gels were stained with ethidium bromide, then photographed and quantified using an Eagle Eye II system (Stratagene).[103] The IC_{50} of each compound was determined as well.

Cleaved Complex Formation Assays: Cleaved complex formation is a measure of the stability of the fluoroquinolone-DNA-topoisomerase ternary complex and is related

to the ability of fluoroquinolones to poison the topoisomerase enzyme. In these assays, the topoisomerases are incubated in buffered reaction mixtures containing ATP, tRNA, and either supercoiled or relaxed DNA. The indicated concentrations of compound were incubated in the first stage. Then, the indicated concentrations of compound were added, and the reaction mixtures were incubated during the second stage. Sodium dodecyl sulfate was added as a detergent and the reaction mixtures were further incubated. EDTA and proteinase K were then and the incubation was continued. The DNA products were purified by extraction with phenol-chloroform-isoamyl alcohol and then analyzed by electrophoresis. After destaining in water, gels were photographed and quantified using an Eagle Eye II system.[119]

Activity against *E. coli* Topoisomerase IV: The ability of the compounds to inhibit *E. coli* Topoisomerase IV and human topoisomerase IIα was determined in a DNA decantenation assay. In brief, TopoIV enzyme harvested from *E. coli* was incubated in buffered reaction mixtures containing ATP, kinetoplast DNA, and the indicated concentrations of fluoroquinolone. Reactions were terminated by adding EDTA and the DNA products were analyzed by electrophoresis. Gels were stained with ethidium bromide and photographed using an Eagle Eye II system (Stratagene).[123]

Activity against human topoisomerase IIα: The ability of the compounds to inhibit human topoisomerase IIα was determined in a DNA decantenation assay. Human cell lines were obtained and human topoisomerase enzyme was purified from these as described previously.[123] In brief, human TopoIIα enzyme was incubated in buffered reaction mixtures containing ATP, kinetoplast DNA, and the indicated concentrations of compound. Reactions were terminated by adding EDTA and the DNA products were analyzed by electrophoresis. Gels were stained with ethidium bromide and photographed using an Eagle Eye II system (Stratagene).[123]

Bacterial strains, growth, and susceptibility determination: The methodology for growing the *E. coli* strains used in the study has been described previously[120] and the

specific cultures are listed in Table 6.1. Cultures of *E. coli* were grown in liquid medium on agar plates at 37 ºC (Miller 1972). *E. coli* strains were deficient in *tolC* to reduce efflux of the test compounds. Inhibition of growth (MIC) was measured by broth dilution. Cultures were grown to A_{600} = 0.3 (about 5 x 10^8 cfu/ml), diluted 5000-fold, and approximately 10^5 cells were applied to liquid medium (1 mL aliquots) containing drugs at various concentrations that differed by 2-fold increments. MIC was taken as the minimal concentration that blocked visible growth following overnight incubation.[120] MIC's determined from these studies were used to determine antimutant activity of the compounds. The antimutant activity of a compound is expressed as a ratio of the compound MIC against *E. coli* mutant cells over the compound MIC against wild-type *E. coli.*

Table 6.1: Cell Cultures for Bacteriostatic Assays

Species	**Strain no.**	**Relevant genotype**	**Reference**
E. coli	KD1397	DM4100 *tolC6*::Tn10 *gyr*$^+$ (wild type)	[120, 122]
	KD2862	KD66 *tolC6*::Tn10 *gyrA* (S83L)	[120], [124]
	KD2866	KD1977 *tolC6*::Tn10 *gyrA* (D87Y)	[120], [124]
	KD2876	KD1909 *tolC6*::Tn10 *gyrA* (S83W)	[120], [124]
	KD2880	KD1913 *tolC6*::Tn10 *gyrA* (D87N)	[120], [124]
	KD2882	KD1915 *tolC6*::Tn10 *gyrA* (G81C)	[120], [124]
	KD2864	KD1975 *tolC6*::Tn10 *gyrA* (A84P)	[120], [124]
	KD2956	DM4100 *tolC6*::Tn10 *gyrA* (D82A)	[120], [124]
M. smegmatis	mc^{2}155 (KD1163)	(wild-type)	[125]

Table 6.1: The cell cultures used in bacteriostatic activity (MIC) assays, later used to determine antimutant activity profiles for the compounds.

CHAPTER VII: CONCLUSIONS AND FUTURE DIRECTIONS

7.1: Brief Restatement of Theory

The research described in this thesis was performed in order to understand what structural features of fluoroquinolones would allow them to inhibit both wild-type and current fluoroquinolone-resistant strains of bacteria. A current theory to explain the emergence of fluoroquinolone resistance in bacteria is that within antibiotic-treated populations of bacteria, there exists subpopulations with point mutations to the bacterial type-II topoisomerases, DNA gyrase and topoisomerase IV, which are the primary targets of fluoroquinolones.

The point mutations primarily responsible for fluoroquinolone resistance are located on the Helix-4 region of the GyrA/ParC-subunit and interfere with the formation of a Mg-water bridge, which is the primary binding interaction for fluoroquinolones bacterial type-II topoisomerases and a key component of the drug-stabilized ternary complex. The ternary complex is a static, inhibited state of bacterial type-II topoisomerase, and is composed of the topoisomerase enzyme, nicked DNA, and fluoroquinolone. The fluoroquinolones generated in this study were designed to explore non-traditional binding contacts within the ternary complex toward identifying new ways to design fluoroquinolones for activity with current fluoroquinolone-resistant strains of bacteria. That is to say, these fluoroquinolones were designed to explore binding contacts separate from the Mg-water bridge which normally anchors fluoroquinolones in the ternary complex.

To accomplish this goal, fluoroquinolones were designed to exploit binding interactions with DNA and with the GyrB/ParE region of the ternary complex. It was believed that fluoroquinolones, which possessed equal binding affinity in the ternary complex either with or without the Mg-water bridge interaction, would be capable of equipotent inhibition of wild-type and current fluoroquinolone-resistant bacterial type-II

topoisomerases, and therefore would be able to target both wild-type and fluoroquinolone-resistant bacteria.

7.2: Studies with Tricyclic Fluoroquinolones

Several attempts were made to generate fluoroquinolones that possessed aromatic extensions of the core structure in the form of either a 5,6-phenyl napthyridone core or 4,5-pyrimidine fluoroquinolone core structure. It was believed that these modifications would increase the ability of fluoroquinolones to form pi-stacking interactions with nucleoside bases of the bound DNA within the ternary complex. In this way, the reliance of these fluoroquinolones on the Mg-water bridge as a primary binding interaction would be diminished. Therefore, the ability of Helix-4 amino acid substitutions that disrupt the formation of the Mg-water bridge as a way of promoting fluoroquinolone resistance would be overcome. Unfortunately, the synthesis of these compounds proved to be more difficult than expected. While a number of viable routes to prepare these target structures remain, and key successes suggest simple modifications to approach would afford the target structures, this part of the project was abandoned in favor of pursuing a promising lead structure that was found to likely bind the GyrB/ParE subunit to overcome Helix-4 resistance mutations.

7.3: Studies with Core-Diverse, C7-Aminomethylpyrrolidine Fluoroquinolones

In this study the effect of the C7-aminomethylpyrrolidine group in conjunction with other structural changes to the fluoroquinolone core was explored in order to determine if there were specific structural requirements of the fluoroquinolone core important to the ability of the C7-aminomethylpyrrolidine group to grant the ability to fluoroquinolones to maintain binding affinity with type-II bacterial topoisomerases possessing Helix-4 substitutions known to cause fluoroquinolone-resistance. The C7-aminomethylpyrrolidine group is believed to contribute to overcoming resistance caused

by Helix-4 amino acid substitutions by making binding interactions through the GyrB/ParE subunit of the ternary complex.

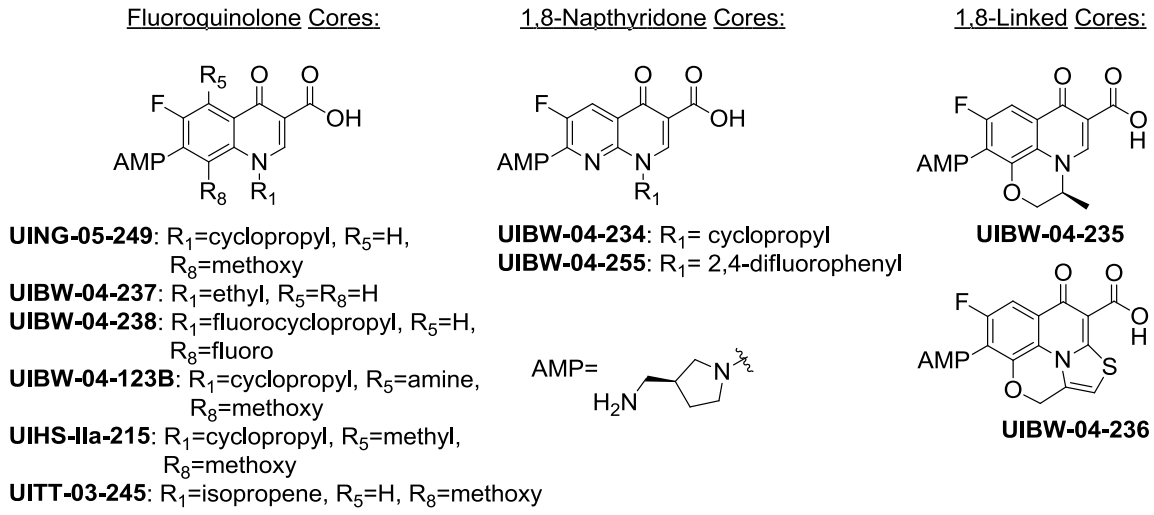

Figure 7.1: Structural diversification of fluoroquinolone cores studied with C7-aminomethylpyrrolidine (AMP) group in Chapter 4.

To accomplish this goal, fluoroquinolones with diverse core structures, each possessing a C7-aminomethylpyrrolidine group, were synthesized, as shown in Figure 7.1. These compounds were subjected to *in silico* docking studies within the crystal structure of a ternary complex of *A. baumannii* topoisomerase IV bound to DNA and moxifloxacin. These docking studies with wild-type topoisomerase IV demonstrate that the compounds generated for this study are capable of binding within the ternary complex through the Mg-water bridge with comparable binding affinity to each other and to the clinical fluoroquinolones ciprofloxacin and moxifloxacin. This serves as an *in silico* proof-of-concept that the C7-aminomethylpyrrolidine group is non-detrimental to fluoroquinolone binding in wild-type topoisomerase IV in a manner analogous to current clinical fluoroquinolones. A future direction of docking studies with these

fluoroquinolones is to test their *in silico* binding affinity in crystal structures modified with known Helix-4 mutations.

The fluoroquinolones synthesized in this study were subjected to *in vitro* testing with purified bacterial and human type-II topoisomerases for their ability: 1) to inhibit the overall DNA supercoiling activity of *E. coli* DNA gyrase, 2) to inhibit the DNA decatenation activity of *E. coli* topoisomerase IV and human topoisomerase IIα, and 3) to poison *E. coli* DNA gyrase and human topoisomerase IIα. The poisoning activity of each of the fluoroquinolones in this study was measured as poisoning fold-stimulation and CC_3 in a DNA cleavage assay that measures the accumulation of cleaved (linear) complexes of DNA as a result of ternary complex formation. The main conclusions from these studies are as follows:

Core-diverse C7-aminomethylpyrrolidine fluoroquinolones display a range of supercoiling inhibition and poisoning activity with wild-type *E. coli* DNA gyrase, but do not inhibit DNA decatenation by *E. coli* topoisomerase IV. This suggests that in *E. coli*, DNA gyrase is the main target of the fluoroquinolones in this study. Previous studies have demonstrated that certain C7-aminomethylpyrrolidine fluoroquinolones are able to poison *B. anthracis* topoisomerase IV.[26] This current study sought to discover if the trends in activity of C7-aminomethylpyrrolidine fluoroquinolones observed in *B. anthracis* (Gram-positive) topoisomerase IV might be found with *E. coli* (Gram-negative) DNA gyrase and topoisomerase IV. Consistent with the studies in *B. anthracis* topoisomerase IV, this study demonstrates that the C7-aminomethylpyrrolidine fluoroquinolones are capable of inhibiting DNA gyrase from Gram-negative bacteria. Furthermore, the consistent pattern between the supercoiling inhibition IC_{50} and CC_3 across the panel of fluoroquinolones demonstrates that supercoiling inhibition for these compound is linked to the formation of the ternary complex. Therefore, all of the fluoroquinolones of this study have demonstrated that they are poisoners of bacterial type-II topoisomerases as opposed to catalytic inhibitors.

Certain C7-aminomethylpyrrolidine fluoroquinolones from the same previous study were found to have crossover activity, meaning that in addition to poisoning *B. anthracis* topoisomerase IV, these fluoroquinolones were also capable of inhibiting the DNA decatenation of human topoisomerase IIα.[26] The only C7-aminomethylpyrrolidine fluoroquinolone generated in the current study found to have detectable inhibition of human topoisomerase IIα was UIBW-04-236, which completely inhibits human topoisomerase IIα at a concentration of 100 μM, with a decatenation IC_{50} of 29.3 μM and a poisoning fold-stimulation of 5.15. To put these values in perspective, the supercoiling inhibition IC_{50} of UIBW-04-236 against *E. coli* DNA gyrase is approximately 300-fold lower than the human topoisomerase IIα decatenation IC_{50} of UIBW-04-236 and the poisoning fold-stimulation with *E. coli* DNA gyrase is 4-fold higher. The current hypothesis to explain the ability of UIBW-04-236 to exhibit crossover activity is that the C2-thioether moiety of UIBW-04-236 is able to bind to a GyrA/ParE arginine residue that is near Helix-4 and is conserved across human and bacterial type-II topoisomerases. The compound UIBW-04-236 is also the only compound found to intercalate DNA (data not shown). Compound UIBW-04-236 is unique in that it has a tetracyclic core structure and in 3D *in silico* modeling is more planar than the other compounds.

This study also sought to discover if the DNA cleavage activity of C7-aminomethylpyrrolidine fluoroquinolones observed in purified topoisomerase IV would translate into bacteriostatic activity *E coli* and *M. smegmatis*. Each fluoroquinolone derivative prepared for this study was tested for its ability to inhibit the growth of *E. coli* and *M. smegmatis* cells in broth-dilution assays. These assays were performed to determine the MIC of the fluoroquinolones with *tolC* KO *E. coli* cells, wild-type *M. smegmatis* cells, and a panel of *tolC* KO *E. coli* strains possessing either current fluoroquinolone resistant Helix-4 substitutions or GyrB/ParE amino acid substitutions. The assays with the *E. coli* strains possessing GyrB substitutions were performed to test the ability of the C7-aminomethylpyrrolidine group of the fluoroquinolones to bind

GyrB. The MIC of each of the fluoroquinolones with the mutant *E. coli* strains was then used to calculate the antimutant activities of each of the fluoroquinolones with each mutant *E. coli* strain as a ratio of MIC with mutant *E. coli* strain over MIC with "wild-type" *E. coli* strain. The conclusions of these studies are as follows:

The compound UIBW-04-237, which has an N1-ethyl group, consistently has the highest MIC across the *E. coli* and *M. smegmatis* cells, and the entire panel of mutant *E. coli* strains. The compounds UIBW04-235, which has N1-C8 2-methylmorpholone core, and UITT-03-245, which has an N1-isopropene C8-methoxy core, also consistently have high MIC values compared to the parent C7-aminomethylpyrrolidine fluoroquinolone UING-05-249. Otherwise most compounds generated for this study have MIC values within a narrower range of (within 10-fold the MIC of UING-05-249, which has an N1-cyclopropyl C8-methoxy group) with each wild-type and mutant *E. coli* strain. Bacteriostatic activity against *M. smegmatis* for compounds is overall weaker. In particular, the compounds UIBW-04-235, UIBW-04-237 and UIHS-IIa-215, which has an N1-cyclopropyl C5-methyl C8-methoxy core, have particularly high MIC with *M. smegmatis* compared to UING-05-249. There does not appear to be a consistent trend of compound MIC's across *E. coli* and *M. smegmatis* cultures. All compounds have inferior antimutant activity profiles to UING-05-249 however they have superior profiles to moxifloxacin and the current fluoroquinolone PD160788, which has a tertiary amine in its C7-group and is not expected to be able to make binding interactions with GyrB. Across the panel of C7-aminomethylpyrrolidine fluoroquinolones, of all the mutant *E. coli* strains tested, the largest antimutant activities are consistently found with the *E. coli* strain possessing the Helix-4 S83W substitution. This is not a surprising observation as the S83 residue is one of the Helix-4 residues that coordinate the Mg-water bridge. There are variations in antimutant activity with the *E. coli* strain possessing the Helix-4 S83W substitution across the panel of C7-aminomethylpyrrolidine fluoroquinolones, which

suggests that fluoroquinolone core structure plays a role in at least partially overcoming resistance caused by this this substitution.

In summary, the core-diverse C7-aminomethylpyrrolidine fluoroquinolones have demonstrated the capability for supercoiling inhibition in *E. coli* DNA gyrase, and furthermore demonstrate that they inhibit the function of DNA gyrase by acting as DNA gyrase poisons. With the exception of UIBW-04-236, the fluoroquinolones generated for this study do not inhibit human topoisomerase IIα. Growth inhibition assays with wild-type and mutant *E. coli* strains demonstrate that the C7-aminomethylpyrrolidine group is able to promote antimutant activity across a panel of fluoroquinolones possessing structural diversification to the fluoroquinolone core. Broadly, none of the compounds generated for this study were found to possess an antimutant activity profile across the *E. coli* mutant strains tested that was superior to the broad antimutant activity profile of the parent C7-aminomethylpyrrolidine fluoroquinolone UING-05-249.

7.4: Studies with C7-Variant Fluoroquinolones

An extension of the studies with core-diverse, C7-aminomethylpyrrolidine fluoroquinolones was to understand the structural requirements of the aminomethylpyrrolidine group to bestow the ability to overcome current fluoroquinolone-resistant Helix-4 mutations to fluoroquinolones by binding through the GyrB/ParE region of the ternary complex. In this study, fluoroquinolones with C7 groups that are structural analogs of the aminomethylpyrrolidine group, referred to as "C7-variant fluoroquinolones," were synthesized, as shown in Figure 7.2. The supercoiling inhibition and poisoning activities of the compounds generated for this study were characterized in the same assays described in Chapter 4 for the core-diverse, C7-aminomethylpyrrolidine fluoroquinolones: *in silico* docking studies, supercoiling inhibition and poisoning against wild-type *E. coli* DNA gyrase, topoisomerase IV and human topoisomerase IIα. These compounds were also tested for bacteriostatic activity

with *tolC* KO *E. coli*, *tolC* KO *M. smegmatis*, and mutant *E. coli* strains possessing fluoroquinolone resistant Helix-4 amino acid substitutions or GyrB substitutions. As before, all compounds dock into the wild-type *A. baumannii* topoisomerase IV crystal structure with comparable affinity to each other and to moxifloxacin, using the Mg-water bridge as the primary binding interaction.

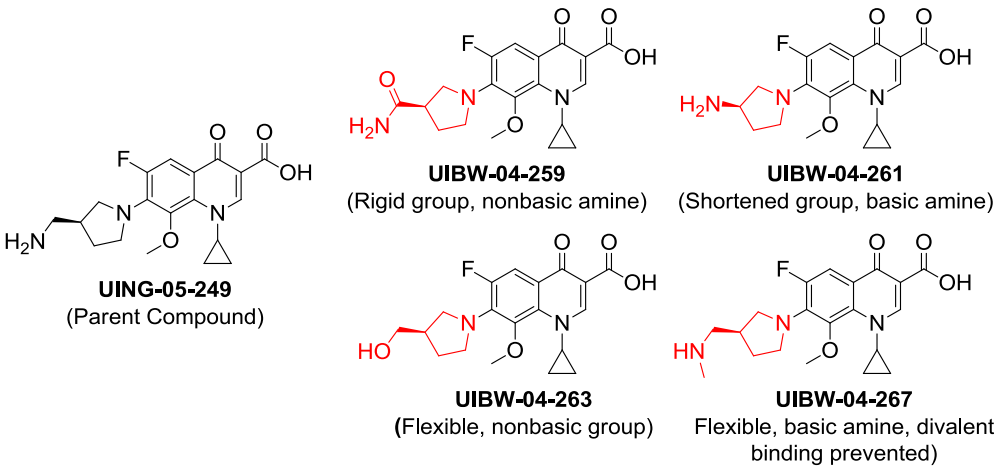

Figure 7.2: The C7-variant fluoroquinolones (C7-groups highlighted in red) with parent compound UING-05-249 and brief descriptions of structural diversification.

The C7-variant compounds have a wider range of IC_{50} values in supercoiling inhibition with *E. coli* DNA gyrase compared to the core-diverse, C7-aminomethylpyrrolidine fluoroquinolones. Specifically, compounds UIBW-04-259 and UIBW-04-263 demonstrate less potent supercoiling inhibition than the other C7-vaiant fluoroquinolones and UING-05-249. Hypothetically, this may be evidence that structural requirement of the aminomethylpyrrolidine side chain to bind through GyrB is the basic amine center. In theory, the side-chain hydroxide of UIBW-04-263 should be able to have a hydrogen-bond donating interaction with the carbonyl oxygen of a GyrB/ParE glutamate residue observed in *in silico* modeling studies with UING-05-249, but perhaps

because this is a weaker interaction because the side chain of UIBW-04-263 does not have a basic center. This hypothesis may also explain the weak supercoiling inhibition activity observed for UIBW-04-259, which also lacks a basic center in its C7-group. The other compounds UIBW-04-261 and UIBW-04-267 have closer supercoiling inhibition IC_{50} values to UING-05-249, and like UING-05-249, both UIBW-04-261 and UIBW-04-267 have a basic amine in their C7-groups. The UIBW-04-261, which has an aminopyrrolidine C7-group, is expected to have diminished capability to interact with the GyrB/ParE residues nut retain capability to interact with DA-20 and DA-16 substructures. The UIBW-04-267 compound has a sterically-hindered amine on its C7-group, compared to the C7-group of UING-05-249, and cannot form the bridging pose between the GyrB/ParE E437 and R418 backbone carbonyl, as observed in docking studies with UING-05-249. The slightly lower supercoiling inhibition of UIBW-04-267 is perhaps evidence that the bridging binding pose is beneficial to binding of the C7-aminomethylpyrroldine in wild-type DNA gyrase. The same consistency of trends between supercoiling inhibition IC_{50} and CC_3 values determined for the C7-variant fluoroquinolones suggest that, similar to the panel of core-diverse, C7-aminomethylpyrrolidine fluoroquinolones, the C7-variant fluoroquinolones are *E. coli* DNA gyrase poisons as opposed to catalytic inhibitors. Only C7-variant compound UIBW-04-261 was found to have detectable inhibition of human topoisomerase IIα decatenation activity, and with half the efficacy at 100 μM as core-variant UIBW-04-236, and with an IC_{50} of 74.4 μM and a poisoning fold-stimulation of 3.95. To put these values in perspective, the supercoiling inhibition IC_{50} of UIBW-04-261 against *E. coli* DNA gyrase is approximately 200-fold lower than the human topoisomerase IIα decatenation IC_{50} of UIBW-04-261 and the poisoning fold-stimulation with *E. coli* DNA gyrase is 5-fold higher.

Interestingly, the compounds UIBW-04-259 and UIBW-04-263 display more potent growth inhibition (lower MIC's) against wild-type *E. coli* in bacteriostatic assays

than the other C7-variant fluoroquinolones. In fact, with a single exception of UIBW-04-263 against the D82A *E. coli* mutant, the compounds UIBW-04-259 and UIBW-04-263 consistently show either superior or equivalent growth-inhibition potency to UING-05-249 with all *E. coli* strains tested. Because the *E. coli* strains used in this study are all *tolC* knock-out, and therefore common mechanisms of drug efflux are disabled, the current hypothesis for the increased potency of these compounds relative to the *in vitro* activity in this study is that they may have marginally superior uptake or penetration into the cells. It is possible that UIBW-04-259 and UIBW-04-263 have better uptake or cell penetration due to the lack of a basic amine within their C7-groups. As a matter of perspective, in bacteriostatic assays with *E. coli* and *M. smegmatis*, all C7-variant fluoroquinolones have comparable MIC values (within 3-fold MIC) to UING-05-249. As observed previously with the core-diverse, C7-aminomethylpyrrolidine fluoroquinolones, the C7-variant fluoroquinolones possess lower growth-inhibition activity in *M. smegmatis* cultures. This is not surprising as lower drug penetration and increased drug efflux are commonly observed with mycobacteria-type species across many drug classes, not just fluoroquinolones. In comparing the activities of the compounds between the two bacteria species, it is observed that the greatest in MIC against *E. coli* verses MIC against *M. smegmatis* is found in the compounds UIBW-04-259 and UIBW-04-263. The C7-variant compounds overall possess inferior antimutant activity profiles compared to UING-05-249. It should be noted, however, that this observation masks the ability of UIBW-04-259 and UIBW-04-263 to more potently inhibit the growth of all tested *E. coli* strains. Furthermore, all C7-variant compounds possess comparable MIC's against wild-type *E. coli* to the clinical fluoroquinolone moxifloxacin and also each has a superior antimutant activity profile compared to moxifloxacin. This is highly encouraging as moxifloxacin is used clinically to treat ciprofloxacin-resistant bacteria. Compound UIBW-04-261, across the panel of Helix-4 mutant *E. coli* strains tested, has the highest antimutant activities and therefore the lowest retention of compound activity against Helix-4 mutants. This may

indicate the importance of GyrB/ParC binding to overcome resistance caused by Helix-4 mutations. The compound UIBW-04-259 (amide variant) has the second highest antimutant activities across the panel of Helix-4 mutants. The fact that, overall, UIBW-04-259 had a less impressive antimutant activity profile than UIBW-04-263 (hydroxyl variant) suggests that side chain flexibility is an important characteristic for overcoming resistance caused by Helix-4 mutants. The capacity for the aminomethylpyrrolidine side chain to bestow the ability for fluoroquinolones to maintain their activity against Helix-4 mutants may be linked to the side chain having multiple options for binding interactions. If that is the case, then side chain flexibility should result in lower antimutant activities across the panel of Helix-4 mutants. This hypothesis is supported by the antimutant activity profiles determined for UIBW-04-263 and UIBW-04-267.

In summary, the studies with the C7-variant fluoroquinolones demonstrate that the C7-aminomethylpyrrolidine, which was observed to bestow activity against current fluoroquinolone-resistant Helix-4 mutations of *B. anthracis* topoisomerase IV, is not the only C7-group capable of doing so. Structural modifications to the C7-aminomethylpyrrolidine group, however, are observed to diminish both supercoiling inhibition and poisoning activity (in terms of CC_3 values) in wild-type *E. coli* DNA gyrase. Other factors, such as superior cell uptake/penetration or reduced efflux, may be the cause of optimized growth inhibition by the C7-variant fluoroquinolones in *E. coli*. Most importantly, antimutant activity profiles of compounds can be altered with variation to C7-group and it may be possible that the C7-aminomethylpyrrolidine can be further modified in order to improve fluoroquinolone binding through GyrB/ParE. This study also demonstrates that the C7-vairant fluoroquinolones possess superior bacteriostatic and antimutant activities than the known clinical agent moxifloxacin in *E. coli* strains.

7.5: Future Directions

With the above conclusions in mind, future directions of these studies include more extensive modifications to the C7-aminomethylpyrrolidine side chain in order to further increase understanding of structural requirements of the C7-group to make binding interactions with GyrB/ParE-region as a way to overcome current fluoroquinolone resistance caused by Helix-4 mutations. Currently, *bis*-substituted pyrrolidine C7-groups are of interest for future modifications, as shown in Figure 7.3. Further *in silico* studies with crystal structures altered to have Helix-4 amino acid substitutions known to cause fluoroquinolone-resistance will be performed to explain variations in supercoiling inhibition IC_{50} and CC_3 values of both series of core-diverse, C7-aminomethylpyrrolidine and C7-variant fluoroquinolones will also be pursued. Docking studies with additional modifications to the C7-aminomethylpyrrolidine will guide future plans for synthesis of fluoroquinolone derivatives. Additionally, further *in vitro* studies with purified bacterial type-II topoisomerases possessing current fluoroquinolone-resistant Helix-4 amino acid substitutions will be performed in an attempt to explain patterns within the antimutant activities of the core-diverse and C7-variant compounds.

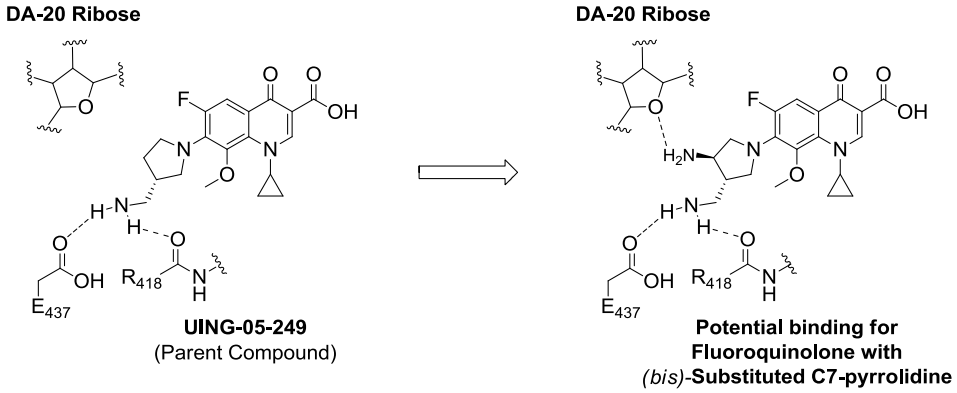

Figure 7.3: Proposed binding for fluoroquinolone with bis-substituted C7-pyrrolidine group.

APPENDIX A: CHAPTER 3 SELECTED NMR SPECTRA

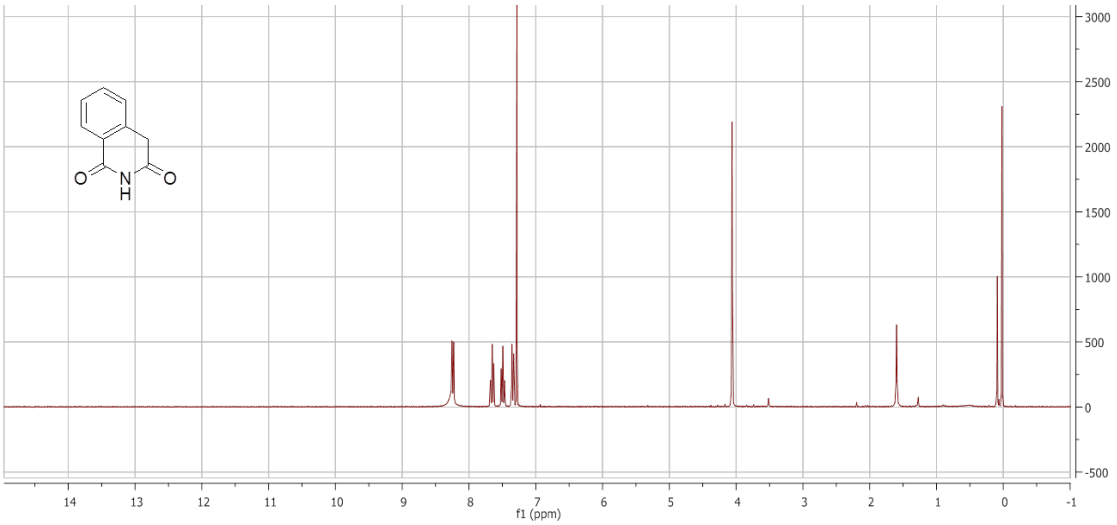

Figure A1. ^{1}H-NMR (300 MHz, $CHCl_3$) of **6** (**UIBW01-236**)

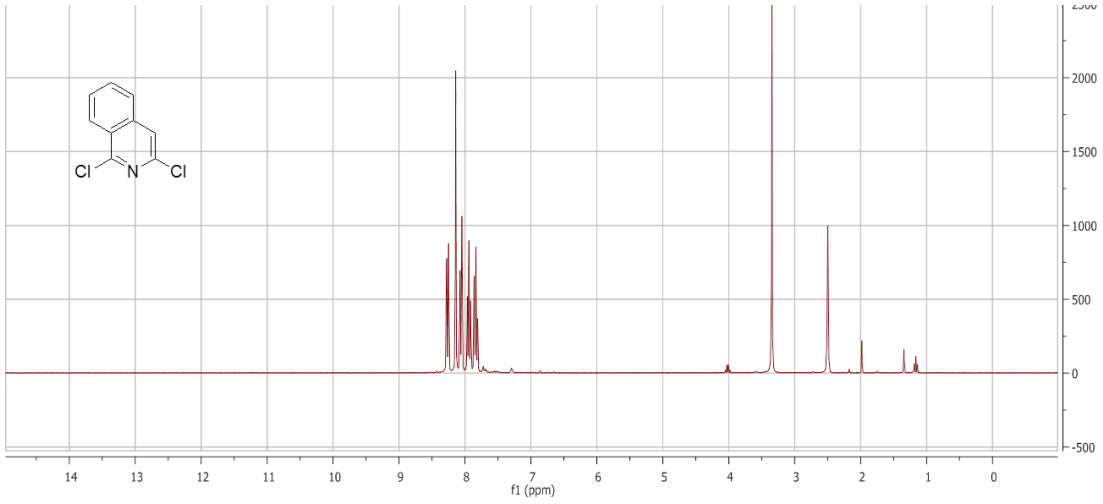

Figure A2. ^{1}H-NMR (300 MHz, DMSO-d_6) of **7** (**UIBW01-239**)

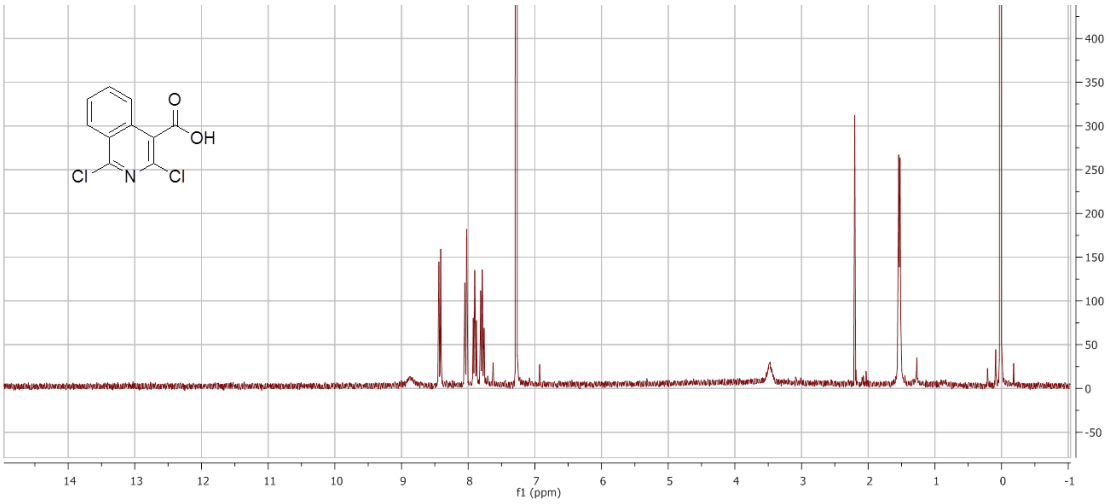

Figure A3. ^{1}H-NMR (300 MHz, $CHCl_3$) of **8** (**UIBW02-121**)

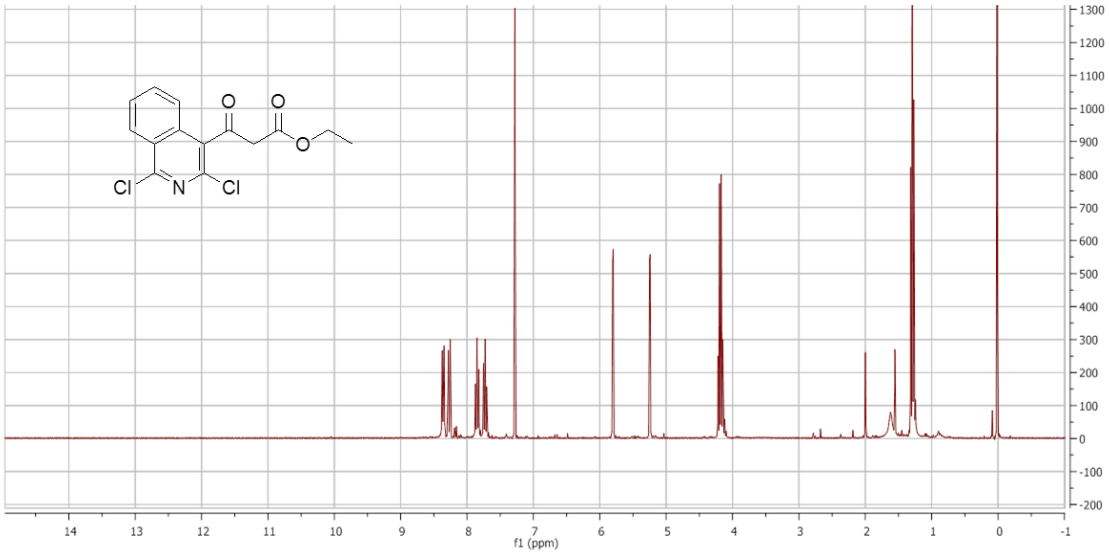

Figure A4. ^{1}H-NMR (300 MHz, $CHCl_3$) of **10 (UIBW02-299)**

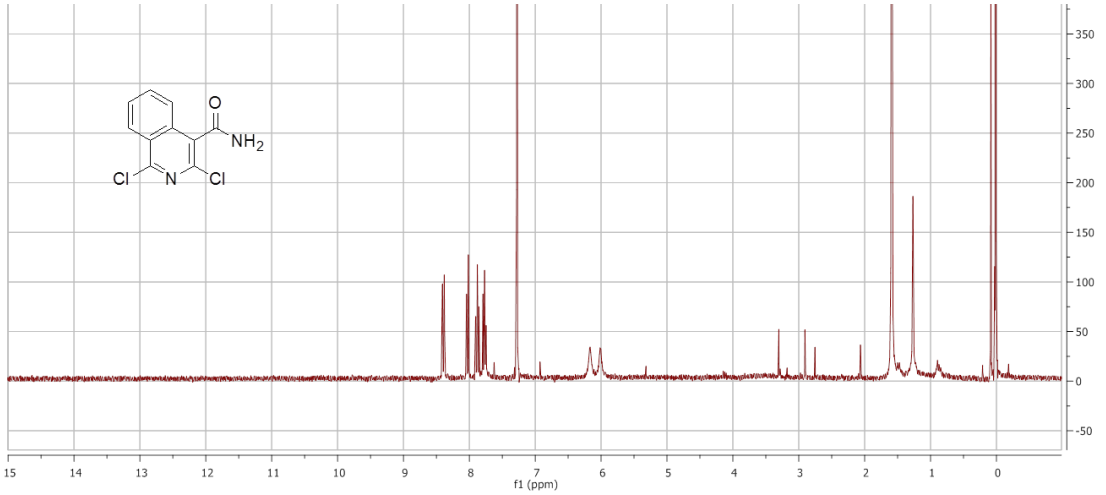

Figure A5. ^{1}H-NMR (300 MHz, $CHCl_3$) of **9** (**UIBW02-297**)

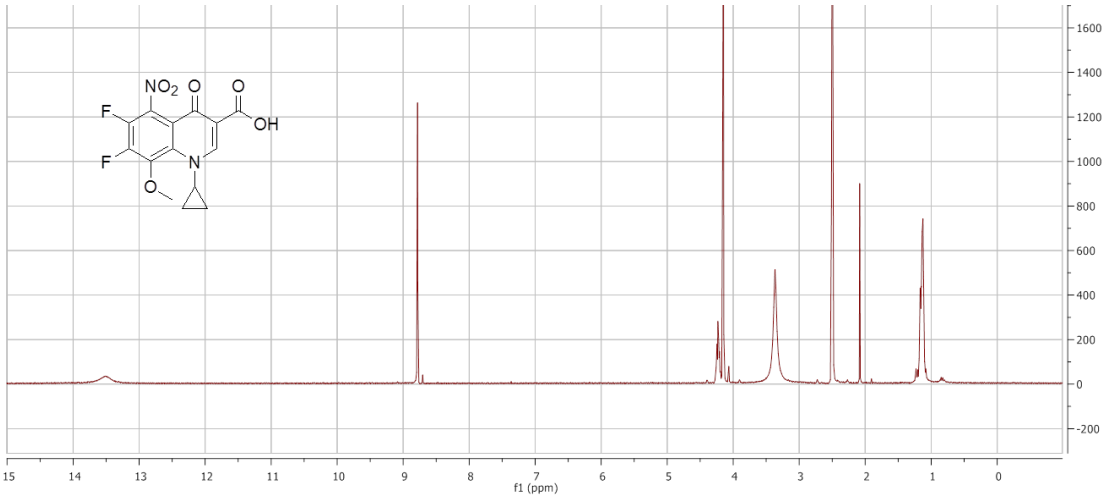

Figure A6. ^{1}H-NMR (300 MHz, DMSO-d_6) of **21** (**UIBW02-067**)

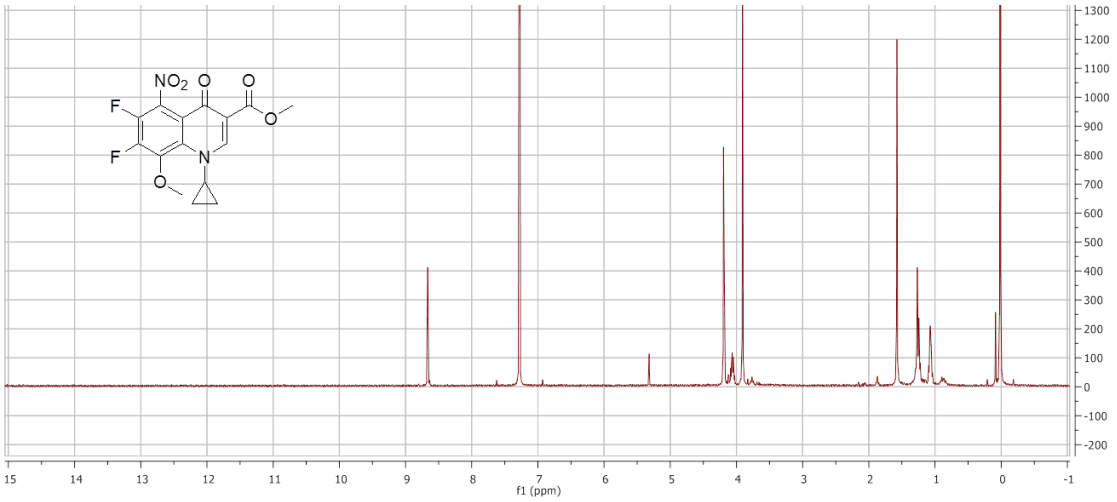

Figure A7. ^{1}H-NMR (300 MHz, $CHCl_3$) of **22** (**UIBW02-068**)

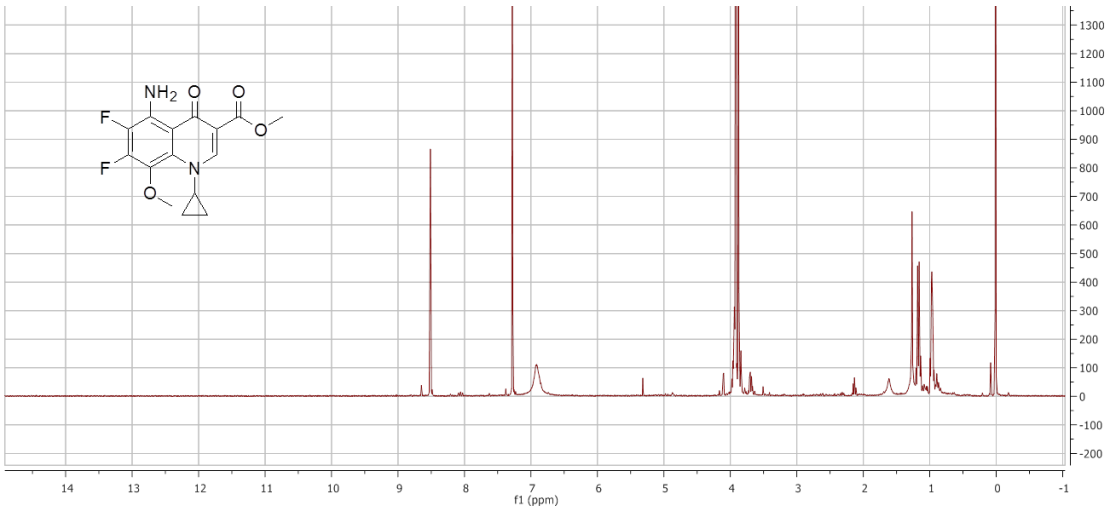

Figure A8. ^{1}H-NMR (300 MHz, $CHCl_3$) of **23** (**UIBW02-196**)

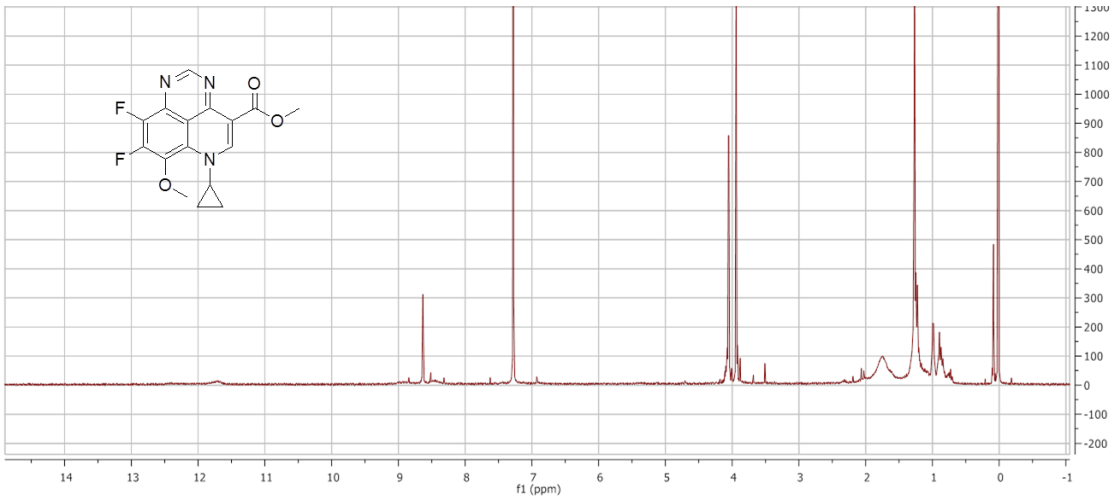

Figure A9. ^{1}H-NMR (300 MHz, $CHCl_3$) of **24** (**UIBW02-157**)

APPENDIX B: CHAPTER 4 AND 5 SELECTED NMR SPECTRA AND HPLC CHROMATOGRAMS

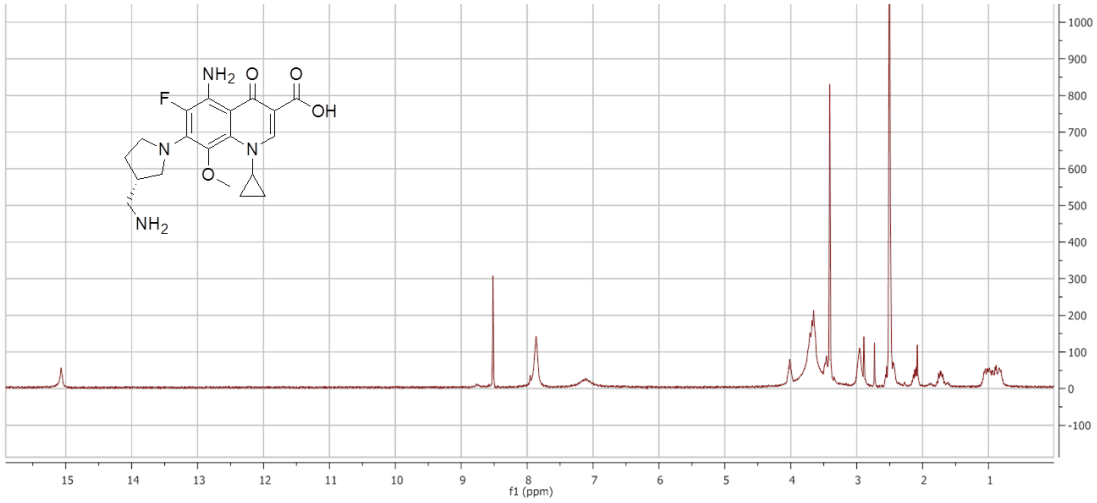

Figure B1. ^{1}H-NMR (300 MHz, DMSO-d_6) of (**UIBW-04-123B**)

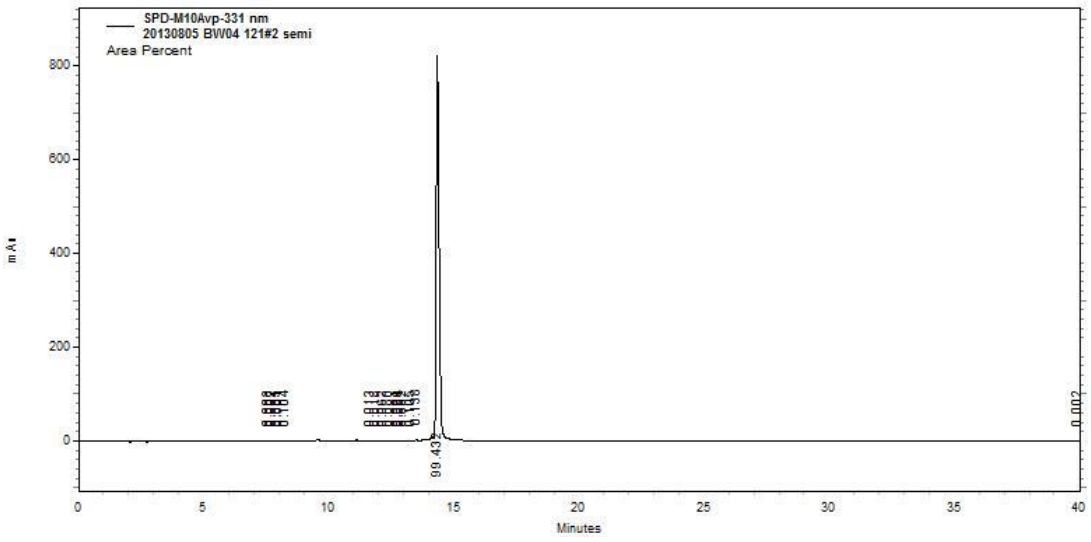

Figure B2. HPLC chromatogram of (**UIBW-04-123B**)

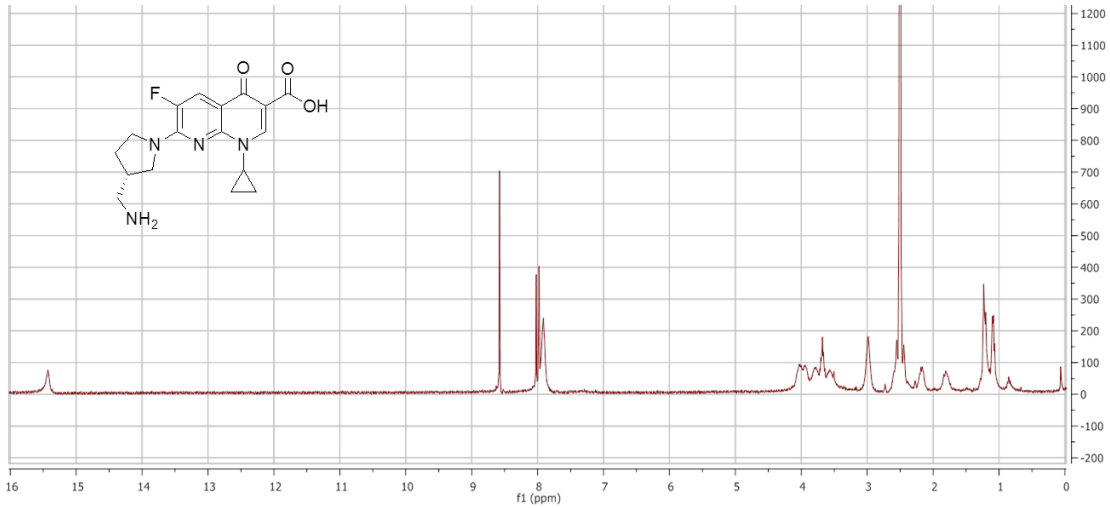

Figure B3. ^{1}H-NMR (300 MHz, DMSO-d_6) of (**UIBW-04-234**)

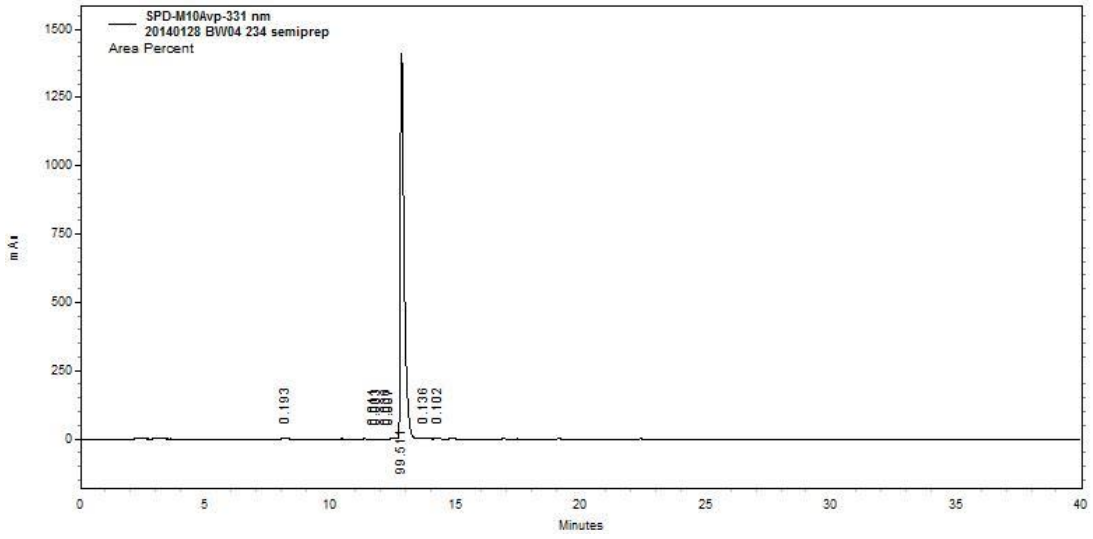

Figure B4. HPLC chromatogram of (**UIBW-04-234**)

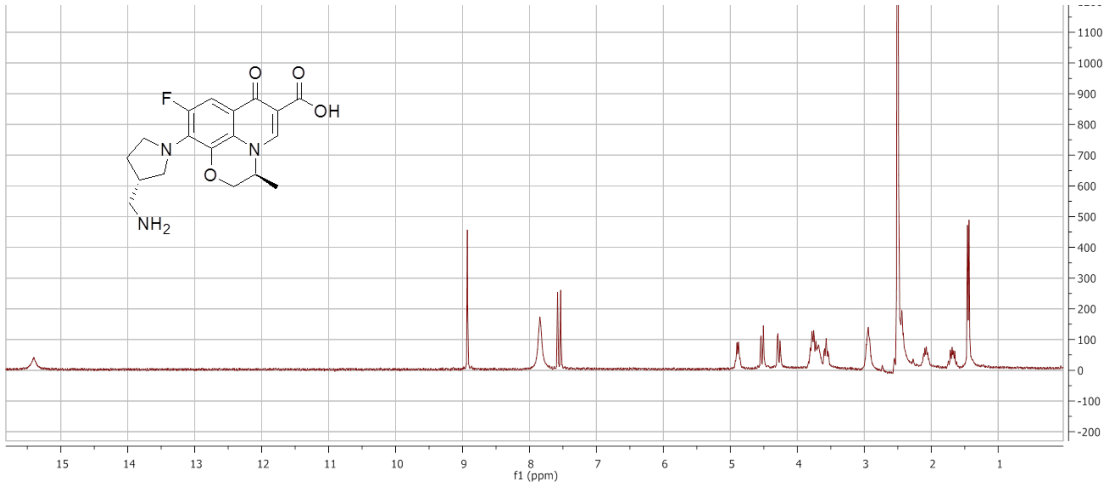

Figure B5. ^{1}H-NMR (300 MHz, DMSO-d_6) of (**UIBW-04-235**)

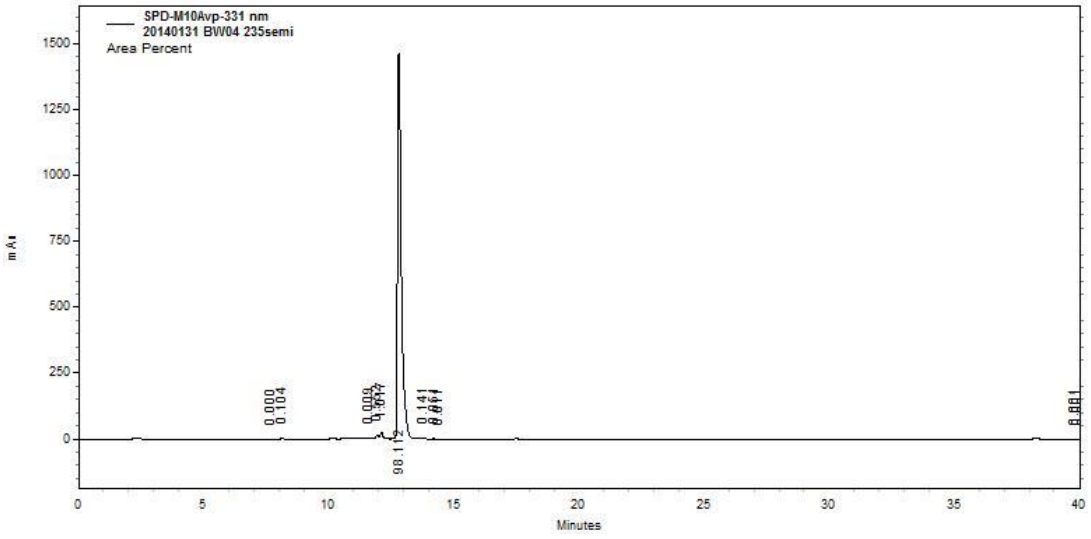

Figure B6. HPLC chromatogram of (**UIBW-04-235**)

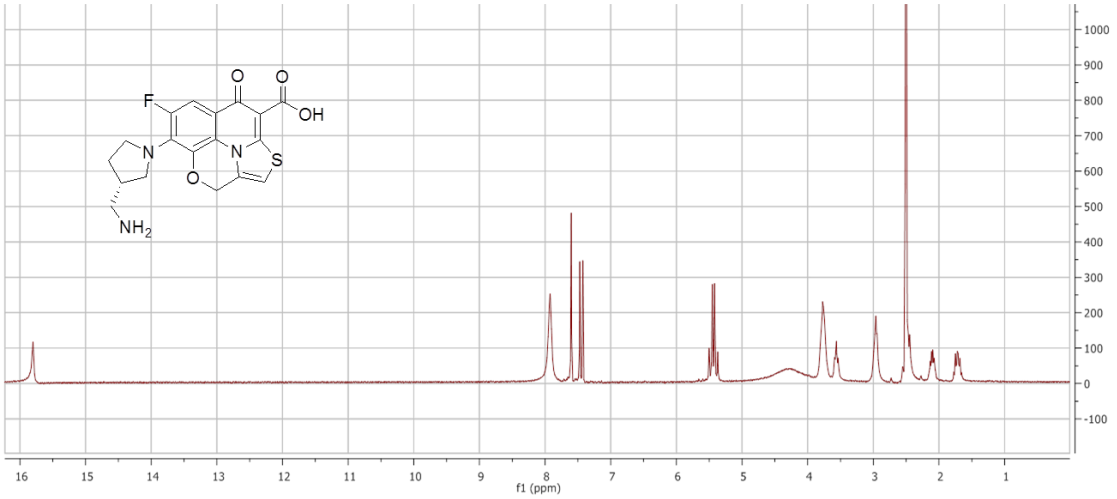

Figure B7. ^{1}H-NMR (300 MHz, DMSO-d_6) of (**UIBW-04-236**)

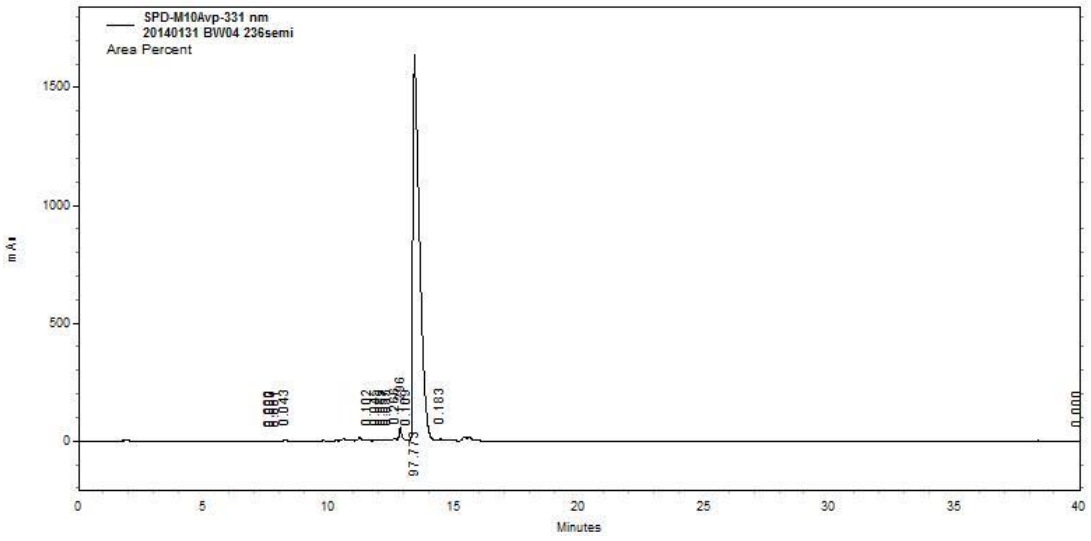

Figure B8. HPLC chromatogram of (**UIBW-04-236**)

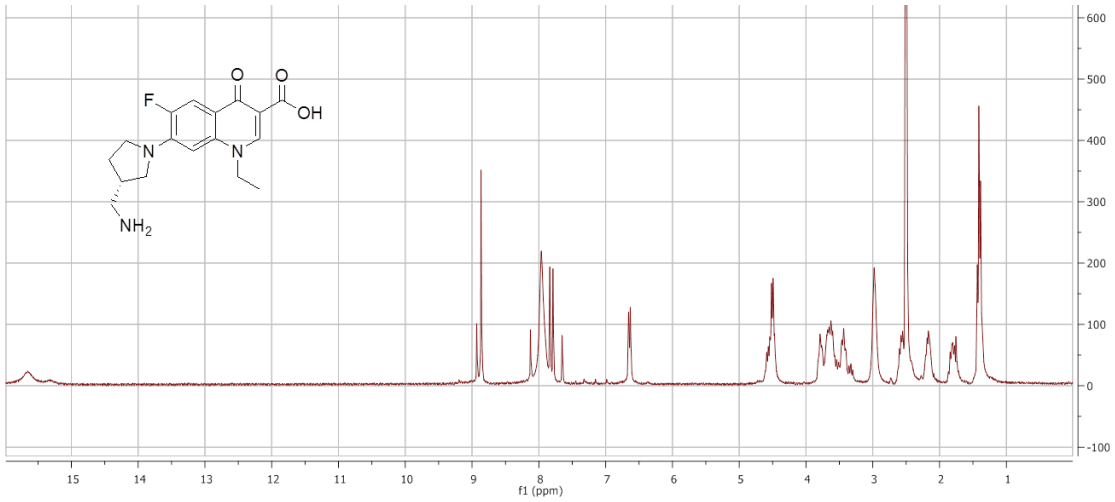

Figure B9. ^{1}H-NMR (300 MHz, DMSO-d_6) of (**UIBW-04-237**)

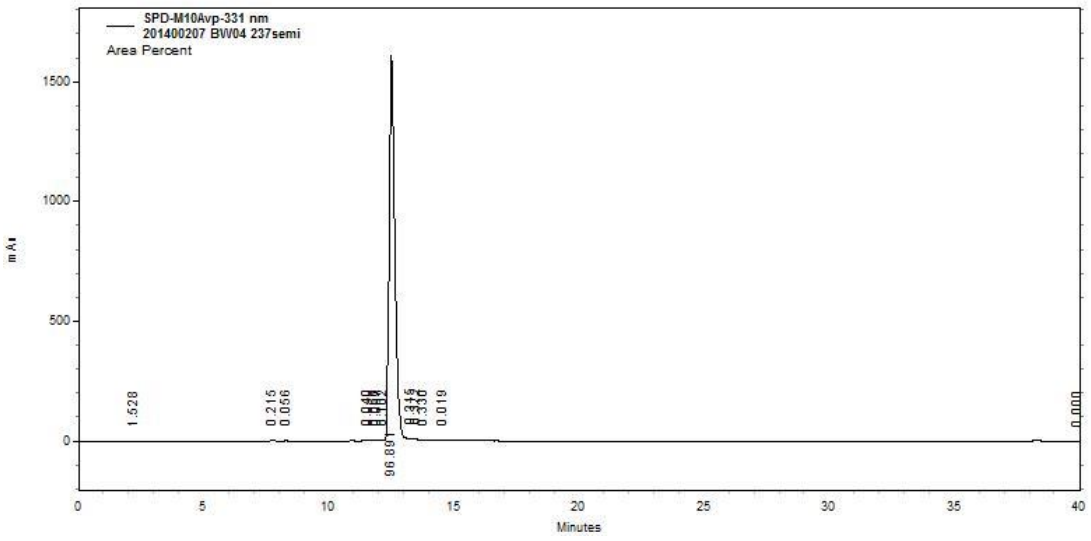

Figure B10. HPLC chromatogram of (**UIBW-04-237**)

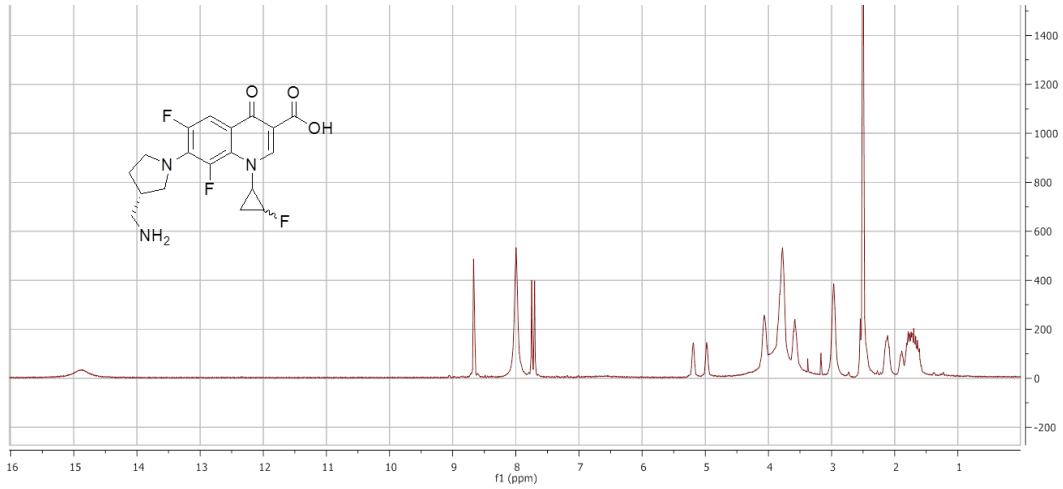

Figure B11. ^{1}H-NMR (300 MHz, DMSO-d_6) of (**UIBW-04-238**)

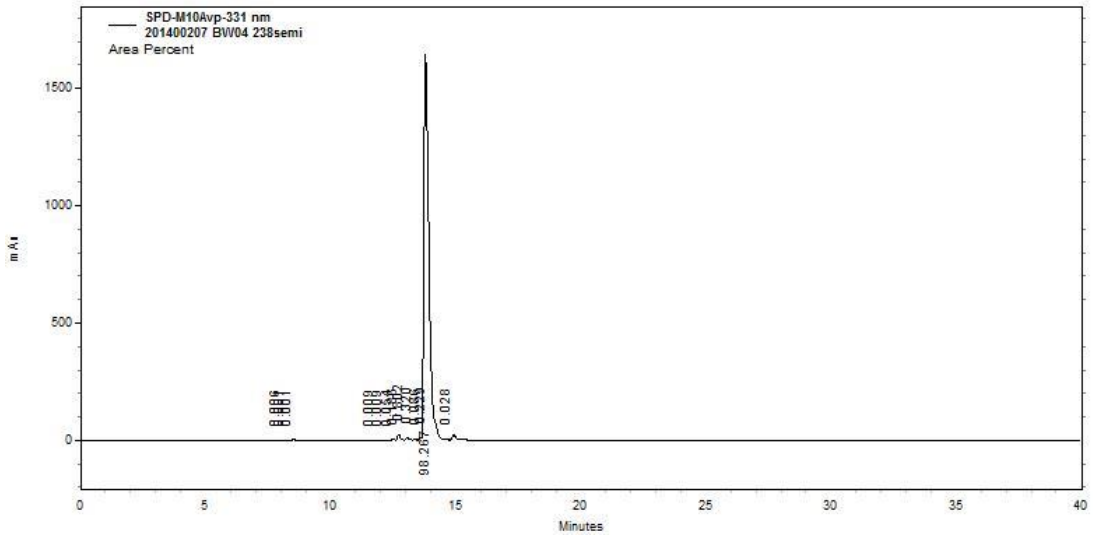

Figure B12. HPLC chromatogram of (**UIBW-04-238**)

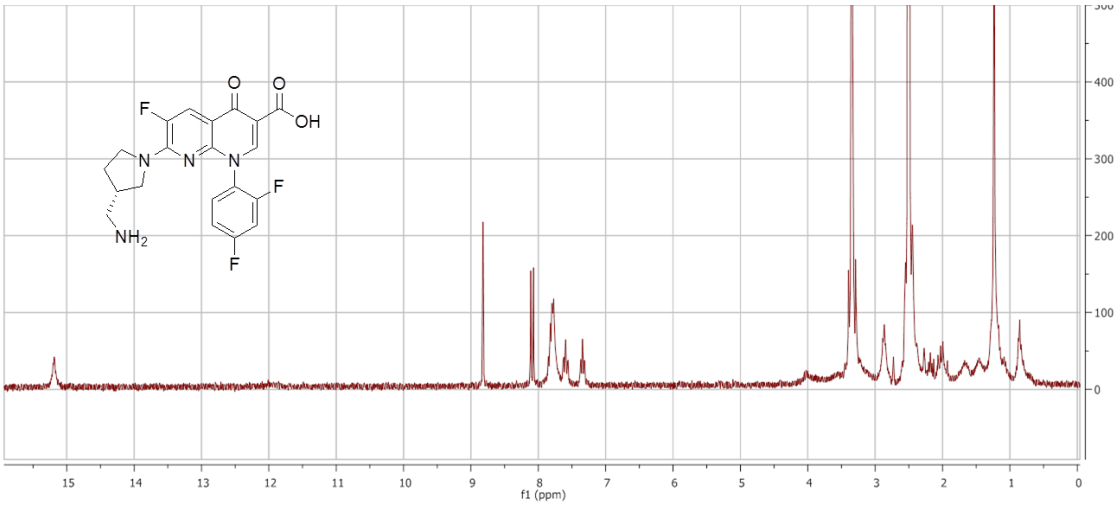

Figure B13. ^{1}H-NMR (300 MHz, DMSO-d_6) of (**UIBW-04-255**)

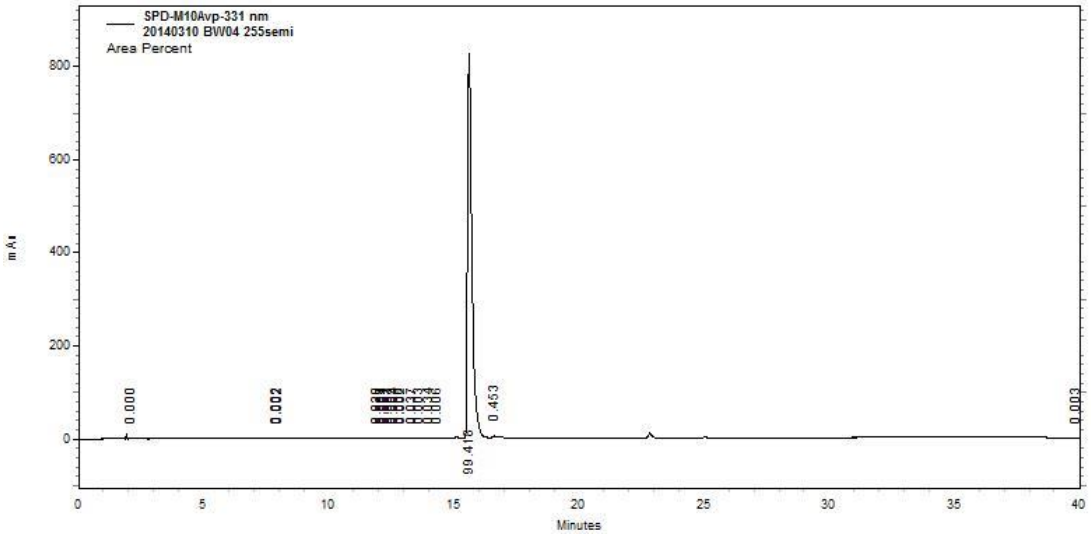

Figure B14. HPLC chromatogram of (**UIBW-04-255**)

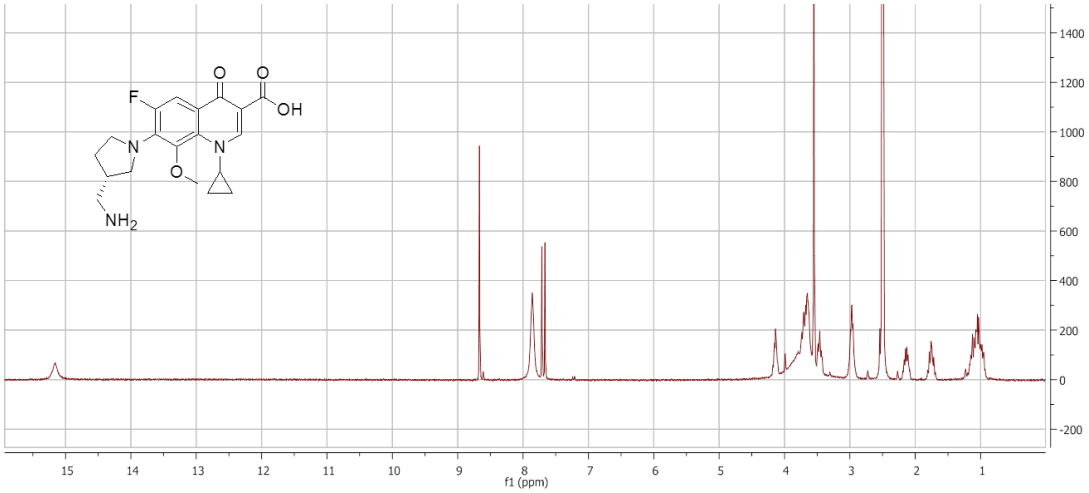

Figure B15. ^{1}H-NMR (300 MHz, DMSO-d_6) of (**UIHS-IIa-77 / UING-05-249**)

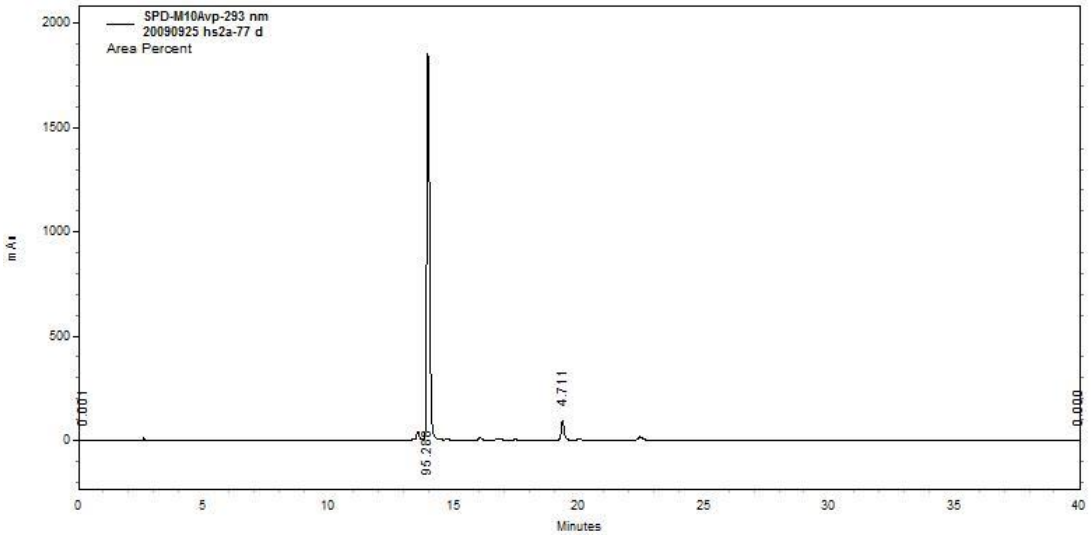

Figure B16. HPLC chromatogram of (**UIHS-IIa-77 / UING-05-249**)

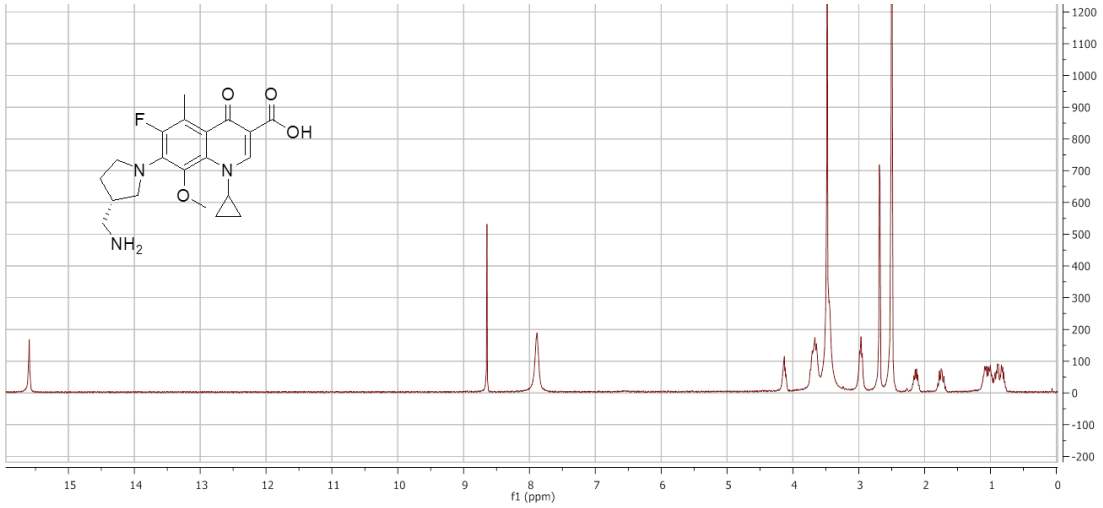

Figure B17. ^{1}H-NMR (300 MHz, DMSO-d_6) of (**UIHS-IIa-215**)

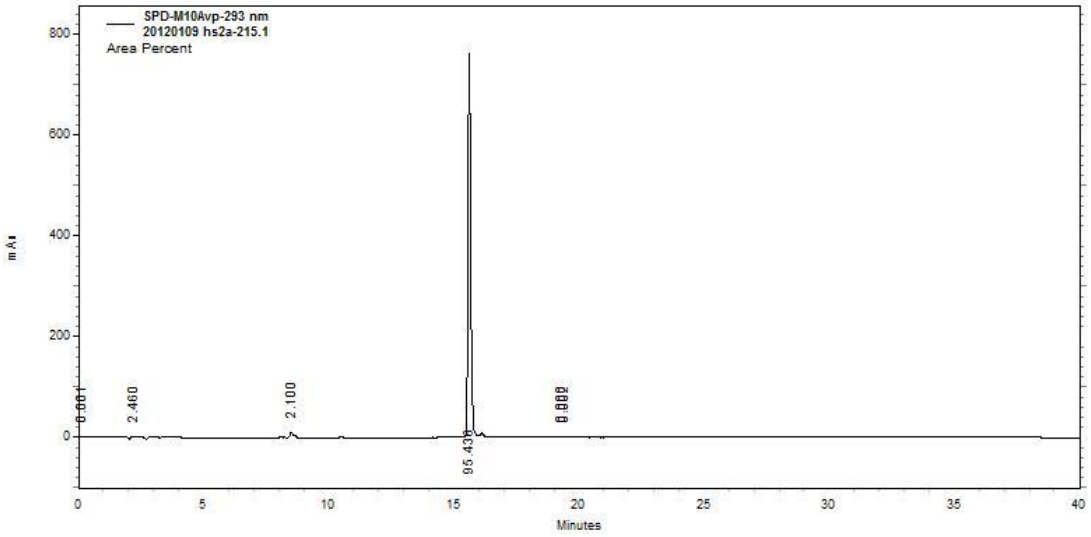

Figure B18. HPLC chromatogram of (**UIHS-IIa-215**)

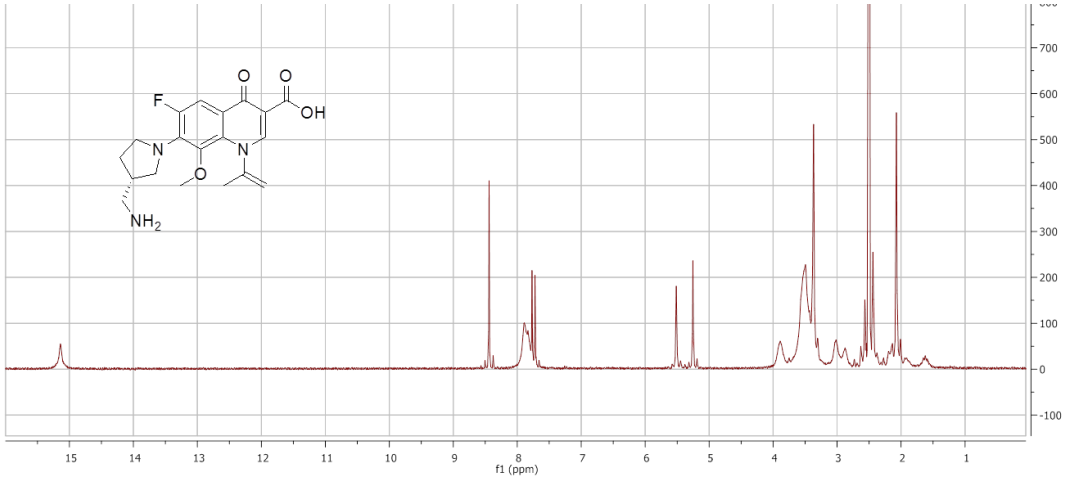

Figure B19. ^{1}H-NMR (300 MHz, DMSO-d_6) of (**UITT-03-245**)

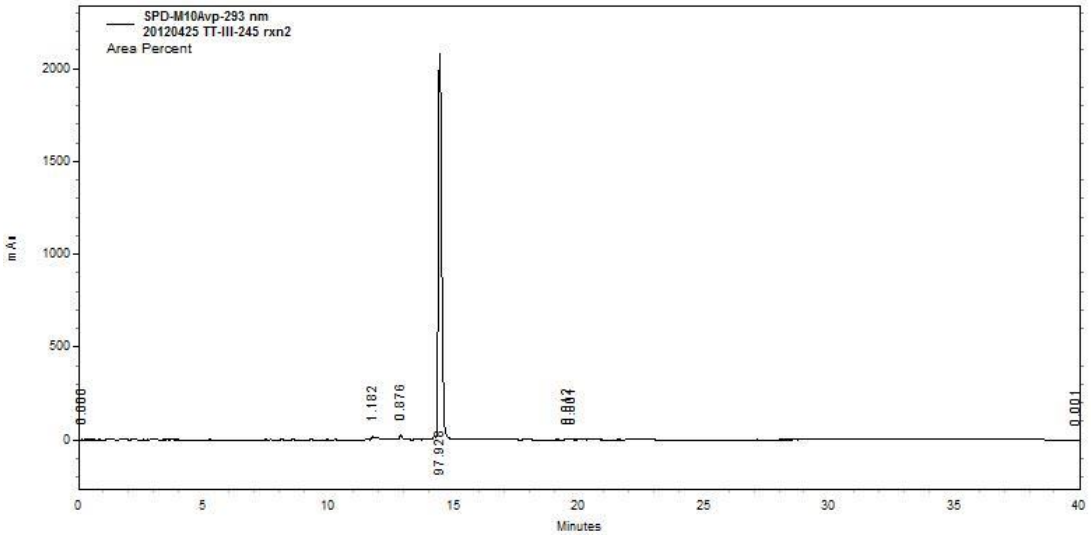

Figure B20. HPLC chromatogram of (**UITT-03-245**)

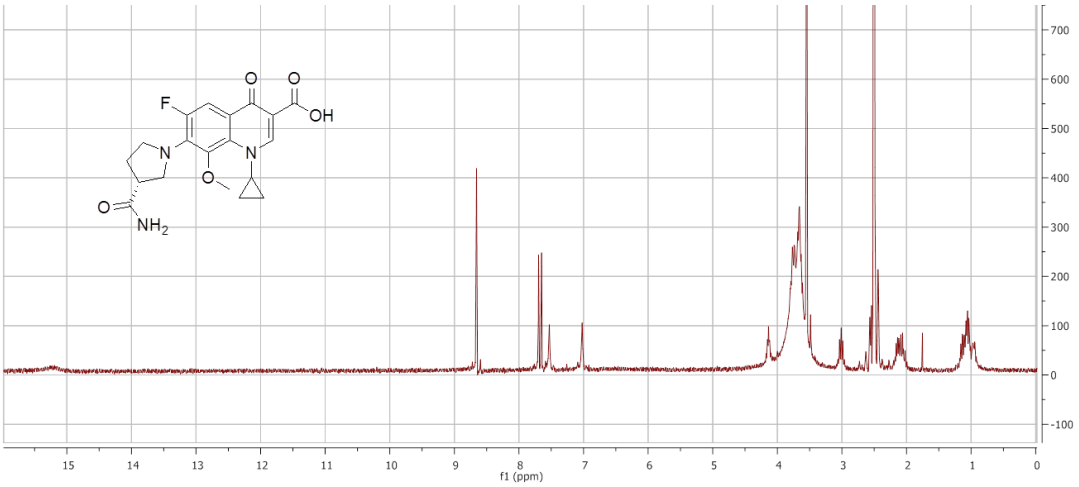

Figure B21. ^{1}H-NMR (300 MHz, DMSO-d_6) of (**UIBW-04-259**)

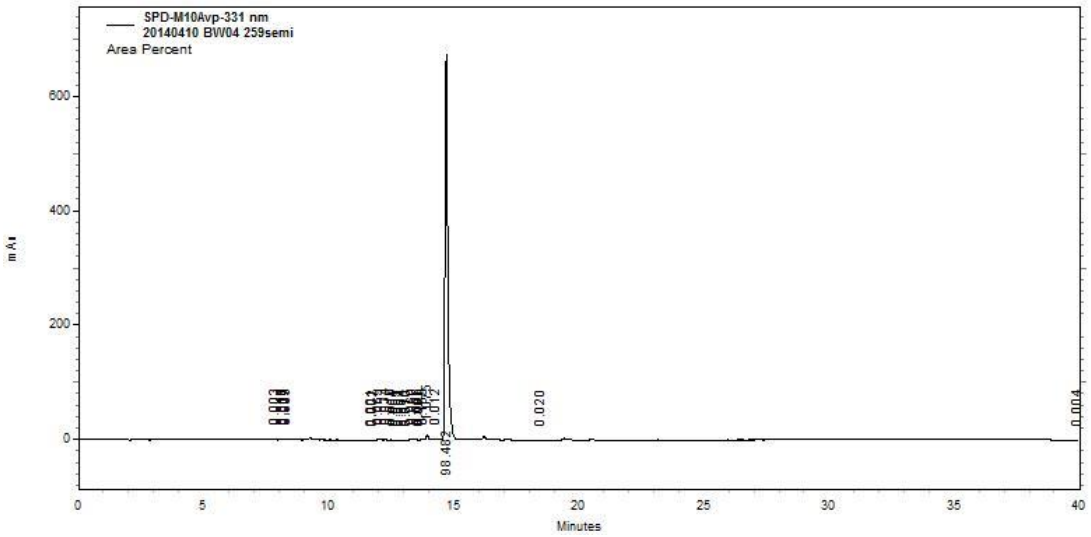

Figure B22. HPLC chromatogram of (**UIBW-04-259**)

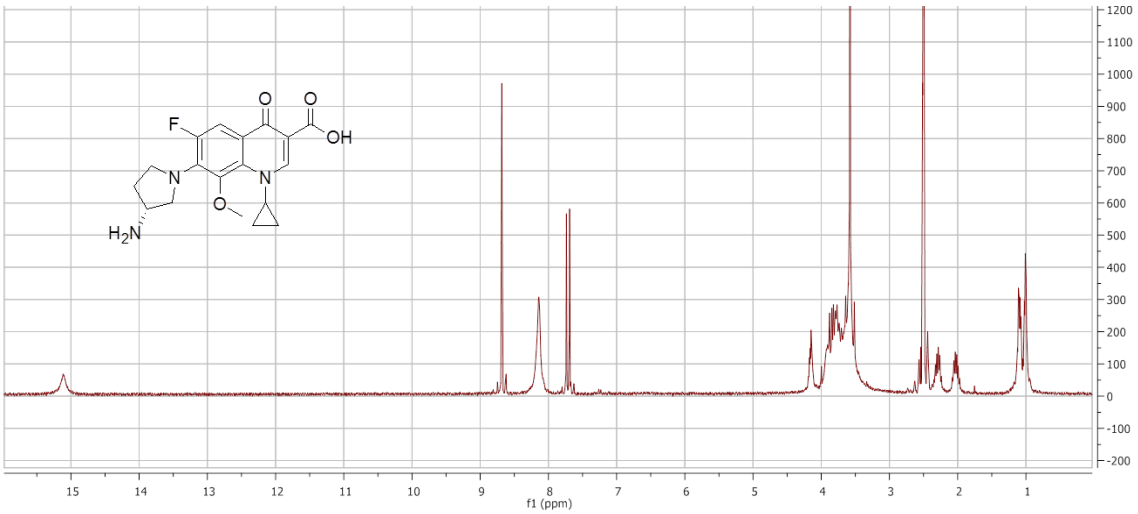

Figure B23. ^{1}H-NMR (300 MHz, DMSO-d_6) of (**UIBW-04-261**)

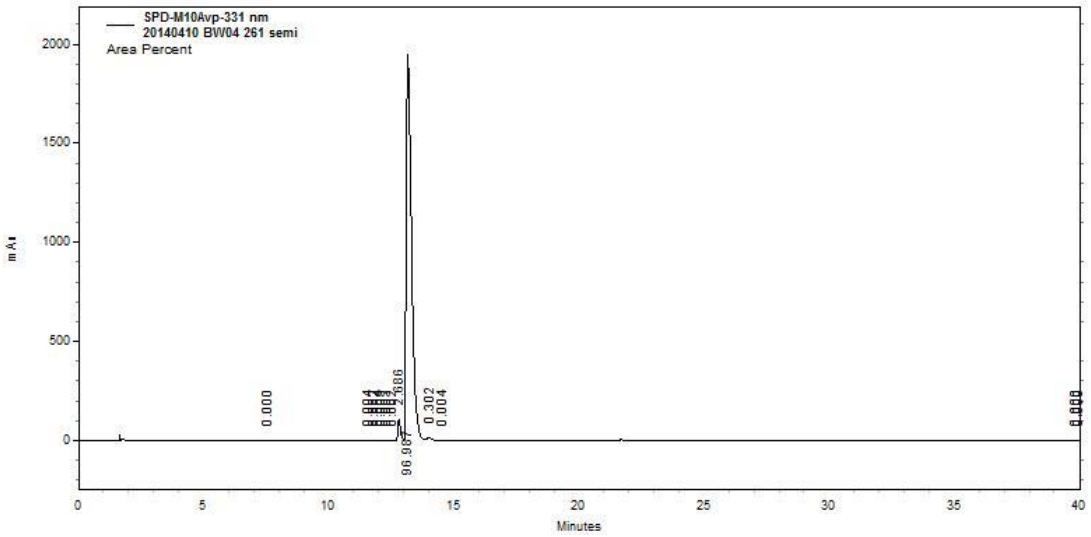

Figure B24. HPLC chromatogram of (**UIBW-04-261**)

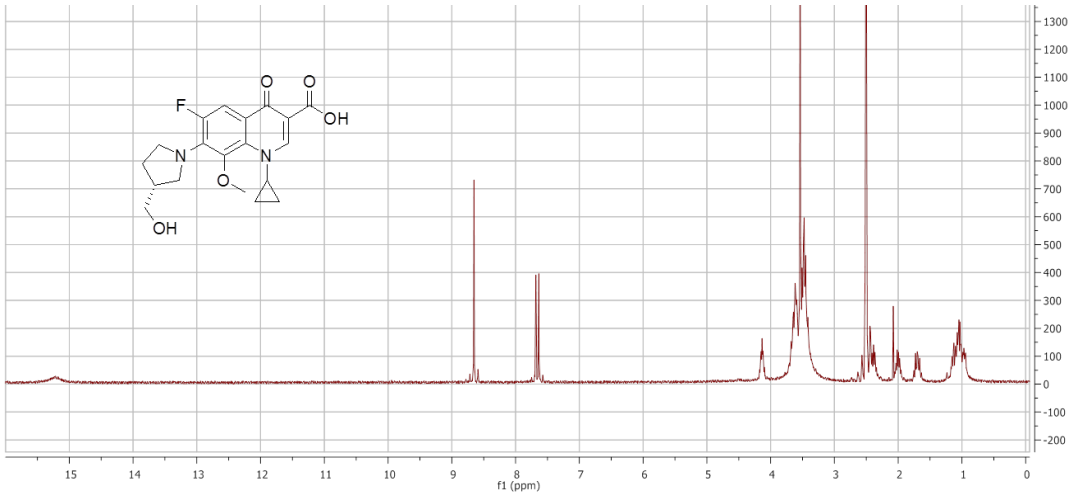

Figure B25. ^{1}H-NMR (300 MHz, DMSO-d_6) of (**UIBW-04-263**)

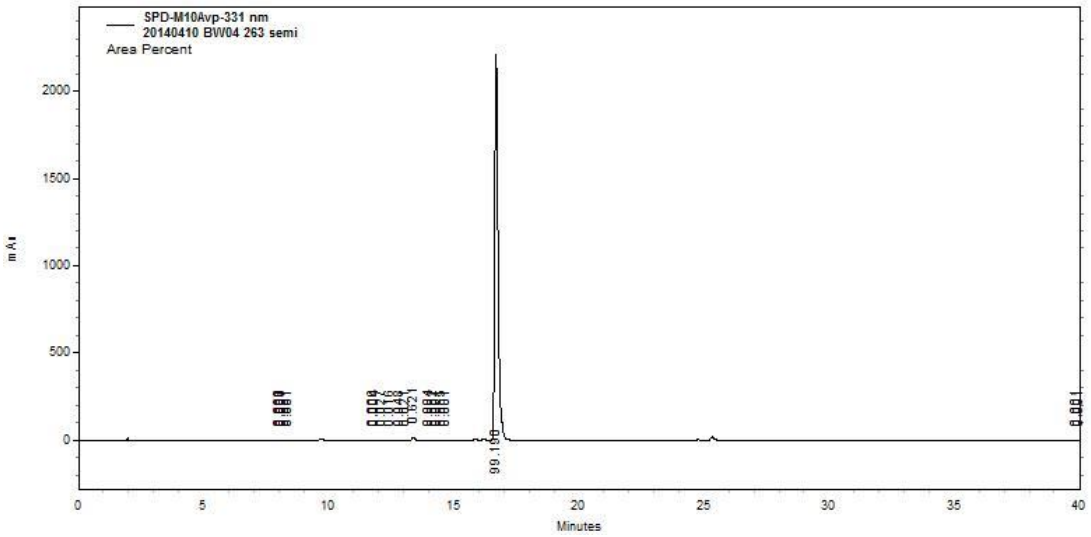

Figure B26. HPLC chromatogram of (**UIBW-04-263**)

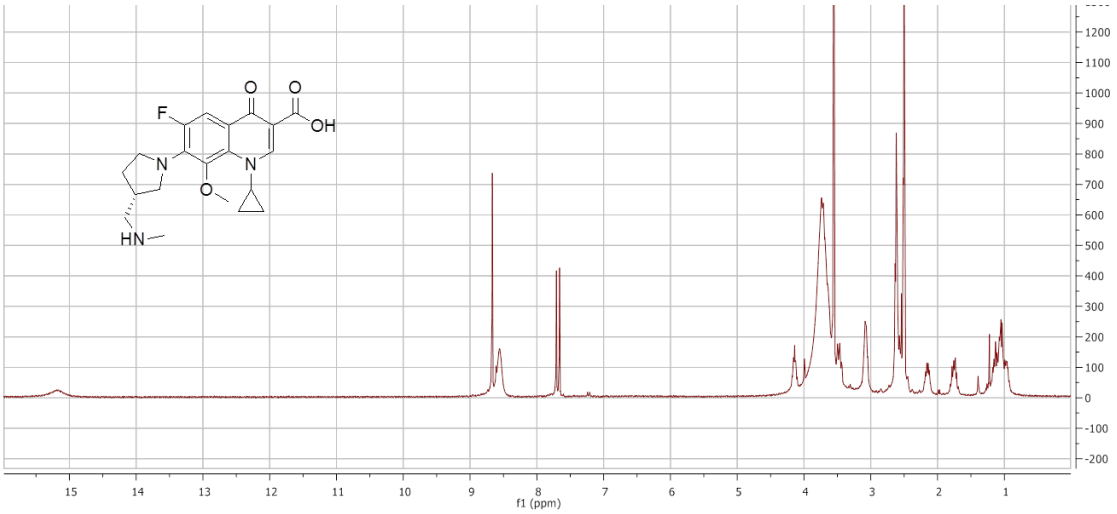

Figure B27. ^{1}H-NMR (300 MHz, DMSO-d_6) of (**UIBW-04-267**)

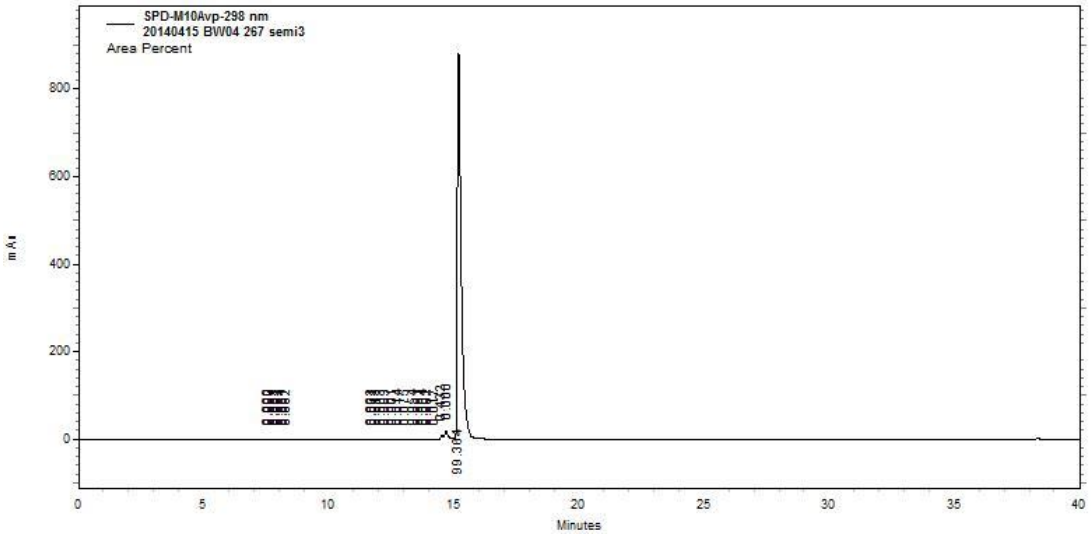

Figure B28. HPLC chromatogram of (**UIBW-04-267**)

REFERENCES

1. Bisacchi, G. S., Origins of the Quinolone Class of Antibacterials: An Expanded "Discovery Story". *Journal of Medicinal Chemistry* **2015, Article ASAP**.
2. Lesher , G. Y.; Froelich , E. J.; Gruett , M. D.; Bailey , J. H.; Brundage, R. P., 1,8-Naphthyridine derivatives: a new class of chemotherapeutic agents. *Journal of Medicinal Chemistry* **1962,** *5* (5), 1063-1065.
3. Cohen, M. A.; Huband, M. D.; Mailloux, G. B.; Yoder, S. L.; Roland, G. E.; Heifetz, C. L., In vitro antibacterial activities of the fluoroquinolones PD 117596, PD124816, and PD 127391. *Diagnosis and Microbiology of Infectious Diseases* **1991,** *14* (3), 245-258.
4. Buchbinder, M.; Webb, J.; Anderson, L.; McCabe, W., Laboratory studies and clinical pharmacology of nalidixic acid (WIN 18,320). *Antimicrobial Agents and Chemotherapy* **1962,** *6*, 308-317.
5. Neu, H., Chemical evolution of the fluoroquinolone antimicrobial agents. *American Journal of Medicine* **1989,** *87*, Suppl. 6C: 2S-9S.
6. Blondeau, J. M., A review of the comparative in-vitro activities of 12 antimicrobial agents, with a focus on five new respiratory quinolones. *Journal of Antimicrobial Chemotherapy* **1999,** *43*, Suppl 2: 1-11.
7. Koga, H.; Itoh, A.; Murayama, S.; Seigo Suzue ; Irikura, T., Structure-activity relationships of antibacterial 6,7- and 7,8- disubstituted 1-alkyl-1,4-dihydro-4-oxoquinoline-3-carboxylic acids. *Journal of Medicinal Chemistry* **1980,** *23* (12), 1358-1363.
8. Davis R; Markham A; JA., B., Ciprofloxacin: an updated review of its pharmacology, therapeutic efficacy and tolerability. *Drugs* **1996,** *51* (6), 1019-1074.
9. Weiss, K.; Laverdiere, M.; Restieri, C., Comparative activity of trovafloxacin and Bay 12-8039 against 452 clinical isolates of Streptococcus pneumoniae. *Journal of Antimicrobial Chemotherapy* **1998,** *42* (4), 523-525.
10. Acar, J.; Goldstein, F., Trends in bacterial resistance to fluoroquinolones. . *Clinical Infectious Diseases* **1997,** *24*, 1 Suppl. S67-73.
11. Zhanel, G. G.; Kelly Ennis; Lavern Vercaigne; Andrew Walkty; Alfred S. Gin; John Embil; Smith, H.; Hoban, D. J., A Critical Review of the Fluoroquinolones Focus on Respiratory Tract Infections. *Drugs* **2002,** *62* (1), 13-59.
12. Andriole, V., The future of the quinolones. *Drugs* **1993,** *45*, Supp. 3: 1-7.
13. Domagala, J. M.., Structure-activity and structure-side-effect relationships for the quinolone antibacterials. *Journal of Antimicrobial Chemotherapy* **1994,** *33* (4), 685-706.
14. Wolfson, J.; Hooper, D., Fluoroquinolone antimicrobial agents. *Clinical Microbiology Review* **1989,** *2* (4), 378-424.
15. Zhanel, G. G.; Walkty, A.; Vercaigne, L.; Karlowsky, J. A.; Embil, J.; Gin, A. S.; Hoban, D. J., The new fluoroquinolones: A critical review. *Canadian Journal of Infectiuos Diseases* **1999,** *10* (3), 207-238.
16. Anderson, V. R.; Perry, C. M., Levofloxacin: A Review of its Use as a High-Dose, Short-Course Treatment for Bacterial Infection. *Drugs* **2008,** *68* (4), 535-565.
17. (a) Allegraa, L.; Konietzkob, N.; Leophontec, P.; Hosied, J.; Pauwelse, R.; Guyenf, J. N.; Petitpretzg, P., Comparative safety and efficacy of sparfloxacin in the treatment of acute exacerbations of chronic obstructive pulmonary disease: a double-blind, randomised, parallel, multicentre study. *Journal of Antimicrobial Chemotherapy* **1993,** *37*, Suppl. :93-104; (b) DeAbate, C. In *Treatment of acute bacterial exacerbations of chronic bronchitis with sparfloxacin and ofloxacin.* , Thirty-sixth Interscience Conference on Antimicrobial Agents and Chemotherapy., New Orleans, September 18-20; The SPAR Multicentre ABECB Study Group.: New Orleans, 1996.

18. Taytard, A.; Aguado, G. A.; Vogel, F. In *Short (5 days) course of sparfloxacin in the treatment of acute exacerbation of chronic bronchitis.*, First European Congress of Chemotherapy, May 14-17; 1996.
19. Jaillon P; Morganroth J; Brumpt I; G., T., Overview of electrocardiographic and cardiovascular safety data for sparfloxacin. . *Journal of Antimicrobial Chemotherapy* **1996,** *37*, Suppl. A: 161-167.
20. Ferguson J; R., D., Phototoxicity in quinolones: comparison of ciprofloxacin and grepafloxacin. . *Journal of Antimicrobial Chemotherapy* **1997,** *40*, Suppl. A: 93-98.
21. Blondeau, J. M.; Laskowski, R.; Bjarnason, J.; Stewart, C., Comparative in vitro activity of gatifloxacin, grepafloxacin, levofloxacin, moxifloxacin and trovafloxacin against 4151 Gram-negative and Gram-positive organisms. *International Journal of Antimicrobial Agents* **2000,** *14*, 45-50.
22. Ball P, F. A., Tillotson G. , Therapeutic advances of new fluoroquinolones. . *Expert Opinions on Investigational Drugs* **1998,** *7*, 761-783.
23. Blondeau, J. M., Expanded activity and utility of the new fluoroquinolones: a review. *Clinial Therapeutics* **1998,** *21*, 3-40.
24. Hooper, D. C., Emerging Mechanisms of Fluoroquinolone Resistance. *Emerging Infectious Diseases* **2001,** *7* (2), 337-341.
25. Bryskier, A.; Chantot, J. F., Classification and structure-activity relationships of fluoroquinolones. *Drugs* **1995,** *49*, Suppl. 2: 16-28.
26. Aldred, K. J.; Schwanz, H. A.; Li, G.; McPherson, S. A.; Turnbough Jr., C. L.; Kerns, R. J.; Osheroff, N., Overcoming target-mediated quinolone resistance in topoisomerase IV by introducing metal-ion-independent drug-enzyme interactions. *ACS Chemical Biology* **2013,** *8* (12), 2660-8.
27. Mizuki Y; Fujiwara I; T., Y., Pharmacokinetic interactions related to the chemical structures of fluoroquinolones. *Journal of Antimicrobial Chemotherapy* **1996,** *37*, Supp. A: 41-55.
28. Deppermann, K. M.; Lode, H., Fluoroquinolones: interaction profile during enteral absorption. *Drugs* **1993,** *45*, Supp. 3: 65-72.
29. Marshall, A. J.; Piddock, L., Interaction of divalent cations, quinolones and bacteria. *Journal of Antimicrobial Chemotherapy* **1994,** *34*, 465-483.
30. Wohlkonig, A.; Chan, P. F.; Fosberry, A. P.; Homes, P., Huang,; J., K., M., ; Leydon, V. R.; Miles, T. J.; Pearson, N. D.; Perera, R. L.; Shillings, A. J.; Gwynn, M. N.; Bax, B. D., Structural basis of quinolone inhibition of type IIA topoisomerases and target-mediated resistance. . *Nature: Structural and Molecular Biology* **2010,** *17*, 1152-1153.
31. Brighty, K. E.; Gootz, T. D., The chemistry and biological profile of trovafloxacin. . *Journal of Antimicrobial Chemotherapy* **1997,** *39*, Suppl. B: 1-14.
32. Keam, S. J.; Perry, C. M., Prulifloxacin: Adis Drug Profile. *Drugs* **2004,** *64* (19), 2221-2234.
33. Domagala, J. M., Structure-activity and structure-side-effect relationships for the quinolone antibacterials. . *Journal of Antimicrobial Chemotherapy* **1994,** *33*, 685-706.
34. Roychoudhury, S.; Twinem, T. L.; Makin, K. M.; McIntosh, E. J.; Ledoussal, B.; Catrenich, C. E., Activity of non-fluorinated quinolones (NFQs) against quinolone-resistant *Escherichia coli* and *Streptococcus pneumoniae*. *Journal of Antimicrobial Chemotherapy* **2001,** *48*, 29-36.
35. Barry, A. L.; Fuchs, P. C.; Brown, S. D., In vitro activities of three nonfluorinated quinolones against representative bacterial isolates. *Antimicrobial Agents and Chemotherapy* **2001,** *45* (6), 1923-7.
36. Kimura, Y.; Atarashi, S.; Kawakami, K.; Sato, K.; Hayakawa, I., (Fluorocyclopropyl) quinolones. 2. Synthesis and stereochemical structure-activity relationships of chiral 7-(7-amino-5-azaspiro[2.4]heptan-5-yl)-1-(2-fluorocyclopropyl) quinolone antibacterial agents. *Journal of Medicinal Chemistry* **1994,** *37* (20), 3344-3352.

37. D. Bouzard; P. Di Cesare; M. Essiz; J. P. Jacquet; P. Remuzon; A. Weber; T. Oki; Masuyoshit, M., Fluoronaphthyridines and Quinolones as Antibacterial Agents. 1. Synthesis and Structure-Activity Relationships of New 1-Substituted Derivatives. *Journal of Medicinal Chemistry* **1989,** *32* (3), 537-542.
38. Nightingale, C. H., Moxifloxacin, a new antibiotic designed to treat community-acquired respiratory tract infections: a review of microbiologic and pharmacokinetic-pharmacodynamic characteristics. . *Pharmacotherapy* **2000,** *20* (3), 245-256.
39. Gellert, M.; Mizuuchi, K.; O'Dea, M. H.; Itoh, T.; Tomizawa, J., Nalidixic acid resistance: A second genetic character involved in DNA gyrase activity. *Proceedings of the National Academy of Science U.S.A.* **1977,** *74* (11), 4772-4776.
40. Rohlfing, S. R.; Gerster, J. F.; Kvam, D. C., Bioevaluation of the Antibacterial Flumequine for Urinary Tract Use. *Antimicrobial Agents and Chemotherapy* **1976,** *10* (1), 20-24.
41. Isao, H.; Tokiyuki, H.; Yoshiaki, T., Synthesis and Antibacterial Activities of Substituted 7-Oxo-2,3-dihydro-7H-pyrido [1,2,3-de] [1,4] benzoxazine-6-carboxylic Acids. *Chemical & Pharmaceutical Bulletin* **1984,** *32* (12), 4907-4913.
42. Ito, H ;Yoshida, H; Bogaki-Shonai, M; Niga, T; Hattori, H; Nakamura, S., Quinolone resistance mutations in the DNA gyrase gyrA and gyrB genes of Staphylococcus aureus. *Antimicrobial Agents and Chemotherapy* **1994,** *38* (9), 2014-2023.
43. Malik, M.; Marks, K. R.; Schwanz, H. A.; German, N.; Drlica, K.; Kerns, R. J., Effect of N-1/C-8 ring fusion and C-7 ring structure on fluoroquinolone lethality. *Antimicrobial Agents and Chemotherapy* **2010,** *54* (12), 5214-21.
44. Hooper, D. C. In *The quinolone antimicrobials.*, American Society for Microbiology, Washington, DC., Washington, DC., **2003**.
45. Levine, C.; Hiasa, H.; Marians, K. J., Review: DNA gyrase and topoisomerase IV: biochemical activities, physiological roles during chromosome replication, and drug sensitivities. *Biochimica et Biophysica Acta* **1998,** *1400*, 29-43.
46. Anderson, V. E.; Osheroff, N., Type II topoisomerases as targets for quinolone antibacterials: Turning Dr. Jekyll into Mr. Hyde. *Current Pharmaceutical Design* **2001,** *7* (5), 337-353.
47. Levine, C.; Hiasa, H.; Marians, K. J., DNA gyrase and topoisomerase IV: Biochemical activities, physiological roles during chromosome replication, and drug sensitivities. *Biochimica et Biophysica Acta-Gene Structure and Expression* **1998,** *1400* (1-3), 29-43.
48. Champoux, J. J., DNA topoisomerases: Structure, function, and mechanism. *Annual Review of Biochemistry* **2001,** *70*, 369-413.
49. Redgrave, L. S.; Sutton, S. B.; Webber, M. A.; Piddock, L. J. V., Fluoroquinolone resistance: mechanisms, impact on bacteria, and role in evolutionary success. *Trends in Microbiology* **2014**.
50. Pommier, Y.; Leo, E.; Zhang, H.; Marchand, C., DNA topoisomerases and their poisoning by anticancer and antibacterial drugs. *ACS Chemical Biology* **2010,** *17* (5), 421-33.
51. Nitiss, J. L., DNA topoisomerase II and its growing repertoire of biological functions. *Nature Reviews: Cancer* **2009,** *9*, 327-337.
52. Dirlica, K., Mechanism of fluoroquinolone action. *Current Opinion in Microbiology* **1999,** *2*, 504-508.
53. Champoux, J. J.., DNA topoisomerases: Structure, Function, and Mechanism. *Annual Review of Biochemistry* **2001,** *70*, 369-413.
54. Schmidt, B. H.; Burgin, A. B.; Deweese, J. E.; Osheroff, N.; Berger, J. M., A novel and unified two-metal mechanism for DNA cleavage by type II and IA topoisomerases. *Nature* **2010,** *465*, 641-644.

55. Malik, M.; Zhao, X.; Drlica, K., Lethal fragmentation of bacterial chromosomes mediated by DNA gyrase and quinolones. . *Molecular Microbiology* **2006,** *61* (3), 810-825.
56. Drlica, K.; Malik, M.; Kerns, R. J.; Zhao, X., *Antimicrobial Agents and Chemotherapy* **2008,** *52* (2), 385-392.
57. Cullen, M. E.; Wyke, A. W.; Kuroda, R.; Fisher, L. M., Cloning and characterization of a DNA gyrase A gene from Escherichia coli that confers clinical resistance to 4-quinolones. *Antimicrobial Agents and Chemotherapy* **1989,** *33* (6), 886-894;
58. Aldred, K. J.; McPherson, S. A.; Turnbough, C. L., Jr.; Kerns, R. J.; Osheroff, N., Topoisomerase IV-quinolone interactions are mediated through a water-metal ion bridge: mechanistic basis of quinolone resistance. *Nucleic Acids Res* **2013,** *41* (8), 4628-39.
59. WHO *Global Tuberculosis Control* World Heath Organization: 2013.
60. Emmerson, A. M.; Jones, A. M., The quinolones: Decades of development and use. *Journal of Antimicrobial Chemotherapy* **2003,** *51*, Suppl. 1 13-20.
61. Mitscher, L. A., Bacterial topoisomerase inhibitors: Quinolone and pyridone antibacterial agents. . *Chemistry Reviews* **2005,** *105* (2), 559-592.
62. Andriole, V. T., The quinolones: Past, present, and future. *Clinical Infectious Diseases* **2005,** *41*, Suppli. 2 S113-S119.
63. Drlica, K.; Hiasa, H.; Kerns, R.; Malik, M.; Mustaev, A.; Zhao, X., Quinolones: Action and resistance updated. . *Current Topics in Medicinal Chemistry* **2009,** *9*, 981-998.
64. Dalhoff, A., Resistance surveillance studies: A multifaceted problem□the fluoroquinolone example. . *Infection* **2012,** *40*, 239-262.
65. Blumberg, H. M.; Rimland, D.; Carroll, D. J.; Terry, P.; Wachsmuth, I. K., Rapid development of ciprofloxacin resistance in methicillin-susceptible and -resistant Staphylococcus aureus. . *Journal of Infectious Diseases* **1991,** *163* (6), 1279-1285.
66. Hooper, D. C., Fluoroquinolone resistance among Gram-positive cocci. *The Lancet Infectious Diseases* **2002,** *2* (9), 530-538.
67. Chen, D. K.; McGeer, A.; de Azavedo, J. C.; Low, D. E., Decreased susceptibility of Streptococcus pneumoniae to fluoroquinolones in Canada. *New England Journal of Medicine* **1999,** *341*, 233-239.
68. Poole, K., Fluoroquinolones in Gram-Negative Efflux-Mediated Resistance to Bacteria. *Antimicrobial Agents and Chemotherapy* **2000,** *44* (9), 2233-2241.
69. Aldred, K.; Kerns, R.; Osheroff, N., Mechanism of Quinolone Action and Resistance. *Biochemistry* **2014,** *53*, 1565-1574.
70. Hooper, D. C., Mode of action of fluoroquinolones. *Drugs* **1999,** *58* (Suppl. 2), 6-10.
71. Hooper, D. C., Mechanisms of action of antimicrobials: Focus on fluoroquinolones. . *Clinical Infectious Diseases* **2001,** *32*, Suppl. 1 S9-S15.
72. Fournier, B.; Zhao, X.; Lu, T.; Drlica, K.; Hooper, D. C., Selective targeting of topoisomerase IV and DNA gyrase in Staphylococcus aureus: Different patterns of quinolone-induced inhibition of DNA synthesis. *Antimicrobial Agents and Chemotherapy* **2000,** *44*, 2160-2165.
73. Price, L. B.; Vogler, A.; Pearson, T.; Busch, J. D.; Schupp, J. M.; Keim, P., In vitro selection and characterization of Bacillus anthracis mutants with high-level resistance to ciprofloxacin. *Antimicrobial Agents and Chemotherapy* **2003,** *47*, 2362-2365.
74. Morgan-Linnell, S. K.; Becnel Boyd, L.; Steffen, D.; Zechiedrich, L., Mechanisms accounting for fluoroquinolone resistance in Escherichia coli clinical isolates. *Antimicrobial Agents and Chemotherapy* **2009,** *53* (1), 235-41.
75. Li, Z.; Deguchi, T.; Yasuda, M.; Kawamura, T.; Kanematsu, E.; Nishino, Y.; Ishihara, S.; Kawada, Y., Alteration in the GyrA Subunit of DNA Gyrase and the ParC Subunit of DNA Topoisomerase IV in Quinolone-Resistant Clinical Isolates of

Staphylococcus epidermidis. *Antimicrobial Agents and Chemotherapy* **1998,** *42* (12), 3293-3295.
76. Blondeau, J. M., Fluoroquinolones: mechanism of action, classification, and development of resistance. *Survey of Ophthalmology* **2004,** *49* (Suppl 2), S73-8.
77. Yoshida, H.; Bogaki, M.; Nakamura, M.; Nakamura, S., Quinolone resistance-determining region in the DNA gyrase gyrA gene of Escherichia coli. *Antimicrobial Agents and Chemotherapy* **1990,** *34*, 1271-1272.
78. Aldred, K. J.; McPherson, S. A.; Wang, P.; Kerns, R. J.; Graves, D. E.; Turnbough, C. L., Jr.; Osheroff, N., Drug interactions with Bacillus anthracis topoisomerase IV: Biochemical basis for quinolone action and resistance. *Biochemistry* **2012,** *51*, 370-381.
79. Aldred, K. J.; McPherson, S. A.; Turnbough, J., C. L.; Kerns, R. J.; Osheroff, N., Topoisomerase IV-quinolone interactions are mediated through a water-metal ion bridge: Mechanistic basis of quinolone resistance. *Nucleic Acids Research* **2013,** *41* (8), 4628-4639.
80. Pan, X. S.; Gould, K. A.; Fisher, L. M., Probing the differential interactions of quinazolinedione PD 0305970 and quinolones with gyrase and topoisomerase IV. *Antimicrobial Agents and Chemotherapy* **2009,** *53*, 3822-3831.
81. Anderson, V. E.; Zaniewski, R. P.; Kaczmarek, F. S.; Gootz, T. D.; Osheroff, N., Action of quinolones against Staphylococcus aureus topoisomerase IV: Basis for DNA cleavage enhancement. *Biochemistry* **2000,** *39*, 2726-2732.
82. Pan, X. S.; Yague, G.; Fisher, L. M., Quinolone resistance mutations in Streptococcus pneumoniae GyrA and ParC proteins: Mechanistic insights into quinolone action from enzymatic analysis, intracellular levels, and phenotypes of wild-type and mutant proteins. . *Antimicrobial Agents and Chemotherapy* **2001,** *45*, 3140-3147.
83. Yague, G.; Morris, J. E.; Pan, X. S.; Gould, K. A.; Fisher, L. M., Cleavable-complex formation by wild-type and quinoloneresistant Streptococcus pneumoniae type II topoisomerases mediated by gemifloxacin and other fluoroquinolones. *Antimicrobial Agents and Chemotherapy* **2002,** *46*, 413-419.
84. Pfeiffer, E. S.; Hiasa, H., Determination of the primary target of a quinolone drug and the effect of quinolone resistance-conferring mutations by measuring quinolone sensitivity based on its mode of action. . *Antimicrobial Agents and Chemotherapy* **2007,** *51*, 3410-3412.
85. Barnard, F. M.; Maxwell, A., Interaction between DNA gyrase and quinolones: Effects of alanine mutations at GyrA subunit residues Ser(83) and Asp(87). *Antimicrobial Agents and Chemotherapy* **2001,** *45*, 1994-2000.
86. Hiasa, H., The Glu-84 of the ParC subunit plays critical roles in both topoisomerase IV-quinolone and topoisomerase IV-DNA interactions. *Biochemistry* **2002,** *41*, 11779-11785.
87. Robicsek, A.; Jacoby, G. A.; Hooper, D. C., The worldwide emergence of plasmid-mediated quinolone resistance. *Lancet: Infectious Diseases* **2006,** *6*, 629-640.
88. Strahilevitz, J.; Jacoby, G. A.; Hooper, D. C.; Robicsek, A., Plasmid-mediated quinolone resistance: A multifaceted threat. *Clinical Microbiology Review* **2009,** *22*, 664-689.
89. Tran, J. H.; Jacoby, G. A., Mechanism of plasmidmediated quinolone resistance. *Proceedings of the National Academy of Science U.S.A.* **2002,** *66*, 5638-5642.
90. Xiong, X.; Bromley, E. H.; Oelschlaeger, P.; Woolfson, D. N.; Spencer, J., Structural insights into quinolone antibiotic resistance mediated by pentapeptide repeat proteins: Conserved surface loops direct the activity of a Qnr protein from a Gram-negative bacterium. . *Nucleic Acids Research* **2011,** *39*, 3917-3927.
91. Robicsek, A.; Strahilevitz, J.; Jacoby, G. A.; Macielag, M.; Abbanat, D.; Park, C. H.; Bush, K.; Hooper, D. C., Fluoroquinolone-modifying enzyme: A new adaptation of a common aminoglycoside acetyltransferase. *Naure: Medicine* **2006,** *12*, 83-88.

92. Guillard, T.; Cambau, E.; Chau, F.; Massias, L.; de Champs, C.; Fantin, B., Ciprofloxacin treatment failure in a murine model of pyelonephritis due to an AAC(6′)-Ib-cr-producing Escherichia coli strain susceptible to ciprofloxacin in vitro. . *Antimicrobial Agents and Chemotherapy* **2013,** *57*, 5830-5835.
93. Yamane, K.; Wachino, J.; Suzuki, S.; Kimura, K.; Shibata, N.; Kato, H.; Shibayama, K.; Konda, T.; Arakawa, Y., New plasmid-mediated fluoroquinolone efflux pump, QepA, found in an Escherichia coli clinical isolate. *Antimicrobial Agents and Chemotherapy* **2007,** *51*, 3354-3360.
94. Cattoir, V.; Poirel, L.; Nordmann, P., Plasmid-mediated quinolone resistance pump QepA2 in an Escherichia coli isolate from France. *Antimicrobial Agents and Chemotherapy* **2008,** *52*, 3801-3804.
95. Fàbrega, A.; Madurga, S.; Giralt, E.; Vila, J., Review: Mechanism of action of and resistance to quinolones. *Microbial Biotechnology* **2009,** *2* (1), 40-61.
96. Poole, K., Efflux-mediated resistance to fluoroquinolones in Gram-positive bacteria and the mycobacteria. *Antimicrobial Agents and Chemotherapy* **2000,** *44*, 2595-2599.
97. Martinez-Martinez, L.; Pascual, A., Garcia, I.; Tran, J.; Jacoby, G. A., Interaction of plasmid and host quinolone resistance. *Journal of Antimicrobial Chemotherapy* **2003,** *51*, 1037-1039.
98. Jacoby, G. A., Mechanisms of resistance to quinolones. *Clinical Infectious Diseases* **2005,** *41*, Suppl. 2 S120-S126.
99. Poole, K., Efflux pumps as antimicrobial resistance mechanisms. *Annals of Medicine* **2007,** *39* (3), 162-176.
100. Goldman, J. D.; White, D. G.; Levy, S. B., Multiple antibiotic resistance (mar) locus protects Escherichia coli from rapid cell killing by fluoroquinolones. . *Antimicrobial Agents and Chemotherapy* **1996,** *40*, 1266-1269.
101. Singh, R.; Swick, M. C.; Ledesma, K. R.; Yang, Z.; Hu, M.; Zechiedrich, L.; Tam, V. H., Temporal interplay between efflux pumps and target mutations in development of antibiotic resistance in Escherichia coli. *Antimicrobial Agents and Chemotherapy* **2012,** *56*, 1680-1685.
102. Wendorff, T. J.; Schmidt, B. H.; Heslop, P.; Austin, C. A.; Berger, J. M., The structure of DNA-bound human topoisomerase II alpha: conformational mechanisms for coordinating inter-subunit interactions with DNA cleavage. *Journal of Molecular Biology* **2012,** *424*, 109-124.
103. Boucher, H. W.; Talbot, G. H.; Bradley, J. S.; Edwards, J., J. E.; Gilbert, D.; Rice, L. B.; Scheld, M.; Spellberg, B.; Bartlett, J., Bad Bugs, No Drugs: No ESKAPE! An Update from the Infectious Diseases Society of America. *IDSA Report on Development Pipeline* **2009,** *48* (1), 1-12.
104. Zhao, X.; Drlica, K., Restricting the Selection of Antibiotic-Resistant Mutants: A General Strategy Derived from Fluoroquinolone Studies. *Clinical Infectious Diseases* **2001,** *33* (Suppl 3), S147-S156.
105. Jianfeng Zhou; Yuzhi Dong; Xilin Zhao; Sungwoo Lee; Amol Amin; Srinivas Ramaswamy; John Domagala; James M. Musser; Drlica, K., Selection of Antibiotic-Resistant Bacterial Mutants: Allelic Diversity among Fluoroquinolone-Resistant Mutations. *Journal of Infectious Diseases* **2000,** *182* (2), 517-525.
106. Laponogov, I.; Sohi, M. K.; Veselkov, D. A.; Pan, X.-S.; Sawhney, R.; Thompson, A. W.; McAuley, K. E.; Fisher, L. M.; Sanderson, M. R., Structural insight into the quinolone-DNA cleavage complex of type IIA topoisomerases. *Nature: Structural and Molecular Biology* **2009,** *16*, 667-669.
107. Sanchez, J. P.; Domagala, J. M.; Hagen, S. E.; Heifetz, C. L.; Hutt, M. P.; Nichols, J. B.; Trehan, A. K., Quinolone antibacterial agents. Synthesis and structure-activity relationships of 8-substituted quinoline-3-carboxylic acids and 1,8-naphthyridine-3-carboxylic acids. *Journal of Medicinal Chemistry* **1988,** *31* (5), 983-991.

108. Perner, R. J.; DiDomenico, S.; Koenig, J. R.; Gomtsyan, A.; Bayburt, E. K.; Schmidt, R. G.; Drizin, I.; Zheng, G. Z.; Turner, S. C.; Jinkerson, T.; Brown, B. S.; Keddy, R. G.; Lukin, K.; McDonald, H. A.; Honore, P.; Mikusa, J.; Marsh, K. C.; Wetter, J. M.; St. George, K.; Jarvis, M. F.; Faltynek, C. R.; Lee, C., In Vitro Structure-Activity Relationship and In Vivo Characterization of 1-(Aryl)-3-(4-(amino)benzyl)urea Transient Receptor Potential Vanilloid 1 Antagonists. *Journal of Medicinal Chemistry* **2007,** *50* (15), 3651-3660.
109. Laeckmann, D.; Rogister, F.; Dejardin, J. V.; Prosperi-Meys, C.; Ge´czy, J.; Delargea, J.; Masereeld, B., Synthesis and Biological Evaluation of Aroylguanidines Related to Amiloride as Inhibitors of the Human Platelet Na+/H+ Exchanger. *Bioorganic & Medicinal Chemistry* **2002,** *10*, 1793-1804.
110. Drlica, K; Mustaev, A; Towle, T. R.; Luan, G; Kerns,R. J.; Berger, J. M., Bypassing Fluoroquinolone Resistance with Quinazolinediones:
Studies of Drug−Gyrase−DNA Complexes Having Implications for
Drug Design. *ACS Chemical Biology* **2014,** *9*, 2895-2904.
111. Pruss, G. J.; Manes, S. H.; Drlica, K., Escherichia coli DNA topoisomerase I mutants: Increased supercoiling is corrected by mutations near gyrase genes. *Cell* **1982,** *31* (1), 35-42.
112. Deitz, W. H.; Cook, T. M.; Goss, W. A., Mechanism of Action of Nalidixic Acid on Escherichia coli III. Conditions Required for Lethality. *Journal of Bacteriology* **1966,** *91* (2), 768-773.
113. Snyder, M.; Drlica, K., DNA gyrase on the bacterial chromosome: DNA cleavage induced by oxolinic acid. *Journal of Molecular Biology* **1979,** *131* (2), 287-302.
114. Chow, R. T.; Dougherty, T. J.; Fraimow, H. S.; Bellin, E. Y.; Miller, M. H., Association between early inhibition of DNA synthesis and the MICs and MBCs of carboxyquinolone antimicrobial agents for wild-type and mutant [gyrA nfxB(ompF) acrA] Escherichia coli K-12. *Antimicrobial Agents and Chemotherapy* **1988,** *32* (8), 1113-1118.
115. Aldred, K. J.; Kerns, R. J.; Osheroff, N., Mechanism of quinolone action and resistance. *Biochemistry* **2014,** *53* (10), 1565-74.
116. Domagala, J. M.; Hagen, S. E.; Joannides, T.; Kiely, J. S.; Laborde, E.; Schroeder, M. C.; Sesnie, J. A.; Shapiro, M. A.; Suto, M. J.; Vanderroe, S., Quinolone Antibacterials Containing the New 7434 1-Aminoethy1)-1 pyrrolidinyl] Side Chain: The Effects of the 1-Aminoethyl Moiety and Its Stereochemical Configurations on Potency and in Vivo Efficacy. *Journal of Medicinal Chemistry* **1993,** *36* (7), 871-882.
117. Suto, M. J.; Domagala, J. M.; Roland, G. E.; Mailloux, G. B.; Cohen, M. A., Fluoroquinolones: Relationships between Structural Variations, Mammalian Cell Cytotoxicity, and Antimicrobial Activity. *Journal of Medicinal Chemistry* **1992,** *35* (25), 4746-4760.
118. Huband, M. D.; Cohen, M. A.; Zurack, M.; Hanna, D. L.; Skerlos, L. A.; Sulavik, M. C.; Gibson, G. W.; Gage, J. W.; Ellsworth, E.; Stier, M. A.; Gracheck, S. J., In vitro and in vivo activities of PD 0305970 and PD 0326448, new bacterial gyrase/topoisomerase inhibitors with potent antibacterial activities versus multidrug-resistant gram-positive and fastidious organism groups. *Antimicrobial Agents and Chemotherapy* **2007,** *51* (4), 1191-201.
119. Oppegard, L. M.; Hamann, B. L.; Streck, K. R.; Ellis, K. C.; Fiedler, H. P.; Khodursky, A. B.; Hiasa, H., In Vivo and In Vitro Patterns of the Activity of Simocyclinone D8, an Angucyclinone Antibiotic from Streptomyces antibioticus. *Antimicrobial Agents and Chemotherapy* **2009,** *53* (5), 2110–2119.
120. Malik, M.; Hoatam, G.; Chavda, K.; Kerns, R. J.; Drlica, K., Novel approach for comparing the abilities of quinolones to restrict the emergence of resistant mutants during quinolone exposure. *Antimicrobial Agents and Chemotherapy* **2010,** *54* (1), 149-56.

121. German, N.; M. Malik; J. Rosen; K. Drlica; Kerns., R., Use of gyrase resistance mutants to guide selection of 8-methoxy-quinazoline-2,4-diones. *Antimicrobial Agents and Chemotherapy* **2008,** *52*, 3915-21.
122. Sadiq, A. A.; Patel, M. R.; Jacobson, B. A.; Escobedo, M.; Ellis, K.; Oppegard, L. M.; Hiasa, H.; Kratzke, R. A., Anti-proliferative effects of simocyclinone D8 (SD8), a novel catalytic inhibitor of topoisomerase II. *Investgational New Drugs* **2010,** *28*, 20-25.
123. Lu, T.; Zhao, X.; Drlica, K., Gatifloxacin activity against quinoloneresistant gyrase: allele-specific enhancement of bacteriostatic and bactericidal activity by the C-8-methoxy group. *Antimicrobial Agents and Chemotherapy* **1999,** *43*, 2969-74.
124. Sternglanz, R.; S. DiNardo, K. A.; Voelkel, Y.; Nishimura, Y.; Hirota, A. K.; Becherer, L.; Zumstein; Wang, J. C., Mutations in the gene coding for Escherichia coli DNA topoisomerase I affecting transcription and transposition. *Proceedings of the National Academy of Science U.S.A.* **1981,** *78*, 2747–2751.